POLITECHNIKA KRAKOWSKA
im. Tadeusza Kościuszki

Wydział Inżynierii i Technologii Chemicznej

CRACOW UNIVERSITY OF TECHNOLOGY
Faculty of Chemical Engineering and Technology

ELECTROOXIDATION OF GUANINE – THE USE IN QUANTIFYING ANTIOXIDANT ACTIVITY AND NANOMOLAR ELECTROANALYSIS

by

Termeh Darvishzad, MSc

Supervision: Professor Dariusz Bogdał

Co-supervision: Dr Stefan Kurek

Kraków 2018

Dedication

To my beloved parents and sisters for their endless love and affections. And to an unforgettable person of my life, my very dear co-supervisor, Dr. Stefan. Kurek who showed me the face of a real human.

Acknowledgments

First and foremost, praises and thanks to God, the Almightly, for his showers of blessings through my life.

This work was impossible without the perfect support of my family specially my dear parents and the huge assist of the greatest human ever in my life, my dear co-supervisor, Dr. Stefan Kurek.

I appreciate my father who accepted the whole expense of this PhD study. And my lovely mother because of her unconditional love and support.

I specially thank my dear co-supervisor, Dr. Stefan Kurek, who taught me not only science but also humanity.

I am grateful to my supervisor, Professor Dariusz Bogdał, who kindly accepted me to study as a PhD student in his faculty.

My profound gratitude goes also to Professor. Krystyna Wieczorek-Ciurowa and Ms. Katarzyna Bieg who kindly helped me to be enrolled in “Cracow University of Technology”.

My sincere gratitude also goes to Prof. Adam Grochowalski, Dr. Szczepan Bednarz, Dr. Mateusz Galica and Dr. Piotr Konieczny (From IFJ PAN) for their kind cooperations in performing some of my measurements.

I deeply thank my colleagues, Dr. Piotr Romańczyk, Dr. Grzegorz Rotko, Gleb Andryianau, Marcin Piotrowski, Adam Żaba, Svitlana Sovinska, Iwona Kamińska-Borek, Jasiek Ozimek and Szymon Bąnk because of their helps and friendly behaviors with me.

I also thank all the Professors in the “Faculty of Engineering and Chemical Technology” of “Cracow University of Technology” who patiently taught me science.

Finally I am extending my appreciation to all the people who have supported me during this journey directly and indirectly.

Abstract

The work focuses on the application of electrooxidation of guanine for quantifying antioxidative activity with the use of specifically developed voltammetric technique, and for guanine trace analysis in nanomolar concentrations on electrodes modified by a polymer strongly interacting with the analyte. The first part is devoted to the determination of guanine solubility in water, the value that has never been correctly obtained before. Using thermodynamic principles and known pK_a values, it was proven that the solubility of the neutral form of guanine is constant and independent of pH. The least square fit gave the concentration value equal to 25.4 μM for the neutral form of guanine. The solubility of guanine as a function of pH can be calculated as a total concentration of all the guanine species present in the solution. The individual concentrations can be calculated based on the pK_a values. However, dissolution of guanine powder leads to the formation of guanine nanoparticles, which is not evident and was apparently the main cause of obtaining too high solubility data published in the literature.

In the second part a new electrochemical method was developed for the evaluation of antioxidants activity based on their ability to inhibit 8-oxoguanine production. It appeared that the antioxidative activity vs. antioxidant concentration follows the exponential decay. Among the applied antioxidants, resveratrol and gallic acid with the exponential decay coefficients of 142.6 mM^{-1} and 91.37 mM^{-1}, respectively, were found the best antioxidants at pH 7. Pyrogallol showed a mixed pro-antioxidative behaviour at pH 9. Ascorbyl phosphate did not show any antioxidative activity even in the presence of a huge amount of it at pH 9.

The last, main part, is devoted to the development of a new electrochemical sensor for trace analysis of guanine. To this end, the surface of a glassy carbon electrode (GCE) was modified by a polymer. The best result was obtained by oxidative electropolymerisation of citrazinic acid, and by swelling the polymer layer in a tetrahydrofuran solution containing iron tetraphenylporphyrin. The limit of detection for this biosensor is about 5 nM. In further studies it was shown that this polymer is capable of forming special multiple hydrogen bonds with guanine which resemble triple H-bonds between guanine and cytosine in DNA. Magnetic susceptibility measurements proved that this polymer is a complex antiferromagnetic compound. Elemental analysis demonstrated that the polymer consisted of linked substituted pyridyl units mixed with considerable amounts of water and inorganic phosphates.

Aim and scope

The aim if this thesis was to develop novel methods based on electrooxidation of guanine in aqueous solutions. Preliminary studies indicated that owing to the importance of guanine oxidation by Reactive Oxygen Species leading to mutations, and consequently to a series of deceases that can be prevented by antioxidants, development of a new method for the assessment of antioxidative activity could be the first aim of this work. There is also a demand for an effective method for trace analysis of guanine. Modification of the electrode leading to an increase in its sensitivity and selectivity in guanine electroanalysis, enabling its detection in nanomolar concentration became the second aim in this work. As it appeared that the aqueous solubility of a compound of such an importance is not known for certain, the determination of its aqueous solubility became an additional aim in this work.

The determination of aqueous solubility of guanine in the pH range of 4 to 9 was carried out with the use of UV spectroscopy for guanine concentration determination. To dissolve guanine in this pH range it was necessary to use sonication and centrifuging. The problems encountered with the reproducibility of the results led to the detection of nanoparticles in the solution. The size distribution of these particles was determined by DLS technique. Thermodynamic analysis of dissociation and protonation equilibria in guanine solutions was also carried out leading to a method that enabled calculating the aqueous solubility of guanine at various pH values.

The method for the assessment of antioxidative activity is based on measuring the reduction in the amount of 8-oxoguanine produced in the reaction of guanine with ROS in the presence of antioxidants. A series of popular antioxidants was tested at pH 7 and pH 9 comprising active polyphenols, like resveratrol, catechol, catechin and gallic acid, but also resorcinol and pyrogallol, glutathione and ascorbic acid. It appeared also that simple alcohols, like methanol and ethanol also exhibit antioxidative properties, however, weak. The studies revealed also strong pro-oxidative properties of some polyphenols, particularly at alkaline pH. The antioxidative assessment could be quantified, and it was proven that this property could be described by an exponential decay curve with the decay coefficient being the measure of antioxidative activity.

An electroanalytical method developed is based on the modification of the carbon electrode by polymerisation of pyridine carboxylic acids. A series of these acids was tested with citrazinic acid yielding the most active layer. Additionally it was shown that swelling the layer in a solution of metalloporphyrins in tetrahydrofuran allows achieving the system capable of trace guanine electroanalysis in nanomolar concentration. The same system was active also in adenine analysis. Both nucleic acids can be determined simultaneously.

The modifying polymer was subjected to a series of tests. Despite its solubility in water, its structure cannot be easily studied as the polymer is paramagnetic and no NMR spectra could be recorded. Magnetic measurements proved that it is indeed paramagnetic and at very low temperatures is antiferromagnetic. Other analytical techniques were also applied to the study of the polymer, like elemental analysis and gel and ion chromatography. The latter revealed that the polymer contains significant amounts of phosphate anions from the buffer solution in which it was

formed. Electrochemical methods were also used to study the interaction of this polymer with guanine and to measure its acidity.

Contents

Dedication 1
Acknowledgments 2
Abstract 3
Aim and scope 4
Contents 6
List of figures 8
List of schemes 12
List of tables 12
Introduction 13
Guanine in nature 13
Guanine solubility 14
DNA damage 15
ROS production in our body 19
ROS paradox in cancer 20
ROS-based therapeutics in cancer 21
Redox homeostasis regulated by enzymes in cells 23
Guanine oxidation 24
Antioxidants effect 26
Antioxidants evaluation methods 27
Modification of the electrode 30
Polymers used to modify the electrode 31
Conducting polymers 32
Adsorption of Graphene and Porphyrins 35
Experimental 38
Guanine solubility 38
Dynamic Light Scattering (DLS) 39
Correlation in Dynamic Light Scattering 39
Obtaining size from the correlogram 39
DLS sample preparation 40
Lower size limit of DLS 40

Upper size limit of DLS 40
Sedimentation 41
Number fluctuation 41
Sample concentration overview 41
Lower concentration limit 41
Upper concentration limit 41
Restricted Diffusion 42
Particle interactions 42
Sample preparation overview 43
Sample dilution 43
Diluent filtration 43
Antioxidant evaluation 43
Guanine electroanalysis 44
Electrode modification 44
Polymer characterisation 45
Guanine trace analysis 46
Results and discussion 48
Guanine solubility 48
Antioxidant evaluation 56
Behaviour of antioxidants at pH 7 59
Behaviour of antioxidants at pH 9 68
Electrode modification for guanine analysis 74
Guanine electroanalysis on modified electrodes 83
Effect of scan rate on guanine oxidation 83
The limit of detection for TD100 86
Other products of guanine oxidation 89
Chronocoulometric results 90
Region number3: Polymer, Guanine and Adenine oxidation 94
Spectroscopic studies of citrazinic acid and its polymer 95
Polymer obtained from citrazinic acid (TD100) 104
Acidity determination 109
The interaction between TD100 and guanine 111
AFM measurements 114
Conclusions 115

Guanine solubility 115
Antioxidant evaluation 115
Guanine electroanalysis and electrode modification 116
Reference 118

List of figures

Figure 1. Structures of different forms of guanine. *13*
Figure 2. Deoxyribonucleic acid (DNA) double helix versus Ribonucleic acid (RNA) single helix with their bases. *14*
Figure 3. Piperlongumine structure. [] *21*
Figure 4. Pl-Fph structure [17] *21*
Figure 5. Quinone based anticancer agents *22*
Figure 6. Intensity, volume and number distributions. Intensity distribution is calculated from the correlogram. Volume and number are calculated from intensity. *40*
Figure 7. Synthesized compounds used for electropolymerisation. *45*
Figure 8. Passing laser pointer beam through the guanine solution. *48*
Figure 9. Typical size distribution of colloidal particles in a solution of guanine in pure water. *49*
Figure 10. Size distribution of colloidal particles in a solution of 0.1 M pH 7 PBS. Directly after preparation and after 14 days. *49*
Figure 11. Size distribution of colloidal particles in a freshly prepared solution of 0.1 M pH 4.0 PBS buffer. *50*
Figure 12. Size distribution of colloidal particles in a freshly prepared solution of 0.1 M pH 5.5 acetate buffer. *50*
Figure 13. Speciation of guanine solution as a function of pH calculated from the pKa values. *53*
Figure 14. pH dependence of guanine solubility. The line was calculated assuming a constant concentration of neutral guanine equal to 25 µM and summing up the concentrations of its ionised forms calculated from the respective pKa values. The inset shows this line over a wide range of pH. *54*
Figure 15. Comparison between our data and what is published by the other authors. Ideal fitting, except for the lowest concentrations (open points refer to pure guanine), dashed lines in our plot denote lower and upper limits. *54*
Figure 16. Voltammograms of 2nd and 5th steps recorded in a saturated solution of guanine in phosphate buffer of pH 7. Details on the applied potential hold and scan steps are given in Experimental. *56*
Figure 17. Voltammograms recorded upon adding increasing amounts of catechol (up to 0.23 mM) to saturated solution of guanine in pH 7 phosphate buffer. The bottom voltammograms were obtained prior to catechol addition (a) Step 2 – no previous dioxygen reduction. No trace of 8-oxoguanine can be seen. (b) Step 5 – directly after dioxygen reduction. 8-Oxoguanine can be seen with its wave decreasing with increasing amounts of added catechol, not totally, but to a limiting value. Significantly higher background (by ca. 3 µA) compared to (a) is due to the reduction of various ROS generated in the dioxygen reduction step and possibly surface oxygenated species on the electrode. *57*
Figure 18. Effect of adding methanol at pH 7. Exponential decay curve for 8-oxoguanine peak current in Step 5, expressed as percent of the peak current obtained for pure saturated guanine solution in phosphate buffer in the absence of methanol. The exponential coefficient in the trend line equation is the decay constant expressed in mM^{-1} (reciprocal of antioxidant (methanol) concentration). *59*
Figure 19. Effect of adding ethanol at pH 7. Conditions as in Fig. 18. ..... *60*
Figure 20. Effect of adding 2-propanol at pH 7. Conditions as in Fig. 18. ..... *60*
Figure 21. Behaviour of glutathione at pH 7. Conditions at Fig. 18. ..... *61*
Figure 22.Behaviour of gallic acid at pH 7. Conditions as in Fig. 3. Up to ca. 0.01 mM concentration, very rapid decay is seen, followed by slower steps, and halting at the level of 33%. *61*
Figure 23. Resveratrol behaviour at pH 7. Conditions as in Fig. 18. ..... *62*

Figure 24. Catechol behaviour at pH 7. Conditions as in Fig. 18. 62
Figure 25. Ascorbyl phosphate behaviour at pH 7. Conditions as in Fig. 18.....63
Figure 26. Pyrogallol behaviour at pH 7 and guanine concentration effect. General conditions as in Fig. 18. 8-Oxoguanine peak current as a function of pyrogallol concentration for two different concentrations of guanine. 63
Figure 27. Catechin behaviour at pH 7. Conditions as in Fig. 18.....64
Figure 28. Antioxidative activity coefficients (exponential decay parameters) for investigated substances at pH 7 expressed in mM^{-1}. Where applicable, the decay parameters were used only from the rapid phase at low concentrations.....65
Figure 29. The limiting values of percent 8-oxoguanine formation for studied antioxidants at pH 7. The complement to 100% could be regarded as antioxidant capacity. In some cases, like resveratrol, further reduction in this level could be elicited by adding much higher amounts of the antioxidant.....65
Figure 30. Guanine, 8-oxoguanine and pyrogallol concentration variation with time. Three peaks correspond the opposite behaviour of guanine and 8-oxoguanine with pyrogallol.....67
Figure 31. Charge versus square root of time. At the constant concentration of pyrogallol. 67
Figure 32. Effect of adding methanol at pH 9. Conditions as in Fig. 18 69
Figure 33. Effect of adding ethanol at pH 9. Conditions as in Fig. 18. 70
Figure 34. Effect of adding 2-propanol at pH 9. Conditions as in Fig. 18.....70
Figure 35. Behaviour of glutothione at pH 9. Conditions as in Fig. 18.....71
Figure 36. Behaviour of resorcinol at pH 9. Conditions as in Fig. 18. 71
Figure 37. Behaviour of resveratrol at pH 9. Conditions as in Fig. 18. 72
Figure 38. Behaviour of catechol at pH 9. Conditions as in Fig. 18. Instead of decay effect, only pro-oxidative effect can be seen.....72
Figure 39. Behaviour of catechin at pH 9. Conditions as in Fig. 18. Instead of decay effect, only pro-oxidative effect can be seen.....73
Figure 40. Behaviour of ascorbyl phosphate at pH 9. Conditions as in Fig. 18. Instead of decay effect, only pro-oxidative effect up to 160% can be seen.....73
Figure 41. Pro-oxidative activity of pyrogallol at pH 9. Conditions as in Fig. 18. Only the first portion of pyrogallol led to a decrease in 8-oxoguanine production. Then, up to 0.2 mM, the amount of 8-oxoguanine increased to begin slowly falling down. 74
Figure 42. CV. Scan rate= 100 mV/s. 1st Scan. Guanine oxidation peak, using modified GCE by GU98015: Pyridine-3,4-dicarboxylic acid, GU103027: Pyridine-4-carboxylic acid, GU106009: Pyridine-2,6-dicarboxylic acid. 75
Figure 43. CV scan rate =100 mV/s.1st Scan. Effect of layer thickness. GU98015: Pyridine-3,4- dicarboxylic acid (32 cycles). GU96016: Pyridine-3,4- dicarboxylic acid (12 cycles). 76
Figure 44. DPV. Guanine dissolved in GU88023: Phosphate buffer solution (KH2PO4(0.2 M)+KOH), GU87011: Phosphate buffer solution (Na_2HPO_4 (1/15 M)+H_3PO_4), GU87035: Phosphate buffer solution (KH2PO4(1/15 M))+KOH).....77
Figure 45. CV. Scan rate: 100 mV/s. 1st Scan. Polymer: Poly-pyridine-3,4-dicarboxylic acid. GU104014: Only Guanine (without any adsorption), GU111016: Guanine (with CoTPP adsorbed), GU112016: Guanine (with H_2-TPP adsorbed), GU114016: Guanine (with ZnTPP adsorbed), Gu98015: Guanine (with FeTPP adsorbed). 78
Figure 46. Semiderivatives of voltammograms with a film prepared by oxidation of pyridine-3,4-dicarboxylic acid treated with THF solutions of indicated tetraphenylporphyrins. 'None' denotes the case of no treatment.....78
Figure 47. CV. Scan rate: 100 mV/s .1st Scan. GU104014: Only Guanine (without any adsorption), GU116013: by immersing polymerised layer in only THF. 79
Figure 48. OSWV. Polymer: Poly-pyridine-3,4-dicarboxylic acid. GU104011: Guanine (electrode not modified by porphyrins), GU111008: Guanine (with CoTPP adsorbed), GU112009: (with H_2-TPP adsorbed), GU114009 (with ZnTPP adsorbed), GU116008: modified by immersing polymerised layer in only THF, GU98021: (with FeTPP adsorbed).....80

Figure 49. Structure, chemical name (full and symbol) and voltammogram of a synthesised derivative of pyridine carboxylic acid. 80
Figure 50. Structure, chemical name (full and symbol) and voltammogram of a synthesised derivative of pyridine carboxylic acid. 81
Figure 51. Structure, chemical name (full and symbol) and voltammogram of a synthesised derivative of pyridine carboxylic acid. 81
Figure 52. Structure, chemical name (full and symbol) and voltammogram of a synthesised derivative of pyridine carboxylic acid. 82
Figure 53. Structure and voltammogram of citrazinic acid in water. 82
Figure 54. Semiderivatives of voltammograms of 25 µM guanine in phosphate buffer, pH7, on GCE with a layer obtained by oxidation of the shown pyridinecarboxylic acid, followed by treatment with FeTPP in THF. Scan rate 0.1 V s^{-1}. 83
Figure 55. Semiderivatives of the first cycles of voltammograms of guanine oxidation. . GU111016C: scan rate=100 mV/s, GU111017C: scan rate=500 mV/s, GU111019C: scan rate=1000 mV/s, GU111020C: scan rate=50 mV/s, GU111021C: scan rate=20 mV/s. 84
Figure 56. Semiderivatives of second cycles of guanine oxidation. GU111016C: scan rate=100 mV/s, GU111017C: scan rate=500 mV/s, GU111019C: scan rate=1000 mV/s, GU111020C: scan rate=50 mV/s, GU111021C: scan rate=20 mV/s. 84
Figure 57. Semiderivatives of third cycles of guanine oxidation.. GU111016C: scan rate=100 mV/s, GU111017C: scan rate=500 mV/s, GU111019C: scan rate=1000 mV/s, GU111020C: scan rate=50 mV/s, GU111021C: scan rate=20 mV/s. 85
Figure 58. Cyclic Voltammograms 1st Scan. 191012 – 200 mV/s, 191013 – 500 mV/s, 191014 – 1000 mV/s, 191015 – 50 mV/s, 191017 – 20 mV/s. 85
Figure 59. Cyclic Voltammograms 1st Scan. 191012 – 200 mV/s, 191013 – 500 mV/s, 191014 – 1000 mV/s, 191015 – 50 mV/s, 191017 – 20 mV/s. 86
Figure 60. SQWV results. Limit of detection-increasing of current versus guanine concentration. 86
Figure 61. Linear relationship between guanine concentration and current down to 0.08 µM. 87
Figure 62. SQWV with subtracted background. 87
Figure 63. Peak current vs. concentration. Problems at the lowest concentrations. Red crosses denote outliers, not taken for the calculation of the regression equation. 88
Figure 64. SQWV with subtracted background. 88
Figure 65. Peak current vs. concentration. Problems at the lowest concentrations. 89
Figure 66. Semiderivatives 2nd Scan. 191012 – 200 mV/s; …13 – 500 mV/s; …14 – 1000 mV/s; …15 – 50 mV/s; … 17 – 20 mV/s. 89
Figure 67. a) Charge versus time and b) Charge versus square rout of time in guanine oxidation process. 90
Figure 68. CV. Scan rate= 20 mV/s. Guanine oxidation and 8-oxoguanine peaks at the GCE modified by polymerisation of pyridine-3,4-dicarboxylic acid and CoTPP adsorption from its THF solution. The numbers and ranges refer to chronocoulometric measurements from Table 3. 91
Figure 69. Scan rate= 100 mV/s. Guanine and adenine oxidation on GCE modified by polymerisation of citrazinic acid and FeTPP adsorption from its THF solution. 92
Figure 70. a) Charge versus time, b) Charge versus the square root of time; 1st region. 92
Figure 71. a) Charge versus time, b) Charge versus the square root of time; 2nd region. 93
Figure 72. a) Charge versus time, b) Charge versus the square root of time; 3rd region. 94
Figure 73. Uv-vis spectra of citrazinic acid itself and after adding guanine in phosphate buffer solution (KH2PO4+KOH, pH=9). 96
Figure 74. Effect of Guanine on the citrazinic acid spectrum. Diff is the differential spectrum from Fig. 73 expanded. Here, it is compared with the spectrum of guanine. 96
Figure 75. Doubly differential spectrum obtained by subtracting guanine spectrum from the differential spectrum of Fig. 74. A new band is seen. 97

Figure 76. Comparison of the spectrum of citrazinic acid in the presence of guanine with guanine itself in the phosphate buffer solution pH 5. 97
Figure 77. No changes could be seen on the spectrum of citrazinic acid by adding guanine at pH 7. 98
Figure 78. Fluorescence spectra of citrazinic acid as the monomer, polymer and monomer in the absence and presence of guanine in water. 99
Figure 79. Fluorescence spctra of citrazinic acid in phosphate buffer solution pH 7 in the absence and presence of guanine. 99
Figure 80. The new band obtained by subtracting the spectrum of citrazinic acid from the spectrum of this acid in the presence of guanine at pH 7. 100
Figure 81. Emission of guanine in 260 nm, 280 nm and 389 nm excitation wavelengths. 100
Figure 82. Fluorescence spectra of citrazinic acid in the absence and presence of guanine at pH 5. 101
Figure 83. The band obtained by subtracting of the spectrum of citrazinic acid from the spectrum of this acid in the presence of guanine at pH 5. 101
Figure 84. Fluorescence spectra of citrazinic acid in the absence and presence of guanine at pH 9. 102
Figure 85. The new peak obtained by subtracting of the spectrum of citrazinic acid from the spectrum of this acid in the presence of guanine at pH 9. 102
Figure 86. Uv-Vis spectrum of citrazinic acid polymer in water. 103
Figure 87. The new bands obtained by subtracting the spectrum of polymer in the absence and presence of guanine. 103
Figure 88. Fluorescence spectra of polymer in the absence and presence of guanine. And the difference between these two spectra at pH 9. 104
Figure 89. Gel permeation chromatography of polymer obtained from citrazinic acid. 105
Figure 90. Isothermal magnetization in 2.0 K. Insert points out the value of coercive field of about 90 Oe. The lines are only guides for eyes. 105
Figure 91. Isothermal magnetization in 2.0K with subtracted diamagnetic contribution (blue circles). The red line represent the Brillouin function for spin 1/2, g=2.0 and with assumption that there is one delocalized electron for each 5 formula unit. 106
Figure 92. Dc susceptibility as a function of temperature in constant field of 1000 Oe. 106
Figure 93. The temperature dependence of χT product. 107
Figure 94. Cyclic voltammograms of citrazinic acid in DMF on Pt electrode. 109
Figure 95. Semiderivatives of the voltammograms in Fig. 94. 109
Figure 96. Cyclic voltammograms of polymer in DMF on Pt electrode. 110
Figure 97. Semiderivatives of the voltammograms in Fig. 96. 110
Figure 98. Guanine-cytosine pair and citrazinic acid structures. 111
Figure 99. Semiderivatives of voltammograms of citrazinic acid, without and with guanine added in DMF at Pt. Scan rate 0.02 V s^{-1}. 112
Figure 100. Semiderivatives of voltammograms at a scan rate 0.2 V s^{-1}. 112
Figure 101. Comparison of semiderivatives of voltammograms of indicated mixtures in DMF at Pt. Scan rate 0.2 V s^{-1}. 113
Figure 102. Representative surface topography images of citrazinic acid layer (a) and citrazinic acid admixed with guanine film (b). Lateral force (c, d) and error signal (e, f) images of investigated samples. Additionally, pixel height distributions are presented in (a') and (b'). 114

List of schemes

Scheme 1. Sources of ROS, antioxidant defences, and subsequent biological effects depending on the level of ROS production. 18
Scheme 2. General Scheme for ROS Production. 19
Scheme 3. ROS Generation Induced by Cellular Enzymes. 19
Scheme 4. Maintenance of redox homeostasis in cells by enzymes. 24
Scheme 5. Oxidation of guanine to 8-oxoguanine. 25
Scheme 6. A correlogram. 39
Scheme 7. Multiple scattering. 42
Scheme 8. HP UV-visible Spectroscopy system. 45
Scheme 9. Different forms of guanine. 51
Scheme 10. The series of antioxidants which were applied in the measurements, by showing their structures. 58

List of tables

Table 1. Ultraviolet spectra of guanine and its conjugated acids and bases used for concentration. 38
Table 2. pKa values of acid-base equilibria for guanine and its conjugate acids and bases. Note: the pK_a value is a mean of two values based on NMR and UV spectroscopic studies. 52
Table 3. Chronocoulometric results obtained from guanine oxidation on modified GCE; voltammograms shown in Fig. 68. Nett charge (Nett Q) for chronocoulograms #023 and 025 were calculated by subtracting the charge used for double layer and polymer charging from the intercept (see text below). 91
Table 4. Chronocoulometric data of the 1st region. 93
Table 5. Chronocoulometric data of 2nd region. 94
Table 6. Chronocoulometric data of 3rd region. 95
Table 7. Elemental analysis of TD100. 107
Table 8. Phosphate ion chromatography analysis results. 108
Table 9. pKa values of citrazinic acid in DMF. 109
Table 10. pKa value of polymer in DMF. 110
Table 11. pKa values of a couple of acids in DMF for comparison [52]. 111

Introduction

Guanine in nature

In nature, guanine is present in the form of nucleosides, in which it is chemically linked to pentoses, either ribose as in guanosine or deoxyribose as in deoxyguanosine. The sugar unit in them is additionally phosphorylated. The presence of such groups makes guanine in the natural form more soluble.

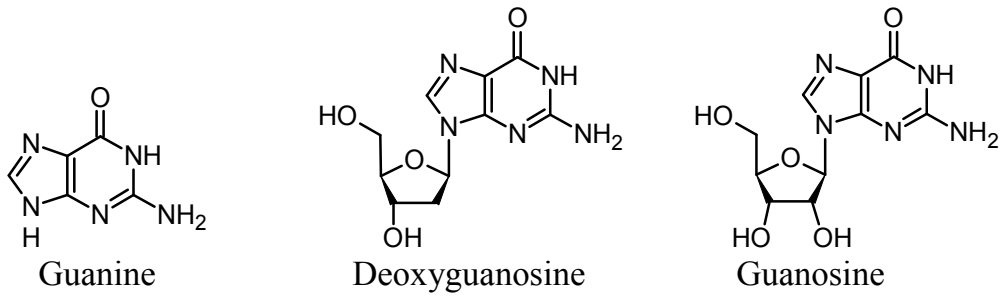

Figure 1. Structures of different forms of guanine.

However, the unsubstituted form of guanine could also be found in nature. Its tiny crystals are responsible for metallic lustre in fish, certain spiders and even for tuning the colour of panther chameleons [1,2]. Guanine as an essential component of DNA and RNA, was identified in guano in 1845 for the first time. Then, in 1861, guanine crystals were identified in the scales and air bladders of fish. Guanine crystals were found in reptiles and arthropods in 1882. By 1893, it was well understood that guanine crystals are responsible for the iridescence of fish skin and that the crystals are located inside specialized cells called iridocytes [2]. These tiny crystals of guanine platelets are used for reflecting light in the concave mirror of the scallop eye [3]. Guanine crystals show a diversity of different functions in organisms, such as manipulation of light to produce structural colours, mirror ingredient of visual systems, protection against excessive heat, and inhibition of gas diffusion. Guanine in nature is used as light manipulator probably because it has one of the highest known refractive indices (n = 1.83) for any natural biological material. This high refractive index occurs along one crystallographic axis, corresponding to the guanine molecules stacking in the crystal structure, while the refractive indices along the orthogonal directions are appraised to be much lower, namely around n = 1.45. Therefore, the interaction with light will depend critically on the direction in which light falls on the crystal and on the crystal shape and size, too [2]. Guanine crystallization is very difficult. The obtained crystal form depends on crystallization conditions, the pH value, above all [4]. Guanine monohydrate is obtained from highly acidic solutions (pH 1-3), anhydrous guanine crystals are obtained from neutral and basic solutions (pH 7-13) and the crystallization of guanine sodium salt is occur from alkaline solutions (pH 14). Anhydrous guanine are found in two crystalline forms, a marginally more stable α-form, and β-form, regarded as more kinetically favoured [5]. However, only β-form was found in nature. Thin plate-like crystal structure of β anhydrous guanine is responsible for the broadband reflectance which is found in silvery fish and spiders, and block- shaped β anhydrous guanine crystals scatter light and make the white colour characteristic of certain spiders. The first crystal

structure of guanine was published for guanine monohydrate in 1971. Due to the role of guanine monohydrate in DNA and its significant interactions with water, its structure is important. Since the structure of guanine monohydrate was reported, many theoretical studies were done on the interactions of guanine and water and also on the structure and properties of guanine monohydrate; however no experimental data on guanine monohydrate crystals were reported, probably because it is very difficult to produce. Guanine microcrystals extracted from fish scales or guano are applied for their pearly and lustrous effect in cosmetics, but also in other commercial products [6]. Guano is excreted by various fish eating sea birds as pelicans, gannets, gulls, petrels, penguins and cormorants. Guano is also a rich fertilizer containing nitrogen and phosphorus. Guano builds up in rainless littoral regions or on islands where birds gather, including the Chincha Islands off the coast of Peru, Galapagos Islands of Ecuador and also on the other Islands of Latin America, Pacific Islands and Grand Canyon Bat cave in Arizona [6]. Orientation of guanine microcrystals along applied magnetic field makes them very interesting material for special applications [7]. Therefore, guanine solubility and its pH dependence should be a very important parameter for designing new crystallization methods.

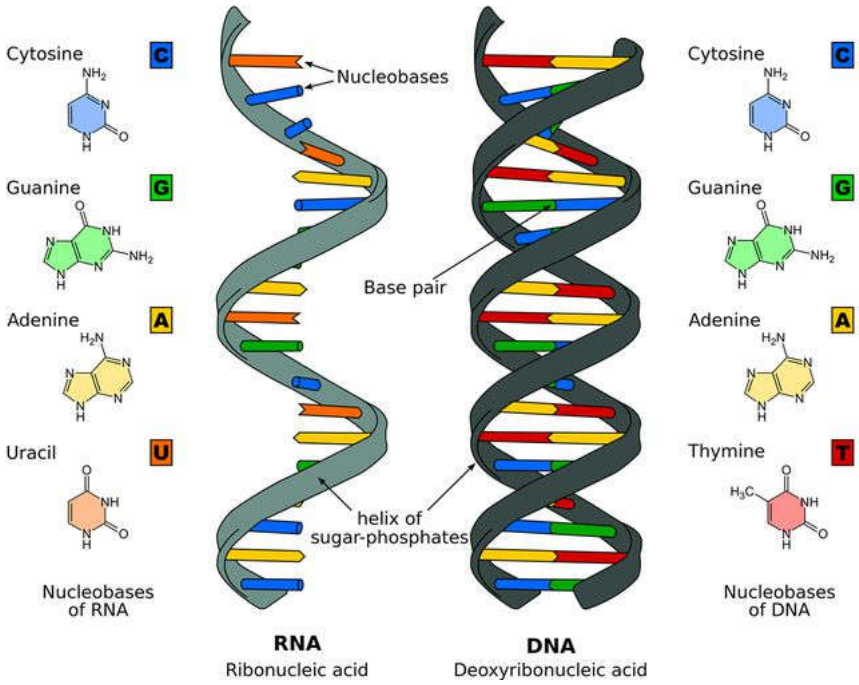

Figure 2. Deoxyribonucleic acid (DNA) double helix versus Ribonucleic acid (RNA) single helix with their bases.

Guanine solubility

Puzzling behaviour of guanine upon dissolution obscures its solubility determination. By looking at the literature, it is only certain that its solubility in neutral solutions is negligible. By adding water to guanine powder, it will be swelled and a thick paste will be formed. By its dilution only a muddy solution could be obtained. When DeVoe and Wasik [8] were studying guanine solubility, they noticed that and then decided to force water through this paste mixed with silanised diatomaceous silica particles in a liquid chromatography column at a high pressure. They could

determine the solubility of guanine at 25 °C to be 39 ± 1 μM with $\Delta_{sol}H$ equal 49.2 ± 0.6 kJ mol^{-1}. However, the pH value of the resulting saturated solution was not given. The authors realized that solubility values reported in the literature are even higher. There is another value of 45 μM (0.068 mg/L) quoted from the literature by the Handbook of Chemistry and Physics, which is relatively high [9]. Another article [10]found in the literature, in 2010, reported that the value of even 100 μM at pH 7 could be reached depending on the amount of guanine powder used for solution preparation. In this experiment, the solutions were prepared by dissolving guanine in citrate buffers at 40 °C and then equilibrated at 25 °C. The method worked faultlessly for the other nucleobases and the lowest value of 40 μM was assumed to be the most reliable for guanine solubility. Also, the authors mentioned that dissolution of guanine led to a regular change in pH.

Because of the biological importance of guanine, there is a great interest, recently increasing, in developing of new methods for guanine analysis, mainly electrochemical. It was claimed in many papers that solutions of concentrations up to 100 μM were used at pH 7, a value exceeding the above mentioned reported values of solubility. However, some other researchers tried to determine the concentration of their own saturated solutions and interestingly, each time obtained slightly different values, but generally close to 25 μM [11].

DNA damage

Deoxyribonucleic acid (DNA) is a biomolecule which contains genetic instructions. It is one of the four major types of macromolecules which is essential for our life. DNA has two strands called polynucleotides which are composed of monomer units called nucleotides. Each nucleotide is formed by covalent bonds between a DNA base, a sugar called deoxyribose and a phosphate group. DNA bases are present in two pairs of guanine with cytosine, and adenine with thymine, which are bound to each other by hydrogen bonds. The sequence of these four types of DNA bases encoded our genetic information. Therefore, any changes on DNA backbone can effect DNA replication process to form proteins.

Study of DNA bases including guanine, cytosine, adenine and thymine, has gained a growing interest in recent decades. Physical chemists, analytical chemists and biochemists have done a lot of research on DNA damage and tried to find some solutions to prevent or repair these defects. What makes this field of research important is its vital effect on health care and specially on medicine. Reactive Oxygen Species (ROS) can damage DNA easily. These harmful species can be produced from endogenous metabolic processes or exogenous sources like carcinogens and environmental pollutants and may cause oxidative DNA damage in living cells [12]. Free radicals are generated in living cells during the metabolic process and by exogenous sources, including carcinogenic compounds and ionizing radiation. It can be estimated that 1−5% of oxygen metabolized in living organisms is reduced to yield free oxygen radicals. A human, while resting, consumes about 500 L of oxygen per 24 hours and generates approximately 1 mole of free radicals. Free radicals can oxidize all biological macromolecules including DNA [13]. Many of DNA damages can be repaired by the human body. Biological systems can neutralize excessive levels of ROS and RNS (reactive nitrogen species) and compensate for oxidative stress by developing some natural defence mechanisms. These inherent protective effects can be preventive, repairing, physical or by the act of antioxidants (AOs). AOs defence can be enzymatic or nonenzymatic.

Superoxide dismutases, catalases, glutathione peroxidases, and thioredoxin act as our enzymatic system. Other than some nonenzymatic small molecules such as glutathione, bilirubin, estrogenic sex hormones, uric acid, ascorbic acid, coenzyme Q, melanin, melatonin, α-tocopherol, and lipoic acid are present in the human organism [14]. But if these damages do not be cured in time then they will cause mutations or tumour cells.

One of the most common DNA damage found properly in the tumour cells is telomeric DNA damage. Telomers are present at the end of chromosomes and they are essential for chromosome stability and genomic totality. A special lariat-like structure called T-loop protects the telomere terminus, which forms by strand invasion of 3' single-stranded DNA into the duplex portion of the telomere and then stabilized by shelterin, a six-subunit protein complex. Telomeric dysfunction is the result of uncapping of the telomere which is characterized by end-to-end fusion and anaphase bridges, and triggers DNA damage responses which lead to either senescence or apoptosis. This telomere maintenance plays an important role in tumorigenesis and is decisive for the unlimited proliferative potential of cancer cells. Thus, inhibition of telomere maintenance is considered a popular strategy in anticancer therapy. In the cells, G-quadruplex structure is formed by folding of the 3'-terminal single-stranded DNA (TTAGGG repeats) which can be detected by G-quadruplex antibodies. There are many studies which prove that telomeric G-quadruplex ligands might perturb telomere replication and cause telomere uncapping. The stabilization of telomeric G-quadruplexes by these ligands can change the T-loop structure, which leads to its degradation through a DNA damage response pathway by releasing some shelterin proteins from the telomeres. This process finally leads to cell cycle arrest, senescence, or apoptosis. Researching in the field of telomeric G-quadruplex ligands as potential anticancer chemotherapy agents has become very attractive recently [15].

DNA damage can lead to many harmful diseases like epilepsy, Acquired Immune Deficiency Syndrome (AIDS), atherosclerosis, chronic hepatitis, cardiovascular diseases, mental retardation, age-related disorders and many kinds of cancer. These diseases are the result of mutations which start with mispairing of 8-oxoguanine with thymine instead of cytosine. It is known that the neurodegenerative disorders are related to the accumulation of 8-oxoguanine in mitochondrial DNA of the brain cells. Most of these defects are due to one electron reduction of dioxygen, , and the release of its uncontrolled product, superoxide anion:

$$O_2 + e^- \rightarrow O_2^{\bullet -} \quad (1)$$

This may happen during the mitochondrial respiratory chain by leaking electrons from complex III in immune cells where NADH is producing superoxide to fight pathogens.

Superoxide anion radical can be protonated in the aqueous environment rapidly to produce hydroperoxide radical, $HO^{\bullet}_2$,which may undergo further reduction yielding hydrogen peroxide H_2O_2.

$$O_2^{\bullet -} + H^+ \rightarrow {\bullet}O_2H \quad (2)$$
$${\bullet}O_2H + e^- \rightarrow HO_2^- \quad (3)$$
$$HO_2^- + H^+ \rightarrow H_2O_2 \quad (4)$$

$2O_2^{\bullet-} + 2H^+ \rightarrow O_2 + H_2O_2$ (5)

$M^{n+} + H_2O_2 \rightarrow M^{(n+1)+} + HO\bullet + OH^-$ (6)

$M^{n+} + H_2O_2 \rightarrow M^{(n-1)+} + HOO\bullet + H^+$ (7)

As we know, there are no 100%-effective treatments for any of these diseases generated as a consequence of the ROS reacting with guanine. For example, cancer kills millions of people in the world every year. Some methods, like chemotherapy and phototherapy have been used to treat cancer cases. However, the results have shown that these methods are not efficient enough.

In biology and medicine, cancer is a very important field of study. In my research, I thought what should be very important at first, it is to decrease the probability of getting cancer. Now, the question is which compounds can help us to protect our body against cancer? And which methodology should be used for this kind of measurement to reach really reliable and helpful results?

By searching the scientific literature in this area one finds a lot of scientific results on the evaluation of antioxidative activity for many years until now. There are some assays reporting the use of Uv-Vis Spectroscopy, which is mainly employed in food chemistry. Electrochemical methods, specially voltammetric measurements, can help us to study redox reactions on the molecular scale. I found them easy to operate, available, yielding fast response and inexpensive that make real time, analysis able to reveal conditions under which the DNA can be damaged.

The oxidation of the purine bases (guanine and adenine) occurs at much lower positive potentials than that of those of the pyrimidine bases (cytosine and thymine), which require very high positive potentials, and consequently their oxidation peaks are more difficult to detect [16]. Among the DNA bases, guanine has the lowest oxidation potential and ionization energy. Therefore, it is the most sensitive base that is oxidized easier than the other DNA bases. And it has become the most interesting DNA base to be studied in the electrochemical investigations preliminarily.

There are many types of ROS, like superoxide anion ($\bullet O_2^-$), singlet oxygen ($^1O_2$), hydrogen peroxide (H_2O_2), nitric oxide (NO), peroxynitrite ($ONOO^-$), hypochlorous acid (HOCl), peroxyl radical, including both alkylperoxyl and hydroperoxyl radicals (wherein R = H) (ROO•), etc., which can oxidize guanine. Among them, peroxide radical produced by the reaction of superoxide with hydrogen cations in aqueous solution is interesting for me to study it in my work.

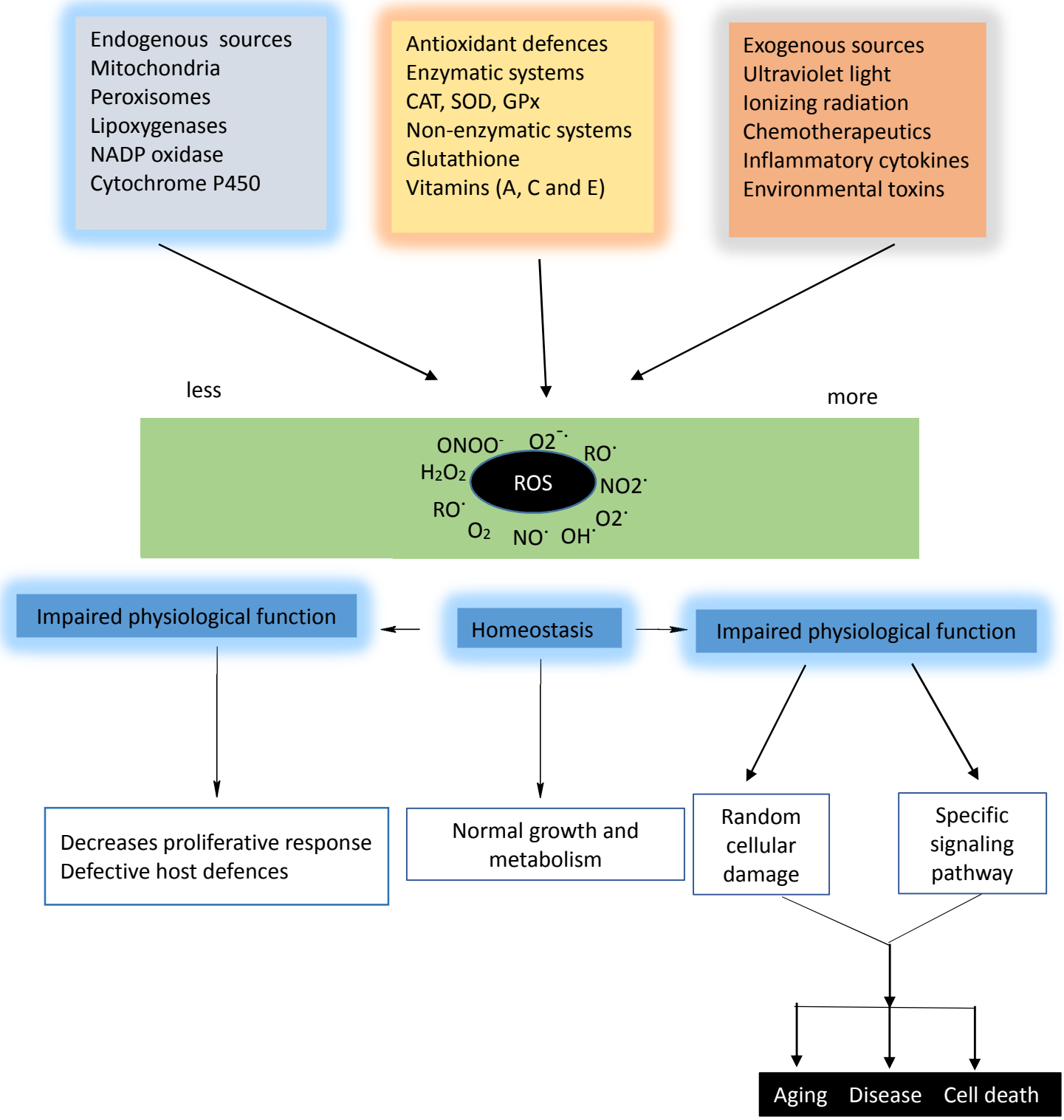

Scheme 1. Sources of ROS, antioxidant defences, and subsequent biological effects depending on the level of ROS production.

ROS production in our body

As it can be seen in scheme 2 superoxide ($O_2^{\bullet -}$) is generated in our body cells by transferring $1e^-$ to O_2 which is possible through the electron transport chain (ETC), or by NADPH oxidase (NOX) enzyme. Superoxide species by dismutation will be transformed to hydrogen peroxide (H_2O_2) and water, the reaction catalysed by a family of enzymes called superoxide dismutases (SOD). Hydroxyl radical (OH•), which is one of the most reactive ROS, is formed through a metal (Fe(II) or Cu (I)) mediation to reduce H_2O_2 by Fenton reaction. Hydroxyl radical reacts with DNA and in this way it causes irreversible damages leading to DNA mutation. The targets of these uncontrolled damages in DNA are sugar backbone and nucleobases. In some of these DNA degradations C-4' tertiary radical in ribose is generated. Guanine is the main target of oxidation by OH• to generate 8-oxoguanine. Thymine is another nucleobase which is oxidized by hydroxyl radical forming thymine radical species which leads to mutation also. Proteins mainly containing amino acids including methionine are attacked by hydroxyl radical to be oxidized to their corresponding sulfoxides (see scheme 2). Those proteins containing amino acids including carboxylic acid groups such as lysine, arginine, proline and histidine will oxidise with OH• . For instance the oxidation product of histidine residues in proteins is 2-oxo-histidine.

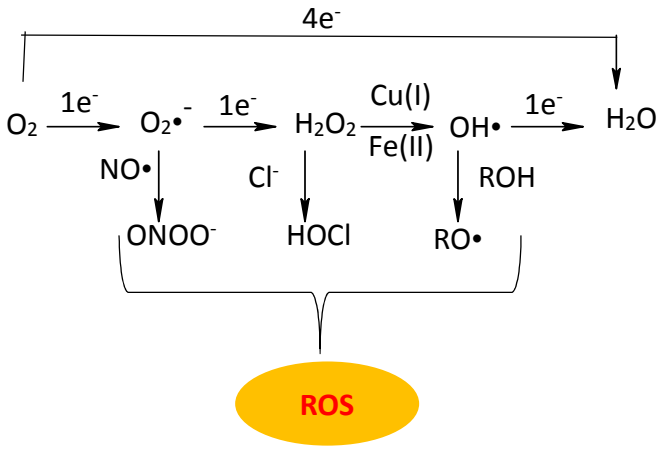

Scheme 2. General Scheme for ROS Production.

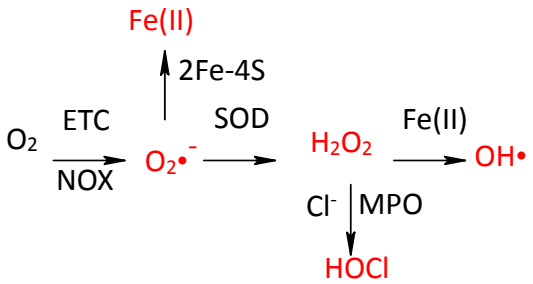

Scheme 3. ROS Generation Induced by Cellular Enzymes.

The enzyme called myeloperoxidase (MPO) catalyses the generation of hypochlorous acid (HOCl) (see scheme 3). This species, HOCl, is able to oxidise some biomolecules such as cysteine residues to cysteine sulfenic acid and tyrosine residues to dityrosines in proteins. As it can be evidenced by the oxidation of glutathione, HOCl is much more active (3×10^7 $M^{-1}s^{-1}$) than H_2O_2 90.9 $M^{-1}s^{-1}$). Other harmful radicals like hydroperoxyl or organoperoxy, which are responsible for the lipids oxidation in our body, can be produced from hydroxyl radicals.

When ROS cause an immune response to combat pathogens, the immune cells will detect the damaging capacity. Except for damaging effects, ROS are known as a key factor in many cellular signalling such as cell proliferation and survival which are necessary to balance ROS production and redox homeostasis maintenance. Therefore, to reduce the oxidative stress to biomolecules and to adjust redox homeostasis, our body has evolved an antioxidant system, like antioxidant thiols and enzymes. For instance, the enzyme superoxide dismutase (SOD) is responsible for quenching the oxidative stress from superoxide radicals by converting O_2• to H_2O_2 and H_2O. Then, another enzyme, catalase, will transform H_2O_2 to water. Determining the safe level of ROS in the biological systems is still challenging due to the mixed effect of ROS in the cells protective in pathogenic conditions and harmful effects to the host cellular components at higher levels. The optimal level of ROS in the cells remains a mystery and a large number of investigations based on chemical biology and medicinal chemistry are underway to discover ROS therapeutic strategies.

ROS paradox in cancer

Mitochondrial genetic mutations may lead also to the cellular ROS increase. Following the mitochondrial mutagenesis in DNA, the electron transport sequence in ETC may be trafficked. Consequently, electrons will accumulate in the mitochondrial membrane and react with molecular oxygen to produce O_2•$^-$, from which H_2O_2 can be generated by dismutation of O_2•$^-$ by SOD. Hydrogen peroxide may diffuse and enter the nucleus, and further damage the DNA inducing genetic mutation. These total genomic instabilities enhance the ROS levels and oxidative stress, trigger cancer metastasis and progression. However, because of the cell proliferation requirements, cancer cells are able to adapt to significantly increased levels of intracellular ROS, which reach almost the toxic level limit. Glutathione and other antioxidant enzyme in the cell are responsible for balancing the overproduction of ROS in the cell. Thioredoxin reductase-1 (TR-1) is one of the antioxidant selenoproteins which will be activated by oxidative stress to prepare the reducing environment in cells. Overexpression of TR-1 and the inhibition effect of TR-1 function in many virulent tumours were recognized and can repeal cancer progression. Applying antioxidants to treat cancer is generally considered a correct strategy, since ROS are assumed to promote cancer. However, there are clinical reports that treatment of cancer with antioxidants, such as N-acetylcysteine, ebselen, edaravone, vitamin A, vitamin C, vitamin E and β-carotene failed to inhibit cancer development in long treatment regimes. Hence, ROS-mediated mutations could develop cancer and, paradoxically, promote intracellular levels of ROS close to the toxic limit for cancer cells, suggesting an opportunity to develop ROS based therapeutics for cancer treatment.

ROS-based therapeutics in cancer

Growth and proliferation of cancer cells increase in conditions of a modest rise in intracellular ROS; on the other hand, apoptosis can be induced at higher levels of ROS. Notwithstanding, maintaining high levels of intracellular ROS, cancer cells are more sensitive to increased intracellular ROS than non-transformed cells. Therefore, using ROS as small molecules targeting cancer cells can be considered as a potential strategy. Piperlongumine, (see Fig. 3) is an alkaloid natural product extracted from a pepper plant.

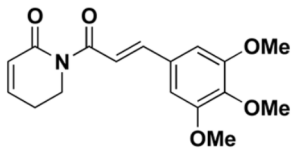

Figure 3. Piperlongumine structure. [17]

This compound is known as one of the effective anticancer agents which kills cancer cells selectively by promoting ROS levels through inhibition of the cellular machinery responsible for quenching ROS and oxidative stress in cells. Cancer selective cytotoxicity induced by this compound is clearly identified in both vitro and vivo models. Proteins responsible for tuning oxidative stress in cells, such as glutathione-S-transferase pi 1 (GSTP1) AND carbonyl reductase 1 (CBR1), were known as binding targets of piperlongumine using as impartial target recognition approach, i.e., stable isotope labelled amino acids in cell culture (SILAC) and quantitative proteomics. Moreover, investigations on cancer cells with built-up mutations of proteins responsible for removing oxidative stress (such as GSTP1 and CBR1) demonstrated sensitivity to piperlongumine, and a reverse sensitivity was observed by co-treatment with antioxidants, therefore exhibiting the involvement of redox modulation in cells by piperlongumine for its action. It was reported about the structure-activity relationships of this compound that had demonstrated a dual activity in cells including ROS generation and a diminution of small molecule cellular antioxidant thiol, GSH. Some of piperlongumine derivatives were found to improperly form ROS better than this substance; however they did not have cytotoxic effect sufficiently to induce death to cancer cells in a comparable concentration with piperlongumine.

Another molecule, Pl-Fph (see Fig. 4), was characterized as highly toxic to cancer cells; however this compound did not increase intracellular ROS in HeLa and H1703 cells. An ROS-independent, irreversible glutathionylation was determined as a mechanism of action for the cytotoxicity of piperlongumine-like molecules. Therefore, a mechanism of antioxidant GSH evaluation and intracellular ROS induction was suggested for the cytotoxic effects of piperlongumine and its action in cancer cells.

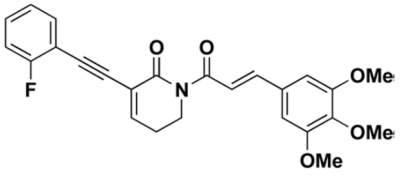

Figure 4. Pl-Fph structure [17]

Quinones are one of the main sources of ROS in the biological cells and it is known that they are responsible for bioreduction in cells. Consecutive reactions of molecular oxygen will produce ROS. Some of the anticancer agents based on well-known quinones, cooperated with ROS-mediated cell-killing by applying another mechanism of action, are mitomycin C (DNA alkylation), geldanamycin (heat shock protein 90 (HS P90), streptonigrin (topoisomerase inhibitor) and mitoxantrone (topoisomerase inhibitor) (Fig. 5). Deoxynyboquinone (DNQ) is a powerful quinone based anticancer agent and a natural abduction of SCH 538415. There is an early report of the mechanism of cytochrome C, which is determined for DNQ to induce apoptosis in cancer cells. Later, another research group developed a synthetic method for this compound and investigated the compound's ability to promote intracellular ROS in cancer cells that participated in cell killing. This compound has been found to have a high potential at nanomolar concentrations against a segment of cancer cell lines including human melanoma cancer (SK-MEL-5), breast cancer (MCF-7), leukaemia (HL-60) and doxorubicin-resistant leukaemia (HL-60/ARD). Experiments carried out under hypoxic conditions showed a decreased effect of DNQ, which proved the importance of oxygen for its action. Moreover, some evidence indicated an ROS based mechanism of DNQ compound for global transcription profiling U-937 cells treated with this substance. Haem oxygenase-1 (HO-1) is one of the antioxidant proteins in the Nrf2 (E2-related nuclear factor 2) pathway that will be activated by the oxidative stress in the cells. It has the highest grade of transcript characterized by the experiments, and heat shock protein-70 (HSO-70) and metallothioneins are other main proteins in this list. Additionally, more Western blotting analysis of the cell treated by various concentrations of DNQ exhibited a concentration dependent improvement of HO-1 and HSP-70 levels. NADP9H quinone oxidoreductase 1 (NQO1) is a 2-electron reductase which is overexpressed in many solid tumours for the detoxification of quinones and reducible xenobiotics, like nitroaromatics and azo dyes. Cancer cells, such as breast cancer, colon cancer, non-small cell lung carcinoma, pancreatic cancer and ovarian cancer are determined by overexpressed NQO1 levels.

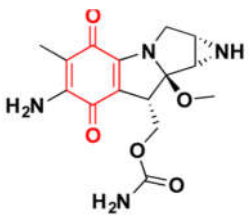

Mitomycin C

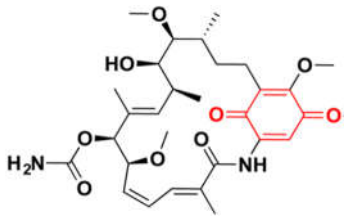

Geldanamycin

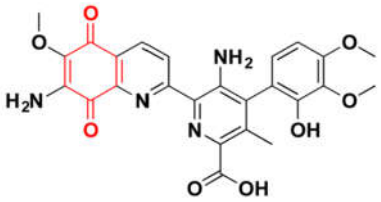

Streptonigirin

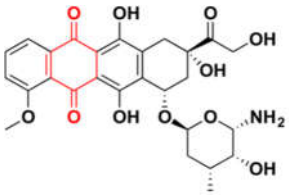

Doxorubicin

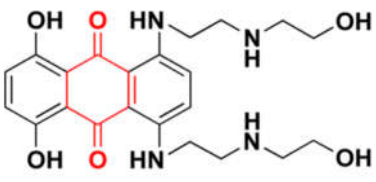

Mitoxantrone

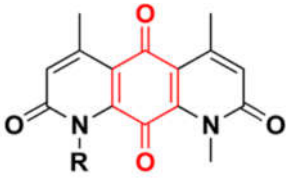

R=H; Deoxynyboquinone
R=CH_3; SCH 538415

Figure 5. Quinone based anticancer agents

Redox homeostasis regulated by enzymes in cells

ROS has an oxidative damaging effect to biomacromolecules like DNA, proteins and lipids. Nonspecific rapid reactions lead to this effect Therefore, ROS are considered harmful species. They lead to overexpression of cellular antioxidant enzymes such as superoxide dismutase and catalase. Until 1990s, the only known ROS generator in phagocytic conditions was the NADPH oxidase. At that time, it was even realized that this biomolecule can be activated in response to growth factors, cytokines and inflammation. Later, some biologically important enzymes were characterized, which could produce ROS as their primary functions. A series including seven enzymes from NADPH oxidase family was characterized as the generators of ROS not only in phagocytes but also elsewhere. Cytosolic NADPH is applied as an electron source, while the electrons are transferred to molecular oxygen upon NADPH oxidase catalysed ROS production. Ligand-receptor interaction with NOX, which mediates ROS formation, includes plate derived growth factors, chemokines and tumour dead states. During the respiration process, molecular oxygen is the last electron acceptor in the ETC, where it will be reduced to water; however due to the escape of electrons in the ETC, partial reduction of O_2 (1-4%) occurs to generate $O_2^{\bullet -}$ and H_2O_2. The other factors which are responsible for the production of mitochondrial ROS are mammalian targets of rapamycin (mTOR), p53 and B-cell lymphoma 2 (BCL-2) family members. Xanthine oxidase (XO), which is a metalloflavoprotein constitutively expressed in cells converts hypothantine and xanthine to urate, while O_2 is reduced into $O_2^{\bullet -}$ during this process. Cytochrome P450 (CYP) enzymes which have an iron-containing haem centre are responsible for oxygen dependent metabolism of cholesterol, steroids and small molecules. The oxygen bound iron haem centre in the CYP molecule is characterized as the source of $O_2^{\bullet -}$ and H_2O_2 generation. ROS are also produced by the metabolism of arachidonic acid with lipoxygenase and cyclooxygenase in different cells (see Scheme 4). Altogether, intracellular ROS are formed by specific enzymes in different parts of cells in a strongly controlled manner for cellular function.

In contrast to a group of identified enzymes that produce intracellular ROS, the only characterized antioxidant systems in the cell for balancing the level of ROS to maintain redox homeostasis, are superoxide dismutase and catalase enzymes. Glutathione (GSH), cysteine (Cys), vitamin C (ascorbic acid) and vitamin E (α-tocopherol) are other non-enzymatic antioxidant molecules that relieve the excess amount of ROS in the cell. Moreover, glutathione peroxidase (GPx), thioredoxin reductase and peroxiredoxin are some of other enzymatic antioxidants which handle ROS levels in cells. GSH is a low molecular thiol and a main antioxidant existing in the cell. This substance uses GPx in wiping out lipid peroxidation and is oxidized to disulfide (GSSG), which can be reduced back to GSH by another enzyme called glutaredoxin, to restitute GSH levels in the cell. Disulfide bonds are formed by oxidation of thiols in proteins, peptides and glutathione by reaction of ROS. The reduced forms are intensively stabilized through the reduction of disulfide bonds by thioredoxin reductase systems using NADPH as a cofactor (see Scheme 4). By timely activation of these precise antioxidant systems, cells are able to efficiently regulate ROS levels and retain redox homeostasis [17].

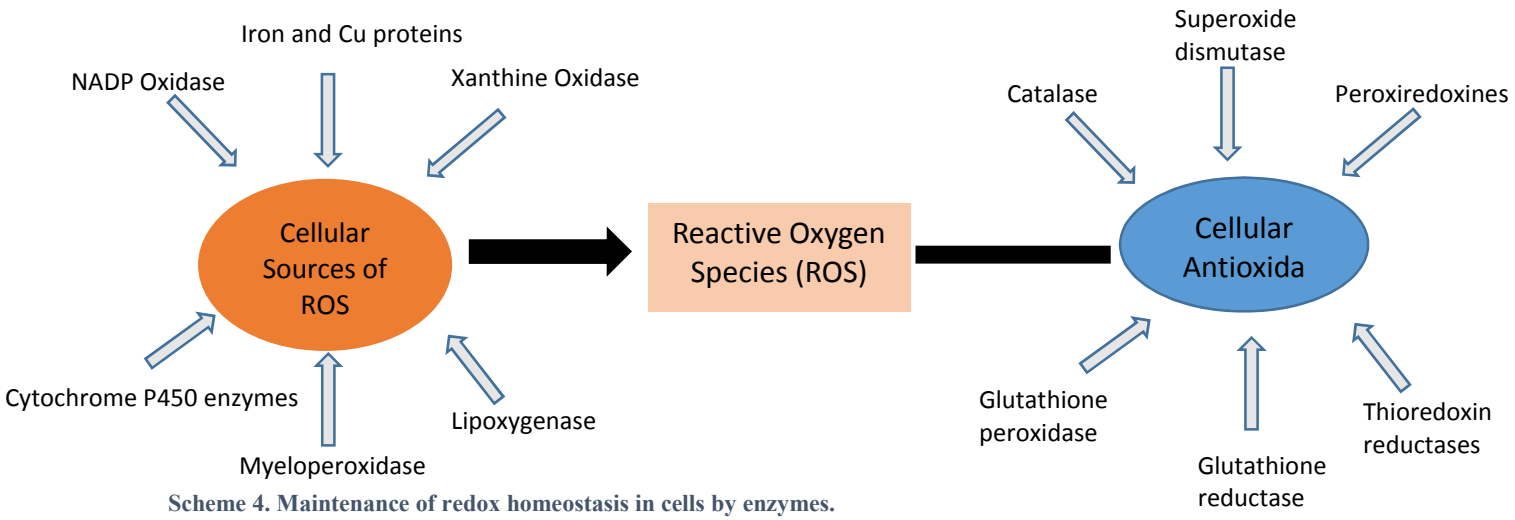

Scheme 4. Maintenance of redox homeostasis in cells by enzymes.

Guanine oxidation

Guanine oxidation is followed by the generation of a lot of intermediates, lesions and products. Currently, more than 50 oxidative DNA lesions have been characterized. The 7,8-dihydro-8-oxo-2-deoxyguanine (8-oxoGuanine) lesion has been studied extensively because it is the most prevalent compound formed upon DNA oxidation [18].The type of every lesion depends on the type of oxidant. The main product of oxidation of guanine with superoxide (or hydroperoxide radical in aqueous solutions) is 8-oxoguanine. It is proven that this compound is really harmful and it is the starting point of mutations in the DNA replication process. 8-Oxoguanine is the product of $2e^-/2H^+$ oxidation of guanine. Electrochemical detection of 8-oxoguanine is rather difficult because this compound gets oxidized at the potential ca. 0.3 V less anodic than guanine. By further oxidation of 8-oxoguanine some other products such as spiroiminodihydantoin and guanidinohydantoin can be also formed [19]. An 8-oxoguanine lesion, spiroiminodihydantoin is not plane but has a propeller-like shape whereas its two rings are connected at closely 90° angle to the central chiral carbon. Both R and S diastereomers can be exist in DNA and both of them can destabilize DNA thermodynamically. According to the prediction of molecular dynamics simulations no of these two forms of diastereomers can intercalate into DNA helix normally. However, formation of this lesion may lead to a mutation in DNA due to the fact that this compound forms a strong block to DNA polymerization that can be bypassed in *vitro* and *vivo* and insert guanine or adenine on the opposite strand instead of the desired cytosine [20].

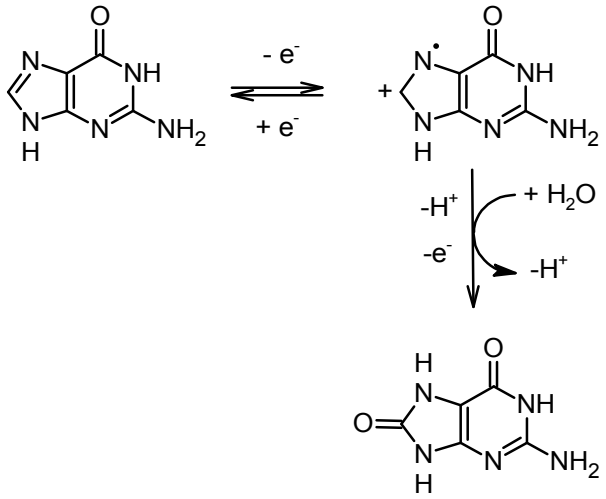

Scheme 5. Oxidation of guanine to 8-oxoguanine.

Moreover, both guanine and 8-oxoguanine undergo the $2e^{-}/2H^{+}$ oxidation processes, which means that the potential will shift by 59 mV per pH unit cathodically with increasing alkalinity, however the difference will stay constant (up to pH 11 [21]). Generation of 8-oxoguanine requires some time because it is the product of consecutive processes. The oxidation peak related to 8-oxoguanine can be observed in the subsequent forward scan only when the scan rate is sufficiently high and the potential scan is reversed at a correct moment [22]. Sometimes it accumulates on the surface of the electrode and it can be observed only after a couple of scans [23].

According to the literature, the number of the electrons involved in the oxidation process of guanine can be calculated by using the Laviron equations which relates oxidation peak height, scan rate and peak area. It has been reported that with a series of scan rates from 0.2 to 1 V/s (on the Au electrode) the process involves $2e^{-}$ both for dsDNA and ssDNA, and a decreasing scan rate leads to $4e^{-}$ oxidation of DNA. Based on these results, we can assume that at the high scan rate an incomplete $2e^{-}$ oxidation process occurs, possibly accompanied by the generation of 8-oxoguanosine (in the same way as for 8-oxoguanine). This oxidation process will be completed at the low scan rate by transferring $4e^{-}$. Interestingly, by applying consecutive scans (8-9 times) in the positive potential area and at the high scan rate, a new peak at +100 mV will appear, which is supposed to be related to the formation of an intermediate product. It is emphasized in this report that this peak never was observed at low scan rates. Similar results were achieved in my experimental measurements (see results and discussions part 2) [24].

It has been proven that in vivo pairing of oxidatively modified guanine (8-OxoG) during DNA replication leads to a transversion of 8-OxoG to thymine and to the formation of oxidation products of other nitrogenous bases. The latter lead to either the transition of Guanine to Adenine or Cytosine to Thymine. Too many transitions and/or transversions in DNA chain lead to the conformational changes of the double stranded DNA [25].

Studying biological systems in vivo or vitro in my work was beyond the available lab facilities. Therefore, I preferred to investigate the redox properties of DNA bases separately.

Antioxidants effect

Antioxidants (AOs) are small molecules able to protect a biological target from oxidation and acting against the adverse effects of reactive oxygen species on physiological functions. Many serious diseases, such as cardiovascular diseases, inflammatory disorders, cancer, Parkinson's disease, diabetes mellitus, and stroke are related to an imbalance between formation of oxidants and the antioxidant system [26]. Therefore, in order to control the oxidative stress in biological systems, it is necessary to include AOs in the daily diets.

Now, the question is what is an antioxidant? Generally, it is not that simple to define the term of antioxidant due to its multifaceted nature. First, the area and protection targets are completely different. Otherwise, a suitable definition can read: the synthetic or natural substances added to products to inhibit or delay their decline caused by the action of oxygen from the air. In food industry, there is a broad use of antioxidants, which in this case mean compounds that protect fats against deterioration or dietary antioxidants that are identified as substances in foods that can diminish the harmful effects of ROS significantly. Another definition says biological antioxidants are molecules that, when present in a small concentration in comparison to the amount of biomolecules, may protect the biological systems against the oxidative stresses or at least they may reduce this risk.

However, we should emphasize that when we are talking about the antioxidants, we mean those dietary, natural or biological molecules that are consumed in our food. Therefore, food and biological samples are the target of antioxidant analytical studies.

However, these definitions for antioxidant do not involve the concept of their mechanism, i.e., how these small molecules act in biological systems to inhibit radical chain reactions, act as metal chelators, prevent oxidative enzymes work and cover antioxidant enzyme cofactors. Moreover, many terms are applied by various investigators to define antioxidant capacity, like efficiency, power or activity. Antioxidant activity measured in any single assay and under specific conditions applied in that assay can reflect only the chemical reactivity in that individual assay, while antioxidant capacity, efficiency or power have similar chemical meaning and they are independent of every specific reaction [27].

AOs react with ROS competitively to reduce these harmful compounds and in this way reduce the probability of those species to oxidise guanine, thus protecting DNA from damage. But is it always so? There are reports in the literature that just the opposite effect may occur. Under some conditions, substances regarded as efficient AOs may act as pro-oxidants. In fact, the addition of AOs promotes the competition with DNA for ROS. For example, pyrogallol is employed in some antioxidant activity evaluation methods as a source of superoxide anion [28]. Another well-known AO, vitamin C, which was recently shown to produce very active hydroxyl radicals [29]. The chemistry of ascorbic acid is very complicated and it appears that at least in alkaline solutions, it can exhibit both oxidative and nonoxidative degradation. However, recently it was demonstrated that at conditions close to physiological pH, ascorbic acid reacts with hydrogen peroxide. To be able to understand the dual behaviour of this compound as an antioxidant or prooxidant, it is crucial that the destiny of ascorbic acid and the product of its reaction with oxygen, it means hydrogen peroxide, is considered. Square wave voltammetry (SWV) presents a suitable analytical technique

to analyse both ascorbic acid and hydrogen peroxide [30]. Even resveratrol may display a complex role by causing massive oxidative stress in mitochondria and, on the other hand, after reduction, by leaking electrons it may also show a strong antioxidant activity [31].The pro-oxidant activity can be seen in the presence of various catalytically active metal ions, too [32]. However, this effect was mostly seen in vitro experiments and in vivo studies revealed different effects. Interestingly, these compounds showed increase in the concentration of ROS to cytotoxic levels mostly in the tumour cells and not in the healthy ones. It means that this effect can be used for the therapeutic purposes. Some macromolecular phenolic substances, such as lignin or melanin, display pro-oxidative activity, also which may be beneficial and is utilized in insect and plant defence system as part of their immune response [33]. Such natural phenolic compounds can be used as antioxidants or prooxidants and, when it is necessary, they may even exhibit UV-protective functions [34].

Antioxidants evaluation methods

In recent years, the degree of AO inhibitory effect against the oxidation of guanine by ROS has been applied for the assessment of AO activity [35]. Antioxidant content of foods became a highly desirable parameter, therefore the need arose for adopting a standardised total antioxidant parameter for application as a nutritional index for food and biological fluids [36]. In my research the change in the peak current related to 8-oxoguanine was measured versus the AO concentration to evaluate the AO capacity.

AOs protect the biological systems against ROS in two competitive mechanisms: one is based on Hydrogen Atom Transfer (HAT) and another by Electron Transfer (ET). For example, radical trapping, like oxygen radical absorbance, is a typical HAT mechanism and trolox equivalent AOs capacity assay is based on the ET mechanism.

Now, why to use electrochemical approaches to evaluate antioxidants activity? Here is a series of keys to understand the relevant role of electrochemical techniques in the evaluation of antioxidant capacity.

i) All natural dietary antioxidants, like vitamin C, exhibit native electroactivity.
ii) Electrochemical methods can evaluate the antioxidant capacity of the compounds present in food and biological samples, without using reactive species, it means by a direct test of total antioxidant capacity based on chemical and physical properties of the antioxidant compound.
iii) The extent of charge based on electron transfer during redox reactions towards a suitable electrode material can be a measure of the antioxidant capacity of natural extracts.
iv) In some controlled-potential techniques, oxidation potential is correlated with the antioxidant capacity. Actually, low oxidation potentials found in food or biological samples determine their high antioxidant capacity. Also, amperometric current and charge measured under certain conditions can inform us about the extension of their capacity. On the other hand, oxidation potential permits selectivity control to find the best

conditions for antioxidant capacity measurements. This approach is really unique in comparison with those offered by spectroscopic methods.

v) Beside the inherent advantages of the electrochemical methods including their sensitivity and selectivity, they are suitable and inexpensive for direct measurements, particularly taking account of the complexity of food and biological samples complexity and the difficulties to separate each antioxidant to study each of them individually.

vi) Electrochemical responses are independent of the optical path length and sample opacity. Additionally, this approach has relatively small instrumental requirements [23].

The evaluation of antioxidant properties is not an easy issue. Numerous methods can be used to determine this activity, and several factors can affect the estimated value, such as conditions and analytical methods. Many assays have been directed to the development of methods that can characterize antioxidants capable of removing harmful radicals in living organisms in an sufficient way. Recently this method has been used for cancer-testing. This progress in application of these methods can be attributed to indigenous characteristics, such as rapid and real time analysis, that increase the assay speed and flexibility as well as the possibility of automatic and multi-target analyses at low cost [37].

The reactivities of various phenols and polyphenols versus superoxide ion ($O_2^{\bullet -}$) were investigated to make an easy electrochemical method for plants and have a chemical evaluating antioxidant capacities. Polyphenols are chemical compounds containing phenolic units. They are substances that, when present at a low concentration, decrease or prevent the oxidation of other molecules. They are found in a number of food products such as fruits, vegetables, beverages or in cereals, nutraceuticals, and medications. They are commonly used as additives for preventing oxidation processes in food. Consuming the food containing these molecules is receiving great interest from the consumers and even by pharmaceutical manufacturers because epidemiologic studies have suggested beneficial effects of preventing or decreasing the risk of getting various pathologies such as cancer, cardiovascular, and neurodegenerative diseases. Many protective actions have been ascribed to the antioxidative activities of polyphenols, notably linked to their power of scavenging free radicals (radical chain breaking) and the protection against ROS.

A lot of researches were devoted to the chemical and physicochemical properties of polyphenols and of their radicals with respect to their activity. Numerous studies have reported the oxidation potentials, p*K*a values, and spectral properties, as well as the reactivities of polyphenol radicals and the generation of secondary oxidised products. However, there are still controversies about how to interpret these data, for example, with respect to apparent oxidation potentials or even the structure of the produced phenoxyl radicals. Therewith, in addition to the fact that phenolic compounds are acids, able to rapidly exchange H^+, they are often determined as efficient H-atom donors or as compounds involved in coupled proton-electron transfer (CPET), resulting in a manifold of possible mechanistic pathways.

Polyphenols are a group of natural antioxidants that inhibit many diseases by reducing oxidative stress. They exhibit a complex antioxidative and prooxidative behaviour, especially in the presence of metal ions. The prooxidant activity of these compounds is based on the formation

of phenoxyl radical, which reacts with oxygen to generate O_2•, H_2O_2, semiquinones and quinones. It is assumed that the prooxidant activity of phenolic compounds may lead to lipid peroxidation, DNA damage and cell death. Notably, many prooxidant compounds can increase the cytotoxic level of ROS in cancer cells more than normal cells because of a higher concentration of copper ions in cancer cells that leads to greater metabolic activity. Therefore, the prooxidant activity of some antioxidants like polyphenols is not always harmful for biological systems and even it can be used for therapeutic treatment of cancer cells. Phenolics are a group of natural antioxidants that exist in the form of glycosides in plants. Consuming vegetables and fruits, which contain these compounds, has health benefits. The regular consumption of these compounds can decrease the risk of chronic illnesses such as neurodegenerative, cardiovascular and coronary heart diseases and cancer.

Polyphenols are a group of aromatic compounds that have received a great attention in recent decades, because of their inhibitory role against some human illnesses (which are mentioned above). They have a diversity of biological properties, such as antioxidant, metal chelation, free-radical scavenging, enzyme modulation and anticancer activities. Prooxidant properties of these compounds can be activated by a high concentration of transition metal ions, alkali pH and the presence of oxygen molecules. Otherwise, the structure of these compounds has a considerable effect on the prooxidant activity of them. For example, compounds containing ortho-dihydroxyl groups or 4-hydroxy-3-methoxy groups indicate a significant DNA damage due to their high prooxidant activity or p-coumaric acid shows the poorest prooxidant effect among hydroxycinnamic acids. Flavonoids are another group of phenolic compounds which are present in the plants. Their prooxidant activity is connected to their ability of metal-chelating, radical scavenging and reducing properties. They can prevent prooxidant enzymes, such as cyclooxygenases and lipoxygenases [28].

Moreover, the biological activity of phenolic compounds is not widely known. Generally, it is accepted that the low molecular weight phenols have a perfect effect in important biological activities. For example, they can facilitate extracellular electron transfer in the soil by forming quinones. And even they can enhance decomposition processes during enzymatic redox cycling reactions. Otherwise, the redox properties of phenolic compounds is not known perfectly as yet and it is under study. For example, lignins and melanins are known as ultraviolet protective compounds, however, their redox activities in biological functions is rarely considered [38].

Unfortunately, most of the studies on prooxidant activity of natural antioxidants have been carried out in *vitro* due to the challenge of extracting the biological matrix intact. Therefore, there is almost no knowledge about their prooxidant activity in vivo that should be explored in the future. However, it was clear for me that applying a living system in my work could make my electrochemical assay much more complicated. Therefore, I had to avoid this complexity to be able to understand the redox properties of the antioxidants tested.

However, the mechanisms, which are responsible for the AO properties of phenols are still the subject of active debates, many methods have been suggested for the estimation of antioxidant capacity, especially in terms of radical-scavenging capacity [39].

All the methods applied to evaluate antioxidant capacity are based on the principle that the antioxidants prevent the oxidative stress in a suitable substrate by preserving the main characteristics of this substrate and a proper measurement of the end-point. When the substrate gets oxidized under standard conditions, the amount of oxidation (or end-point) will be measured at a certain time point over the range, which is specific for the formation of free radical by using optical measurements. Some instances are FRAP (Ferric ion reducing antioxidant power), TEAC (Trolox equivalent antioxidant capacity), ORAC (oxygen radical absorbance capacity) and TRAP (total radical trapping antioxidant parameter) methods. These methods are characterised by a free radical generation system, molecular target, end-point and the time of resistance in the reaction medium. Therefore, the description of the results obtained from every method is not simple. Moreover, the protective effect performed by antioxidant substances at the cellular level can be achieved only by monitoring the inhibitory effect on DNA oxidative damage [40].

Studies with the use of Fenton processes and applying radical scavengers may show high accuracy, however, they include complex operations and are costly. Moreover, the other methods like using ultraviolet light, gamma (γ) or X-ray irradiation of cultured cells or animals, often used in biological laboratories were not appropriate in my work.

Modification of the electrode

Carbon-based electrodes, especially, Glassy Carbon Electrodes (GCEs) have been often used due to their high biocompatibility, low fouling effect and low residual current over a large potential range. GCE has a wide application in electrochemical assays due to its high conductivity, hardness and inertness.

Generally, it is believed that direct oxidation of guanine with respect to slow electron transfer, kinetics and high oxidation potential is very difficult, because it requires a high overpotential. Therefore, numerous researches have prepared sensitive and selective sensors to detect DNA damage at a low limit of detection. Clark is the pioneer of this technology. Afterwards, this concept was further developed by other researchers.

Electrode surface modification is a very important in modern electrochemistry because a modified electrode can significantly extend the application ranges. Generally, chemical modification of an electrode is based on the deposition of a thin film onto the surface of the electrode. Recently, chemical modification of glassy carbon electrode has received a great attention due to its potential for analytical purposes and ease of preparation. Coating the surface of the electrode by generation of conducting polymers can lead to unique physical and chemical properties [41].

There have been a big number of attempts to enhance the electrode kinetics using various electroactive compounds. To date, several kinds of materials, such as transition metals, transition metal complexes, ionic liquids, fullerenes, redox polymers, graphene and carbon nanotubes have been explored for their potential utility in the detection of guanine. However, such systems may led to a decrease in overpotential of guanine oxidation, increase in the stability of the electrode, and improvement in sensitivity, some of them required complex electrode preparation process,

exhibited a short linear range, high background current and fouling of the modified material. Therefore, it is still a challenge to discover a novel and stable electrode modifying material with high sensitivity and selectivity [42]. Series of reports demonstrate that there is a direct correlation between the oxidation current and the degree of DNA damage. There have been considerable efforts to prepare a very accurate and reliable method that would enable the quantification of a very small amount (at least in nanomolar scale) of the major product of guanine oxidation, it means 8-oxoguanine in biological fluids like blood or urine. Particularly, making sensors able to yield information associated with the degree of disease development or status of disorders has received a great interest in the electrochemical research area and even in clinical applications. Many biochemical compounds, like enzymes, have also been used. Clearly, the advantage of application of enzymes is their perfect biocompatibility and selectivity. However, many good results can be obtained with the use of metals (like Pb, Cd, Ni, etc) to modify the surface of the electrode. The obvious advantage of using metals is increasing the electro-conductivity, but unfortunately, most of these metals are very toxic. Graphene, a two dimensional material, is another compound that has attracted considerable attentions from both the experimental and theoretical scientific communities in recent years, because of some unique properties like its extremely high thermal conductivity, good mechanical strength, high mobility of charge carriers, high specific surface area, quantum Hall effect and outstanding electric conductivity [23]. Nevertheless, immobilized DNA has been successfully used for a screening method to detect DNA damage in many studies.

Investigation of surface modified electrode needs studies of the electrochemistry of the attached molecules, to develop specific applications in such widely varying areas as analytical determinations. One of the methods used for the modification of electrode surfaces is electropolymerisation. By applying electropolymerisation, it is possible to accelerate transmission of electrons onto the surface of the electrode, which is highly selective and sensitive due to the film homogeneity in electrochemical deposition, and strong adherence to the electrode surface, and large surface area [43].

Polymers used to modify the electrode

Polymers are a noticeable group of compounds which have been applied on the electrode surface to enhance the voltammetric response. Polymers have also good stability and reproducibility, which makes them useful to detect biological substances. Among the large group of polymeric compounds, the natural polymers, which can be obtained by polymerisation of natural substances, have received a great interest. One of these natural polymers is melanin. Melanin is a big group of natural pigments including eumelanin, pheomelanin, neuromelanin, allomelanin, and pyomelanin. The real structure of melanins remained undefined during the last 50 years. However, we can define melanin simply as "heterogeneous polymer derived by the oxidation of phenols and subsequent polymerisation of intermediate phenols and their resulting quinones"[44]. Otherwise, there are many scientific data determining the role of melanin in the protection of our body against the ultraviolet radiation of the sun. The protective activity of melanin is due to its large π conjugated system. The electron generated by radiation will lose energy gradually by passing through the π electron system of melanin. When its energy is sufficiently low, it can be trapped by a stable free radical present in the pigment. This effect

prevents the occurrence of secondary ionization and the formation of damaging free radical species [45]. On the other hand, there is a controversial concept of the melanin role in human body providing evidences for dual role of melanin as both protector and the damaging agent. However, the mechanism of phototoxicity of melanin is not known.

Polyaniline (PANI) can be deposited on the surface of GCE electrochemically. In this way, a highly porous and stable for a long time (as long as it is not damaged mechanically) coating layer can be obtained. However, there are some aspects about PANI, such as relatively small specific surface area and especially its poor electroconductivity in non-acidic solutions, which make it unfavourable for the construction of an efficient electrochemical sensor.

A layer of electropolymerised pyridine-2,6-dicarboxylic acid on a glassy carbon electrode proved useful in simultaneous determination of guanine and adenine. The intensity of the peak current increased by about 50 percent, when also graphene was used. Interestingly, pyridine-2,6-dicarboxylic acid (dipicolinic acid) is used by some bacteria to increase their resistance against heat denaturation and protect their DNA. On the other hand, nicotinamide adenine dinucleotide (NAD), which is found as a coenzyme in the living cells is a chemical compound that involves redox reactions in metabolism. This coenzyme exists in two forms in the living cells: NAD^+ which is an oxidizing agent to accept electron from the molecules and becomes reduced, then the product of this reduction, NAD, will be used as an reducing agent to donate electron to the other molecules. Interestingly, the structure of NAD contains the nicotinamide unit, hence a derivative of a pyridinecarboxylic acid.

Conducting polymers

The electrodeposited conduction polymer possess advantages such as: 1) thin, uniform and adherent polymer will be obtained, 2) polymer layer can be deposited on the small area of the electrode surface [46]. Generally, conductive polymers (CPs) can be good candidates to be applied as biosensors due to their π electronic structure. Chain conformation induced by interaction with analytes, showing high sensitivity, can be converted to an electrical signal. These properties make the conductive polymers very promising generation of polymers applicable in many research fields. Typically, they associate with conventional polymers and they also may show electrical and optical properties similar to metals and inorganic semiconductors. They exhibit perfect conductivity and high mechanical strength, and their processability makes them efficient materials for application in many research areas. Principal properties of CPs, such as the ability to be structurally and electronically modified, can be used for the generation of desirable properties [47]. Functionalized CPs, such as carboxylic acid functionalized ones, can be applied to fabricate biosensors due to the ability of carboxylic groups to form covalent binding of biomolecules modified by amino groups [48]. Since CPs enable simulating of the natural environment for biomolecules, CPs are appealing materials for the immobilization of biomolecules in the biosensor construction. Combining the biorecognition abilities with the efficiency of transducers has led to the development of biosensors as sensitive and selective instruments. Since CPs are used to produce most of the transducer biosensors, the deposition of electropolymerized films as a biomolecular method has received much attraction in recent years [27].

CPs can be synthesized by chemical methods or by applying electrochemical procedures. Both of these methods are used to produce high quality polymers. Electropolymerization can be applied usually by using cyclic voltammetry. This is a simple method to prepare the polymer layer on the surface of the electrode reproducibly. The advantage of this method is the ability to control the polymerization process easily. For example, by changing the scan rate, the potential range or the number of scans, it is possible to obtain a polymer with certain thickness. However, commercial methods to produce polymers chemically dominate and they are widely used, when bulk quantities of the polymer are necessary. Chemical synthesis proceeds by normal oxidation process in solution [49]. A useful way to control polymer important properties, such as conductivity, thermal and mechanical stabilities, is preparing the polymeric chain in the nanometer scale. Nanostructural polymers can be prepared by surfactant-free chemical methods. In this way, the monomers form micelles in an self-assembly process, which then act as templates for the generation of nano structures.

Recently, CPs have received a great attention in fundamental studies and especially in various applications such as biosensors due to their unique properties at the nanoscale. These days, biosensors are widely used in many areas such as in clinical analysis, environmental monitoring and food industry. A biosensor tool can convert the biological response to an electrical signal. This measured signal is the biosensor response to a special analyte in the test solution [27]. Producing a biosensor to be able to detect a very small amount (at nano scale) of oxidative products of DNA bases is crucial to recognize various fatal diseases, such as epilepsy, Acquired Immune Deficiency Syndrome (AIDS), atherosclerosis, chronic hepatitis, mental retardation, age-related disorders and many kinds of cancer. Especially, analytical methods enable the detection of cancer. Therefore, assays for accurate and sensitive identification and detection of cancer cells is of great importance to an early diagnosis and integrity treatment.

We may also consider another group of CPs called “intrinsically conducting polymers (ICPs)”. They are known as materials that utilize conjugated polymers and at least one secondary component that can be inorganic or organic components or biologically active species. The aim is to produce a novel composite material that has distinguished properties that cannot be observed in the individual components. This includes either new or improved chemical properties that may be employed for chemical or biological sensing. The combined physical or chemical properties of the components are elicited for chemical sensing when the materials are combined. Differences in the properties of composites containing similar components are often due to the method of preparation. Therefore, preparation methods should be probed in more detail with respect to the “how” the secondary component is incorporated in the ICPs. The most important advantage of ICP composite materials over the ICP alone is based on the expansion in active surface area and ability to make good electronic contact between the composite compound and the transducer. The main polymer provides excellent dispersion composite components and large surface area for the secondary components to be integrated and prepares templates for chemical reactions and interactions. The intrinsic stability and symbiosis between the two components used to produce the composite material is often preferable to the bulk components alone [50].

As another approach, plastic antibodies show a new advantage in detecting 8-oxoguanosine. These synthesized compounds are obtained by using molecularly-imprinted technology and they possess longer stability properties and lower production cost than their natural counterparts. As far as I know, this context is present in the literature targeting 8-oxoguanosine. Creating of imprinted sensing films by using metal chelating agents as monomer cross-linked with bisacrylamide have been studied. The sensitivity of these compounds to 8-oxoguanosine were measured by using QCM gold electrodes however the obtained detection limits were not lower than 0.01 μM. Such compounds were reported in 2008-2009, and afterwards a significant development on molecular-imprinting technology have been evidenced in the research reported.

Today, molecular imprinting technology has become a very efficient tool to design nanostructural compounds with highly adjustable detection properties. Conclusively, molecular imprinting polymers (MIP) are synthetic polymers with specific recognition sites which are perfected in size, shape and functional groups to the target molecule. Particularly, MIP approach has arisen from the need to obtain facile, burly and cost effective alternative methods. Currently, MIPs exhibit a wide range of applications, such as drug delivery systems, stationary phases, solid phase extraction and biosensor instruments. Recently, the high stability and specificity of MIPs have made them suitable substances to produce immunosensors. Moreover, the possibility of applying different detection techniques like Surface Plasmon Resonance (SPR), Voltammetry, EIS, Voltammetry and fluorescence quenching turned these materials to very useful chemical sensors. The association of imprinting approach with electrochemistry to make sensing techniques has improved both sensitivity and selectivity of the sensors.

In the biosensors field, the most important feature is related to the association of MIP between transducer and recognition elements. At this point, electropolymerisation can form selective binding sites, at an accurate spot and closer to the electrode surface. By changing the voltage, charge, number of cycles, supporting electrolyte, etc in electrochemistry, it is possible to accurately adjust the rate of polymer growth, the film thickness and their morphological properties. The most important advantage of using electropolymerization to produce MIP is the ability of this approach to synthesise and immobilise the biomolecule in a one-step procedure. Moreover, as we know, electrochemistry is a simple, cost-effective and sensitive method and easily applied to electroactive species in the aqueous environment. Recently, a simple and successful approach was demonstrated by using MIP as a sensor to detect dopamine based on a chitosan-graphene mixture. Furthermore, in many studies carbon nanotubes and supramolecules cyclodextrins have been applied to modify electrodes for simultaneous determination of various DNA bases. During the last decade, the application of MIPs as recognition elements for biological molecules has been reviewed , specially the effect of experimental conditions such as pH, the nature of buffer and functional groups. MIPs are phenolic polymers which can be prepared by electropolymerisation and they possess the ability to interact with various analytes through hydrogen bonding and π-π stacking [51].

Some well-known CPs may be named here, such as poly(3,4-ethylenedioxythiophene) (PEDOT), poly(sulfur nitride), poly(p-phenylene), polypyrrole, polyaniline, poly(thiophene), poly(3,4-ethylenedioxythiophene), poly(p-phenylenesulfide), poly(acetylene), poly(p-

phenylenevinylene). Conductivity of the all of these polymers is the consequence of presence of the delocalized electron(s) (the same as TD100) and extended π bond structure.

It may be mentioned here that the acidity of organic compounds, including polymers, can be determined by electrochemical methods, particularly in non-aqueous solvents like DMF or DMSO [52].

Adsorption of Graphene and Porphyrins

There are many reports on electrodes modified by using adsorbed graphene or graphene oxide (GO) which exhibit a range of functional properties for many applications, such as batteries, supercapacitors, catalysts, solar cells, and electrochemical sensors. Extensively used as an electrochemical biosensor for many years has been graphene with hexagonal lattice structure, the thickness of 0.35 nm, high surface area (2600 m^2g^{-1}), mechanical strength (breaking strength ~40 Nm^{-1}), outstanding heat conductivity (500 $Wm^{-1}K$), exceptional electronic conductivity (200000 $cm^2V^{-1}s^{-1}$ at room temperature), weakly scattered charge carrieres ($\lambda_{scattering} > 300$ nm), ballistic transport of its charge carriers at room temperature, a chemically and geometrically controllable band gap, and quantum Hall effect at room temperature. However, some substantial disadvantages of this compound such as easy aggregation, poor solubility and/or processability, are the big impediments to the various applications for electrochemical biosensors [53].

Graphene nanosheets when compounded with conducting polymers such as PANI can improve not only the electrical conductivity, but also the mechanical strength of the resulting composites. There have been several studies for sensor application of graphene oxide/PANI composites as an electrocatalyst. However, most of graphene-based composites, are prepared via a noncovalent mixing/adsorption route. The preparation of composites with a homogeneous dispersion of graphene sheets within the smooth thin polymer layer is often difficult. Using these methods lead to a decrease in the electrocatalytic activity of the resulting composite. Therefore, developing new methodologies is necessary to prepare hybrids with enhanced properties through the synergistic effects between the two components [54].

Recently, covalently-grafted PANI on GO or reduced graphene oxide was produced. The composites synthesized by applying these new methods showed high electrical conductivity and high stability, which are necessary for their application as electrode materials as supercapacitors or sensors. However, most of the covalent connections in those composites are based on the functional groups of GO, which cannot form a π-conjugated molecular linkages and led to make some limitations on the total conductivity of the composite. Therefore, to improve the overall performance of covalently RGO/PANI composites, the synergistic effect between PANI and RGO is still necessary [55].

In my work, graphene or graphene oxide could not receive much attraction to be researched. The main reason for that is due to the presence of some barriers for the application of graphene (as mentioned above) which makes it an unfavourable compound to modify GCE (at least in my work). Otherwise, graphene has been used in many studies extremely, until now.

Porphyrins are called 'the pigments of life'[56]. Porphyrins are famous for playing a vital role in biological important processes such as the transfer and storage of oxygen in haem or in chlorophyll for the photosynthesis in green plants. Moreover, they can also be applied for the photodynamic therapy purposes, or they can be used as electrocatalysts for the reduction of inorganic and organic nitro compounds, or in form of assemblies as chemical sensors [57]. Many efforts have been applied on mimicking photosynthesis, such as constructing the architecture of dyads or triads consisting of donors and acceptors, with bridges of altering length, to illuminate the energy/electron-transfer process and obtaining high performance in photon-to-electron conversion. The photosynthesis process may be mimicked in a wide gap semiconductor by by the electron transfer between the conduction band of the electrode and photoinduced dyes [58]. In the visible light range, porphyrins have a very high extinction coefficient. This makes them promising photoelectron transfer agents. Moreover, their structures are rigid. Nanoparticles modified by porphyrins exhibit great optoelectronic properties. As a well-known functional dye, for achieving novel optoelectronic properties, derivatives of porphyrins have been employed to modify carbon nanotubes. Through connecting optoelectronically active porphyrin molecules and two-dimensional graphene nanomaterials, multipurpose nanometer-scale materials for optics and/or optoelectronics could be produced. Taking advantage of strong affinity of the explosives to porphyrins, and good capability of charge transfer and high ratio of surface to volume of graphene, porphyrin functionalized grapheme with good sensitivity may be an excellent choice for the electrochemical ultratrace detection of explosives [31].

Porphyrin compounds due to their aromaticity, good stability, wide spectral response and powerful complexing ability with metal ions can also be used for the electrode modification purposes. Recently, the porphyrin (especially metal porphyrin) graphene composite materials have been synthesized by using the covalent bond, π-π stacking and electrostatic attraction. Metal porphyrin-graphene nanocomposites have been researched for the catalytic oxygen reduction and the other reactions [59]. Porphyrins, which are in the active sites of many important enzymes, have been extensively used to study the oxidation and reduction of many biological molecules. In recent years, FeTPP has received more attention because it can be adsorbed onto the multiwall carbon nanotubes (MWCNTs) surface through π-π interactions. The functionalization of MWCNT sidewalls because of non-covalent interactions is an effective way to preserve the sp^2 nanotube structure and electronic characteristics. Additionally, the strong interaction between the aromatic groups of FeTPP with the π-π stacking of MWCNTs is similar to reach the favourable purpose. Immobilization of molecules and biomolecules on MWCNTs has been used in the past, with was motivated by the prospects of using MWCNTs as a novel type of sensors. The formed hybrid nanocomposites (FeTPP/MWCNTs) are characterised by a fast electron transfer, which leads to perfect electrode performance. These nanocomposites have previously been used to detect many substances, such as trichloroacetic acid, nitric oxide, oxygen and neurotransmitters [60].

Metalloporphyrins, are well recognised supramolecular complexes because of their perfect physicochemical properties, rich electrochemistry and high versatility as powerful electrocatalysts that could be applied for the fabrication of electrochemical sensors. The advantage of metalloporphyrins is their strong adsorption on the surface of of graphite and carbon-based

electrode materials such as GCE to detect biological molecules. The potential of these molecules to achieve applications at electrode modification technology needs to use a thin layer of them immobilized on to solid supports such as the glassy carbon electrode (GCE). Some metalloporphyrin complexes like cobalt have been reported as efficient electrocatalysts for several environmental and biomedical molecules such as thiols, nitric oxide, nitrite and oxygen, however, the use of their conjugates in electrocatalysis or electrochemical sensing is under-researched [61].

The major interest is in using these chemically modified electrodes (adsorbed by porphyrins) as biochemical sensors for analytical purposes. Methods which are applied for attaching metalloporphyrins to electrode surfaces include adsorption, direct chemical bonding, ion exchange and electrochemical polymerisation. One of the most widely employed techniques to modify carbon-based electrodes is based on the oxidative electropolymerisation of appropriate metalloporphyrins. This procedure help to adhere the complexes onto an electrode and to stabilise the active sites of the catalysts. Electropolymerisation can be carried out by galvanostatic methods, potentiostatic methods or cyclic voltammetry, in which the electrode potential is scanned over the polymerisation range. The last method is very convenient because of it giving the possibility of continuous monitoring the electropolymerisation process. It also helps to deposit a controlled amount of polymer and therefore the film thickness onto the electrode surface [62].

Some water-soluble metalloporphyrins were found to show an electrocatalytic effect in the reduction of dioxygen to hydrogen peroxide or water. Several studies were directed to adsorbed metalloporphyrins. Besides, there are many reports based on the oxidative electropolymerisation of metalloporphyrins. Electropolymerisation can also be carried out with pyrrole, aniline, hydroxyphenyl and pyridinium substituted porphyrins. Metalloporphyrins are very stable π-conjugated macrocyclic molecules generating a diverse class of multifunctional materials, which show interesting catalytic, optical, electronic and biological properties. Therefore, metalloporphyrins have potential applications in electrochemical sensing [63].

Numerous studies about porphyrin electrochemistry were initially directed towards the elucidation of the role played by porphyrin-containing molecules in the biological electron transfer chain. Lately, applications of widespread nature have been suggested, such as adsorbed electrocatalysts, in the modification of electrode surfaces, and as an integral ingredient for composite electrodes. In natural systems the porphyrin ring almost always contains a central metal cation. A large number of investigations have presented that the electrochemistry of metalloporphyrins is, in good approximation, a superposition of the effect of the ring structure and the effect of the central metal cation, which can be confirmed by relatively simple Hückel-type calculations. There are many important and useful studies about porphyrin free bases to clarify the role of the central metal cation. A large number of these free bases have been studied by regarding their electrochemical reduction and conclusions drawn with respect to ring substituent effects on electrochemical behaviour. It should be noted that, for many organic compounds, the electrochemical response can be changed due to electrode material, solvent, and added electrolyte changes. Some oxidation investigations have been done by using platinum electrodes as work electrodes [64].

Experimental

Guanine solubility

Guanine 98% and the other reagents were purchased from Sigma-Aldrich and used as received. Mili-Q water was applied for the preparation of all the solutions.

A HP 8453 Spectrophotometer was used to record the UV spectra in 10 mm quartz cuvettes and a Zetasizer Nano ZS (Malvern) Instrument was used for DLS measurements.

1 mg guanine (but 5-100 mg in preliminary measurements) was added into 10 ml water or buffer solution. All the mixtures were sonicated in a laboratory ultrasonic bath (100 W) at 25.0 °C for 20 minutes with removing the mixtures from the bath and shaking them every 5 minutes. Then, the mixtures were equilibrated at 25.0 °C for 30 minutes. Eventually, the excess amount of guanine was centrifuged off by using a laboratory centrifuge (16000 g RCF) with its rotor brought to 25 °C just before starting it. After 5 minutes centrifuging the supernatant solution was transferred to another tube and centrifuged for another 10 minutes. All the spectra recorded on supernatant only after the second centrifuge step.

The concentrations of guanine were determined from UV spectra of obtained solutions. A stock solution of guanine was prepared by dissolving it in phosphoric acid 5% and then this solution was used to prepare the standard solutions of guanine in the buffer solutions. The data in Table (from the literature) were used to calculate guanine concentrations. These values agreed well with the absorption coefficients measured. In pH ranges, where more than one guanine species was present, I calculated the ratios of these species from known pK_a values at the given pH (*vide infra*) and based on them ratio-weighed mean absorption coefficients, which I used to calculate the concentration.

Species	λ_{max}/nm log ε	Ref
$GuaH_2^{2+}$	236 (4.01); 252 (3.95)	65
$GuaH^+$	248 (4.03); 271 (3.85)	66
Guanine (Gua)	246 (4.01); 275 (3.89)	66
Gua^-	245 (3.78); 273 (3.87)	66
Gua^{2-}	221 (4.12); 274 (3.94)	66

Table 1. Ultraviolet spectra of guanine and its conjugated acids and bases used for concentration.

Dynamic Light Scattering (DLS)

In my work guanine nanoparticles were discovered for the first time by applying DLS measurements. Brownian motion which is the random movement of particles due to the bombardment by the solvent molecules that surround them is the basis of this method. Smaller particles show more rapid Brownian motion. DLS measures fluctuations in the scattered light intensity caused by Brownian motion. Small particles move faster and the signal intensity fluctuates faster.

Correlation in Dynamic Light Scattering

It is a technique for extracting the time dependence of a signal in the presence of noise. It constructs the time autocorrelation function G(τ) of the scattered intensity. Essentially, it applies an artificial variable to an intensity/time trend and assesses the correlation of the delayed trends with the primary trend. Delay time symbolized as τ.

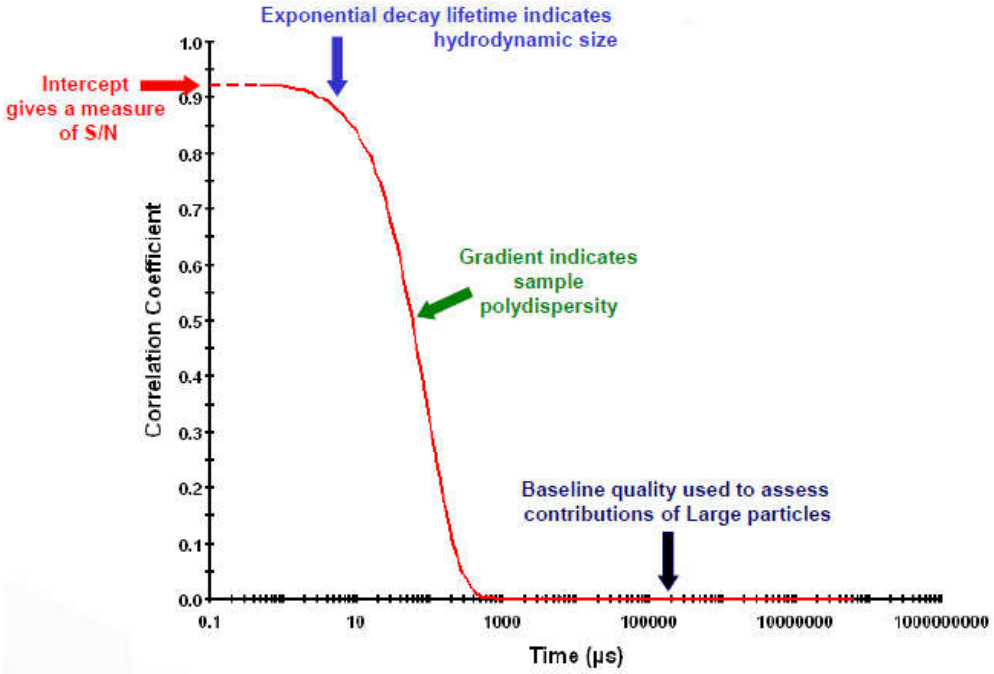

Scheme 6. A correlogram.

Obtaining size from the correlogram

Particle size information is obtained by analysing the correlogram with various algorithms:

- Cumulants (ISO13321): It applies the single exponential fit and then calculates the mean size (z-avg diam.). This algorithm can estimate the width of the distribution (PDI).
- Non-negative least squares: It applies the multi-exponential fit and then calculates the distribution of particle sizes by intensity, volume or number.

Here, a mixture of equal numbers of 5 and 50 spheres may be considered.

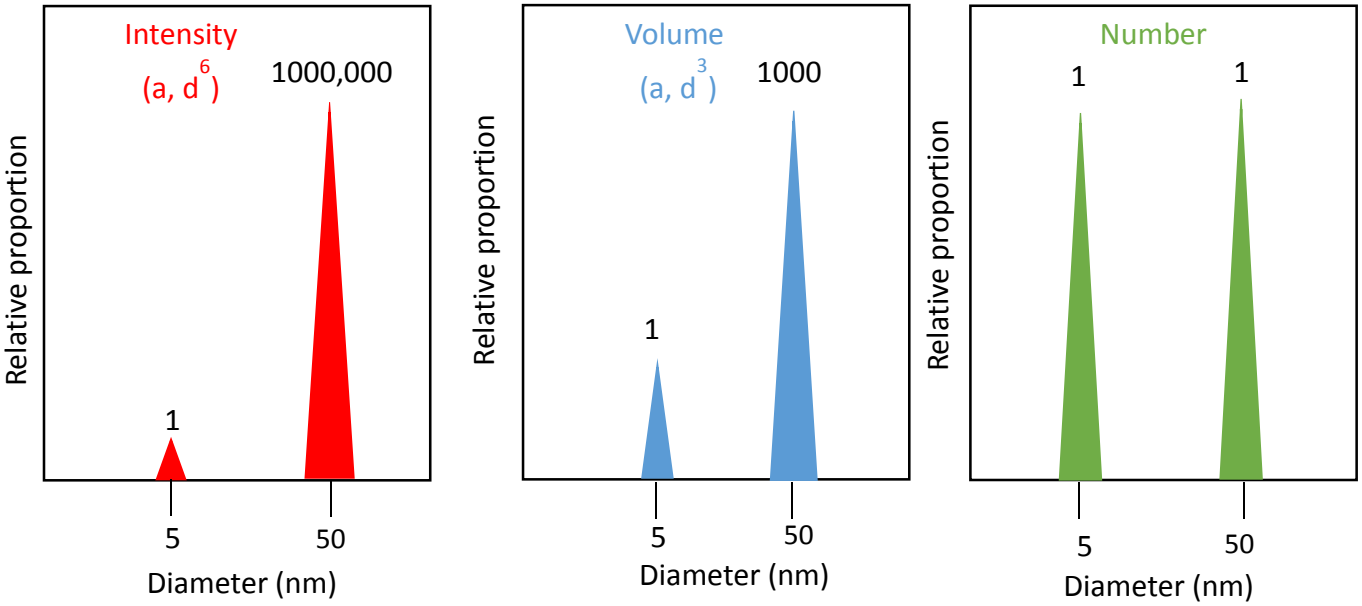

Figure 6. Intensity, volume and number distributions. Intensity distribution is calculated from the correlogram. Volume and number are calculated from intensity.

DLS sample preparation

- Sample requirements
  - The sample should consist of a dispersion of particles in a liquid medium.
  - Ideally, the dispersant should meet the following requirements:
    - It should be transparent
    - Its refractive index should be different from the particles
    - It should 0.5%
    - It should be clean and filterable

Lower size limit of DLS

It depends on:

- The amount of scattered light from the particles
  - Relative refractive index
  - Sample concentration
- Instrument sensitivity
  - Laser power and/or wavelength
  - Detector sensitivity
  - Optical configuration of the instrument

Upper size limit of DLS

DLS measures the random movement of particles undergoing Brownian motion, so it will not be suitable when the particle motion is not random. The upper size limit is sample dependent and is defined by:

- Onset of sedimentation
- Number fluctuations

Sedimentation

All particles will sediment and the rate will depend upon the particle size and relative densities of the particles and suspending medium. For successful DLS measurements, the rate of sedimentation should be much slower than the rate of diffusion since a consequence of slow diffusion is long measurement times. The presence of sedimentation can be determined by checking the stability of the count rate from repeat measurements of the same sample and the expert advice system will highlight this. It may be advantageous to suspend the particles in a medium of similar density, e.g., 13% sucrose has the same density as polystyrene latex.

Number fluctuation

Another factor will be the number of particles present in the measurement volume (the intersection of the laser beam and detector optics). The intensity of scattered light produced by large particles would be sufficient to make successful measurements. However, the number of particles may be so few that serve fluctuations of the momentary number of particles in the measurement volume will occur i.e. number fluctuation. This results in large fluctuations in the scattered intensity which masks those due to Brownian motion.

Sample concentration overview

The result obtained from a DLS measurement should be independent of sample concentration. Each type of sample material has its own ideal range of concentration where measurements should be made. If the concentration is too low, there may not be enough light scattered to make a measurement. If the concentration is too high, the result may not be independent of sample concentration. During method development, determining the correct sample concentration may involve several size measurements at different concentrations.

Lower concentration limit

It depends on:

- The amount of scattered light from the particles
  - Relative refractive index
  - Particle size
- Instrument sensitivity
  - Laser power and/or wavelength
  - Detector sensitivity
  - Optical configuration of the instrument

Upper concentration limit

- Multiple scattering

The ideal situation in a DLS measurement is to have singly scattered light. This means that every photon which reaches the detector was scattered by only one particle. This will be the case for samples at low concentrations. However, as the sample concentration is increased, the probability of the scattered photon being “re-scattered” by second, third,… particle increases. The presence of multiple scattering during a DLS measurement will reduce the measured size.

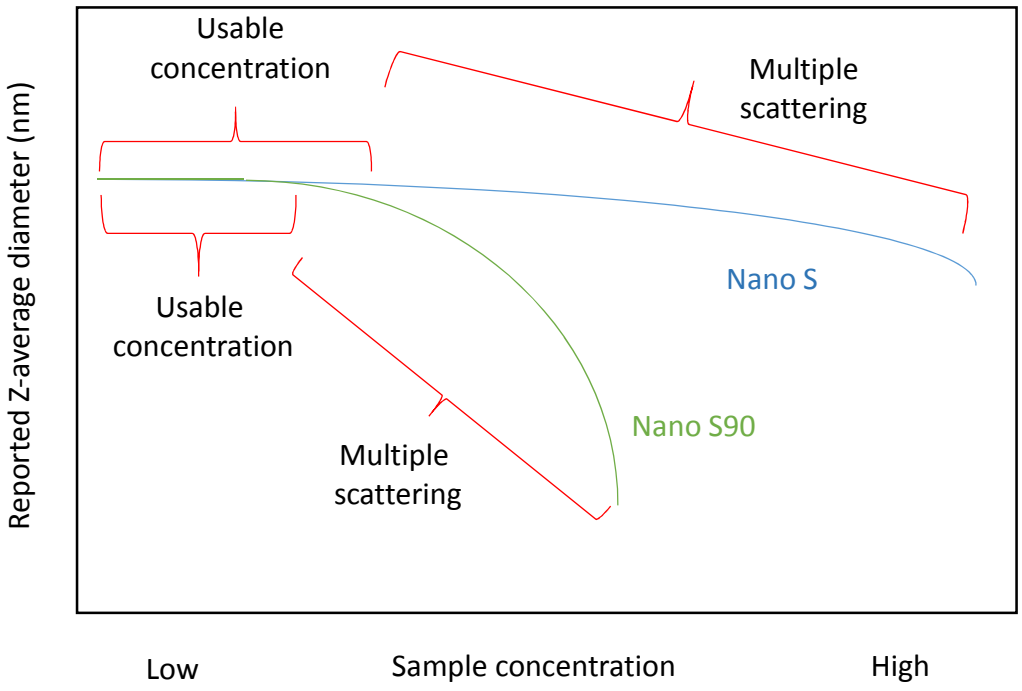

Scheme 7. Multiple scattering.

Restricted Diffusion

It describes the phenomenon where the presence of other particles hinders free particle diffusion. Symptoms of restricted diffusion effects include:

- Shifting of the size distribution, with no change in the modality or polydispersity, to larger sizes when the solvent viscosity values are used for size calculations at high sample concentrations.
- A concentration dependence of the z-average which parallels that of the bulk viscosity of the sample.

As a general rule of thumb, restricted diffusion effects can be minimized by using the bulk, rather than the solvent, viscosity for the size distribution calculations.

Particle interactions

At higher concentrations, particle interactions can modify the free diffusion of particles and this can lead to non-specific aggregation that modifies the size distribution obtained. Symptoms of particle interaction effects include:

- Increase in the distribution modality
- Increase in the sample polydispersity
- Z average diameter and viscosity concentration dependence are uncorrelated

There is no correction for particle interactions, but to increase confidence in the distribution results we should use the bulk viscosity to correct for excluded volume effects and measure near the edge of the sample cell to minimize multiple scattering effects. The addition of electrolyte may reduce interactions by modifying the influence of charge around the particles. This needs to be determined by experiment.

Sample preparation overview

A backscatter instrument can measure the size of any sample in which the particles are mobile. Therefore, high sample concentrations can be measured. However, each type of sample has its own ideal range of concentration where measurements should be made. This should be determined through a series of measurements to ensure that the size obtained is independent of concentration.

Sample dilution

Any sample dilution needs to be carefully performed to ensure that the equilibrium of any absorbed species between the particle surface and bulk solution is preserved. The diluent should be the same as the continuous phase of the original sample. The diluent could be obtained by:

- Filtering the original sample and obtaining a clear supernatant suitable for dilution
- Centrifuging the original sample and obtaining a clear supernatant suitable for dilution
- Making up a continuous phase as close as possible to that of the sample

Diluent filtration

Dust is one of the major problems in DLS measurements and may bias the results obtained. To avoid any possible dust contamination during dilution, the medium should be ideally filtered. Commercial syringe filters are available for use with pore sizes ranging from 2 µm down to 20 nm.

Antioxidant evaluation

All the measurements during my electrochemistry research were done with a BAS 100B/W electrochemical analyser. The first part of my measurements with the purpose to evaluate antioxidant activity were done under air atmosphere in a typical 3-electrode cell with a glassy carbon type K working disk electrode (2.3 mm^2, Mineral, Poland) and platinum wire as the auxiliary. Potentials are conveyed against the Ag/AgCl (3 M NaCl) reference electrode. Saturated solutions of guanine were prepared in the phosphate buffers of pH 7 and 9 (0.1 M KH_2PO_4/KOH) and then sonication (15 min) was used to dissolve guanine followed by centrifuging to separate the excess solid material.

I applied the new invented electrochemical method including following program of alternating potential hold and scan steps:

1st step – Hold at +400 mV for 15 s (electrode stabilisation)

2nd step – Scan from −200 to +1200 mV at 500 mV s−1 (checking for 8-oxoguanine residues)

3rd step – Hold at +1200 mV for 2 s (cleaning the electrode)

4th step – Hold at −1000 mV for 2 s (oxygen reduction – generation of superoxide)

5th step – Scan from −200 to +1500 mV at 500 mV s−1 (detecting 8-oxoguanine and guanine)

6th step – Scan from +1500 to −200 mV at 500 mV s−1 (reverse scan)

The whole program must be run several times (usually 8 times) in the saturated solution of guanine in phosphate buffer to get identical voltammograms for step 5.

Applying this program let me see the production of 8-oxoguanine and check its presence before the generation of superoxide. In order to eliminate suspicion that after step 3 (oxidation at +1.2 V),

8-oxoguanine may remain on the electrode, I applied an additional step of holding the potential at +300 mV for 15 s, and checked for the presence of 8-oxoguanine by scanning the potential in the range −200 mV to +1200 mV. Because no amount of 8-oxoguanine was detected, I did not repeat this step in the subsequent measurements.

The antioxidants were added by small portions (µl) from the stock solution into the phosphate buffer solutions during the experiments. To avoid excess dilution of guanine solutions in the cell, the maximum amount which was added was not more than 1/3 of the initial volume of guanine solution. To be able to cover the initial range of antioxidant concentration, first, it was tried to do the measurements using a more concentrated stock solution and then it was repeated by using the stock solution of a lower concentration. A fresh stock solution was prepared for every measurement due to the tendency of antioxidant solutions to get oxidised, however at pH 9 it was decided to use oxidised stock solutions by leaving them overnight exposed to the air. Before every measurement the cell solution was stirred very well to saturate it with oxygen.

The 8-oxoguanine peaks height was calculated by fitting 5^{th} degree polynomials for the sections of background before and after 8-oxoguanine peak, and by subtracting the background current calculated at the potential of the peak from the peak current. Additionally, it was tried to select a suitable potential range to fit the polynomials to correct the background by visually assessing the interpolated line under the 8-oxoguanine wave. Also, these corrections were checked by drawing the plots of all the 8-oxoguanine oxidation waves together. It could be realized that the waves obtained by this way were more or less symmetrical and they did not demonstrate any limiting diffusion current. Therefore, it was clear that these waves are related to the pure adsorbed 8-oxoguanine, however, as expected, the diffusion current was proportional to the concentration, so it should not affect the value of 8-oxoguanine determined.

All substances were purchased from Sigma-Aldrich in their highest purity grade available and used as delivered.

Guanine electroanalysis

Electrode modification

All pyridine carboxylic acids, pyridine-3,4-dicarboxylic acid, pyridine-2,6-dicarboxylic acid and pyridine-4-carboxylic acid were purchased from Merck in their highest purity grade available and used as delivered.

The electropolymerization of these acids on the surface of GCE was carried out by running cyclic voltammetry between −0.3 V and 1.7 V, at the scan rate of 20 mV/s and at the optimum number of cycles of 32, mostly in the saturated aqueous solutions of these acids and in the presence of KCl, assuming the presence of a salt could help to dissolve the carboxylic acids.

The porphyrins which are used to modify GCE by adsorption were previously synthesised in our lab. Tetrahydrofuran (THF) which is used as the solvent for porphyrin solutions was freshly purified by distillation under argon gas atmosphere. For this series of measurements, first the polymer was prepared electrochemically on the surface of GCE and then the electrode was immersed in the solution of a certain porphyrin in THF overnight. Next day, this prepared electrode

was used to detect guanine. The concentration of the porphyrin solution was measured by using Uv-vis spectroscopy.

Also, the other synthesized compounds with the short names of CCA, TPA, CAF and CATF which are tried in my work by their polymerization to modify GCE, were used as received from Dr Wiktor Kasprzyk from the cooperating chemistry lab.

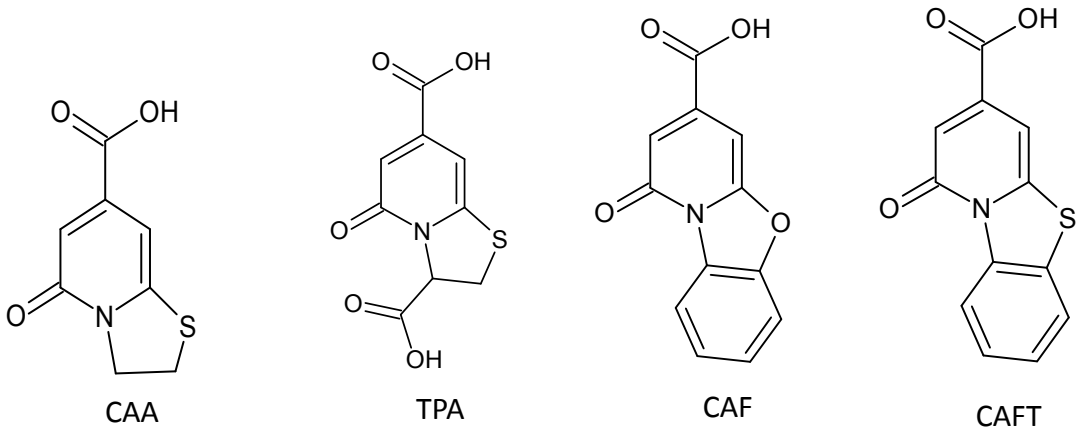

Figure 7. Synthesized compounds used for electropolymerisation.

For all these measurements, guanine was used in its saturated solution, prepared by adding solid guanine in phosphate buffer solutions of pH 7 and 9 (0.1 M KH_2PO_4/KOH) and then sonication for 15 minutes, as described in the guanine solubility section.

All the Uv-vis spectroscopic measurements on guanine was carried out by using HP UV-visible Spectrophotometer.

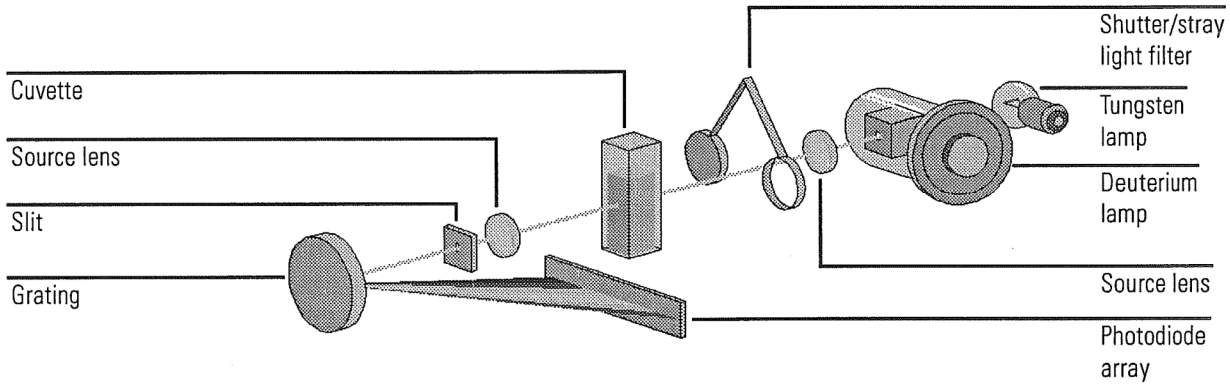

Scheme 8. HP UV-visible Spectroscopy system.

And the fluorescence spectra of guanine were measured by using CCD stellar net silver nova miniature spectrometer.

Polymer characterisation

The polymer obtained from electropolymerisation of citrazinic acid was named TD100. To produce TD100, citrazinic acid (1 mM) in phosphate buffer pH 7 in the presence of $NaBF_4$ (0.1 M) was polymerised on the surface of a platinum plate (1 cm^2) as the work electrode. The polymerisations were carried out between −0.05 V and 1.2 V for 40 cycles at the scan rate of 20

mV/s every time. Then, the polymer deposited on the surface of the platinum plate was scratched or dissolved by rinsing the electrode with water. In this was a very concentrated water solution was obtained. Afterwards, this polymer solution was evaporated in vacuum at 40 °C.

Size exclusion chromatography (SEC) was used to determine TD100 the molecular mass distribution of this new electrochemically synthesized polymer. The "Phenomenex PolySep 3000" column was used and water was applied as the eluent at the flow rate of 0.8 ml/min at 40 °C. For every measurement, 20 µl of sample was injected into the column which kept the concentration of TD100 as 20 mg/ml through the column. UV-vis spectrophotometer and refractive index (RI) detectors were used. Uv detector was set up at 218 nm wavelength. The pump, column oven and detectors were received from Knauer company.

A "Vario EL III" analyser was used for the elemental analysis of TD100. And an ion chromatograph type of "Dionex ICS-1100" with the column characteristics of "IonPac AS19 4×250 mm (Dionex, USA)" was used for phosphate ion chromatography of TD100.

The magnetic susceptibility measurements of TD100 were carried out in the cooperating physics lab (Institute of Nuclear Physics, Polish Academy of Sciences) by using MPMS XL Squid magnetometer from Quantum Design.

Citrazinic acid was purchased from Aldrich with 97% purity and used as delivered.

To determine the acidity of citrazinic acid and its polymer (TD100) I used a BAS 100 B/W electrochemical workstation with a C3 Cell Stand (Bioanalytical Systems, USA) for cyclic voltammetry. The cyclic voltammetry measurements were carried out under the scan rates of 200, 100, 50 and 20 mV/s. The working electrode was a 1.6 mm diameter platinum disk electrode (Mineral, Poland). The potentials were measured against an Ag/AgCl (3M NaCl) electrode that was immersed in supporting electrolyte solution. The working electrode was polished with 0.05 µm alumina (Buehler), rinsed with distilled water in an ultrasonic bath for 10 minutes and dried in an oven (120 °C) just prior to recording each voltammogram. Due to the sensitivity of the system to ohmic drop compensation, all the measurements were carried out under pure argon (Messer, Ar-N5.0). Ferrocene (0.5 mM) was added to the solution along with the first portion of the acid. Tetra-n-butylammonium tetrafluoroborate (TBABF4) was obtained from Fluka, then it was recrystallised from ethanol and water, and before use it was dried under vacuum for several hours. Dimethylformamide (POCh, Poland) was distilled twice under vacuum (by adding toluene and water to the first distillation). To protect the solvent from degradation it was kept in the dark and avoiding exposure to temperatures beyond 100 °C during distillation was applied.

For AFM measurements the aqueous solutions of TD100 and TD100 admixed with guanine in water were cast on mica plates. Samples were prepared and dried in ambient conditions.

Atomic force microscopy (AFM) working in contact mode, Xe120 Park system (IFJ PAN), was used to study surface topography of samples. Topography, lateral force and error signal images were recorded using ORC8-D (Bruker) cantilever.

Guanine trace analysis

To determine the limit of detection of guanine, the electrode was prepared as follows. The citrazinic acid was polymerised on a glassy carbon electrode (GCE) from a solution of this acid in phosphate buffer pH 7. Polymerisation was carried out under argon atmosphere by applying 40

cycles between −0.3 and 1.7 V at the scan rate of 20 mV/s. The modified GCE was immersed in an iron porphyrin solution in THF overnight.

Three stock solutions of guanine in phosphate buffer pH 7 were prepared for detection limit measurements:

1. Guanine saturated solution
2. Solution of 300 µl of saturated solution dilute in 25 ml of buffer
3. Solution of 1500 µl of saturated solution diluted in 25 ml of buffer.

Preconcentration time for every single measurement was 15-30 minutes, depending on the concentration. For the trace analysis, square wave voltammetry (SWV) was found to be the only useful technique and was applied for all this series of the measurements.

Electrochemical measurements were conducted with the use of Ag/AgCl (3 M NaCl, aqueous) as the reference. The potentials reported in the thesis are against this electrode. The potential of this standard is 0.209 V vs. SHE.

Results and discussion

Guanine solubility

Dissolution of guanine in neutral solutions is pretty difficult. I have decided to use sonication at 25 °C, and centrifuging off the excess guanine as described in detail in Experimental Section. The supernatant solution seemed always to be clear, however UV spectra always exhibited a slight steady rise in the baseline towards shorter wavelengths, which may indicate the presence of colloidal particles. First, I checked this phenomenon simply by passing laser pointer beam through the supernatant guanine solution. The DLS measurements confirmed it later.

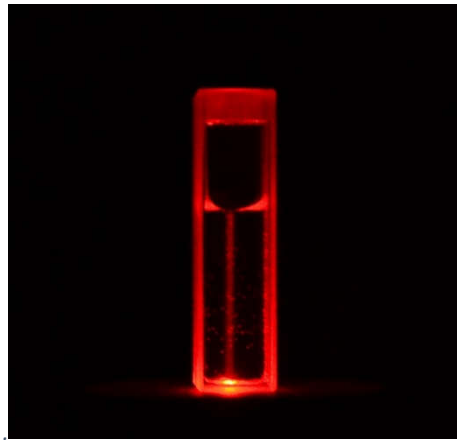

Figure 8. Passing laser pointer beam through the guanine solution.

Generally, the concentration of the colloidal particles was high and I had to dilute solutions for several times to be able to get the size distribution data. The reproducibility was not very good for the initial results. The fraction and size of smaller particles from single measurements were different, however, the size of large particles, of ca. 700-800 nm, was reproducible. Fig. 9 shows a typical size distribution of guanine colloidal particles in pure water. I stress that all the solutions were visibly clear. However, they scattered light, as can be seen in Fig. 8 by passing a laser beam through the supernatant guanine solution.

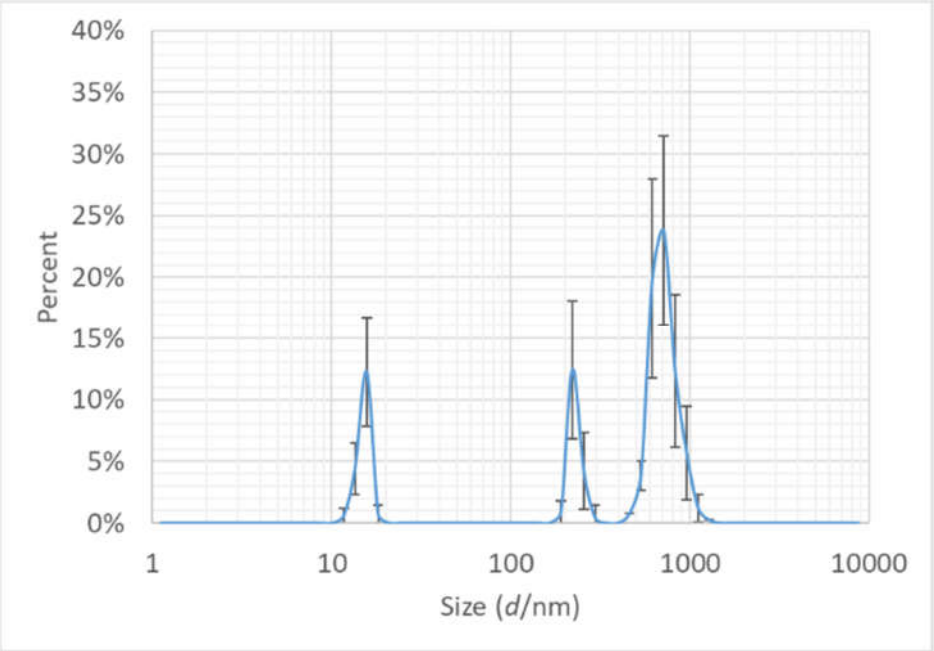

Figure 9. Typical size distribution of colloidal particles in a solution of guanine in pure water.

The smallest colloidal particles tend to aggregate and as it can be seen in Fig. 10 after about 10 days, the curves shift to larger particle sizes. Colloidal particles are also formed in acidic solutions. As it can be seen in Fig. 11 again there is a group of small and bigger particles that tend to aggregate.

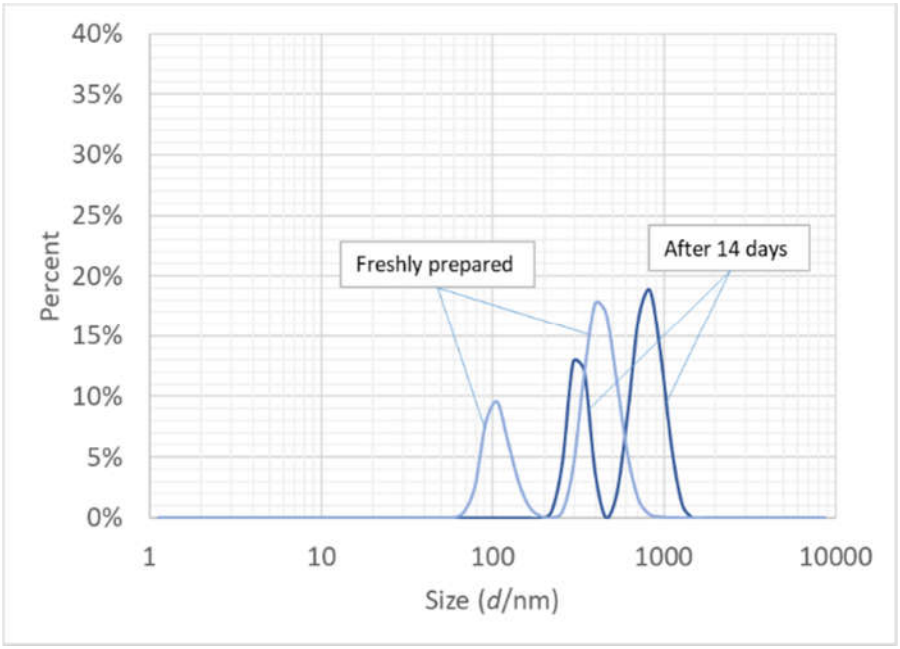

Figure 10. Size distribution of colloidal particles in a solution of 0.1 M pH 7 PBS. Directly after preparation and after 14 days.

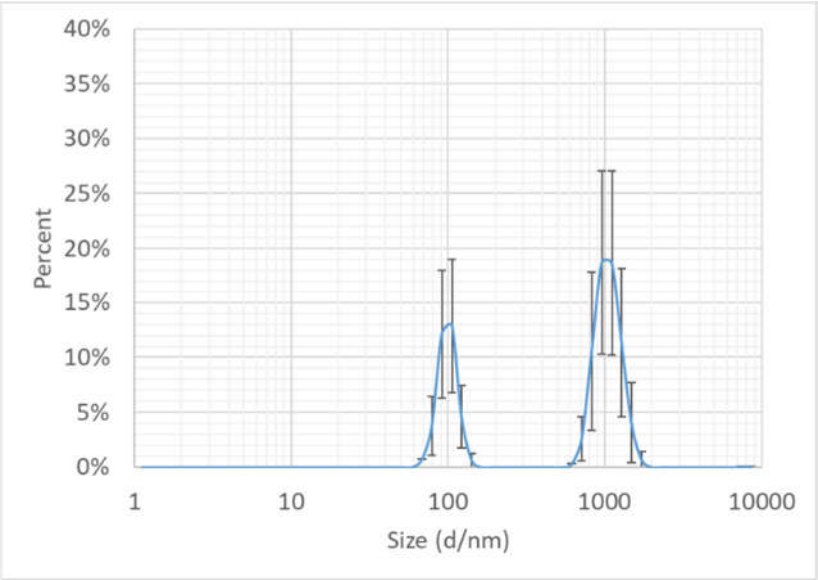

Figure 11. Size distribution of colloidal particles in a freshly prepared solution of 0.1 M pH 4.0 PBS buffer.

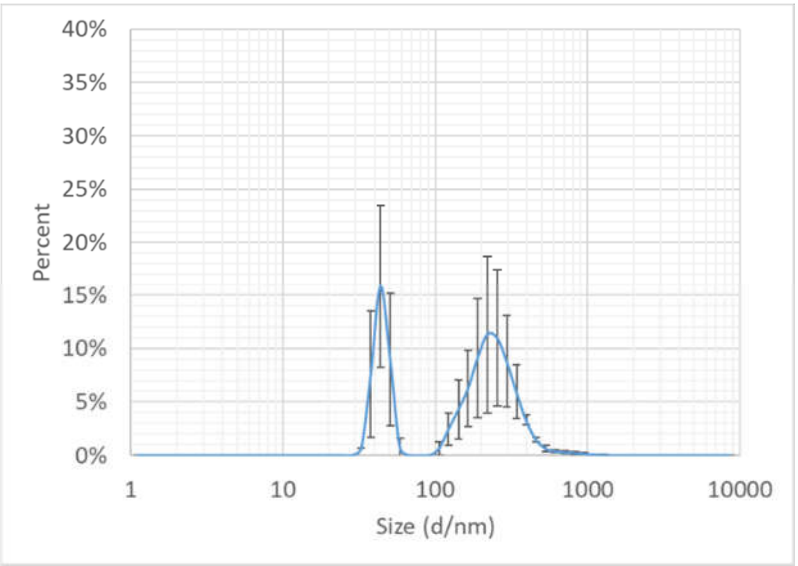

Figure 12. Size distribution of colloidal particles in a freshly prepared solution of 0.1 M pH 5.5 acetate buffer.

Additionally, I tried to pass water through a Pasteur pipette filled with guanine powder. The only result was swelling the powder layer and in fact it was impossible to collect any supernatant liquid. The resulting suspension was rather stable and did not settle down even after a couple of days. I centrifuged a sample of this suspension three times for 20 minutes and then I measured the pH of supernatant which was equal to 3.38. The UV spectrum of this solution indicated that guanine was present predominately in its monoprotonated form ($GuaH^+$). I calculated the concentration of guanine in this solution and I obtained the value of 55 µM. I did most the measurements in the phosphate buffer solutions (PBS), however, I used also acetate buffer

solutions only to check whether the electrolyte type affects the solubility. It appeared that there were no significant differences between the buffers. As it is known, some cations such as potassium cations promote the formation of guanine tetrads, and consequently, guanine quadruplexes [67], I checked whether there is a difference between phosphate buffers containing sodium and those with potassium cations. I could not observe any significant differences, therefore I used only potassium containing phosphate buffers in subsequent measurements. I have also checked the effect of ionic strength by applying 0.5 M sodium chloride and 0.5 M sodium sulphate. In both cases, only a small decrease up to 0.5 pH unit was noticed, but the concentration was roughly the same as obtained in buffer solution of the same pH.

As I mentioned above, dissolving guanine in water decreases the pH of the solution. The same concerns to a lesser extent buffer solutions, particularly diluted ones, which was also observed previously [68]. In my study, when I dissolved 5 mg guanine in 10 ml water then 0.3 M phosphate buffer was required to keep the pH value constant to 0.01 units. However, for 1 mg guanine, 0.1 M buffer solution was sufficient.

In my work, sometimes ultrasonication led to undesirable results. For example, during one of my measurements when I added 0.8 g guanine in 10 ml 0.1 M pH 7 PBS, and then sonicated this mixture as usual, the UV spectrum of the supernatant after centrifuging was very complex with multiple bands in the UV range. This result indicated a partial breakdown of guanine. However, if I used only 1 mg guanine in 10 ml water or a buffer solution, no problems occurred.

By applying more efforts to get highly reproducible, accurate results, I repeated the measurements at pH 7 in 0.1 M PBS 20 times and got the mean value of 25.7 μM with the standard deviation of ±1.4 μM. Other points in the pH range 4-9 were obtained as the average of 3-5 measurements. Fig 14 shows the results.

As shown below, guanine may dissociate or undergo protonation, and hence may be present as a neutral molecule, but also it may occur as mono- and diprotonated conjugate acids or mono- and dianionic conjugate bases.

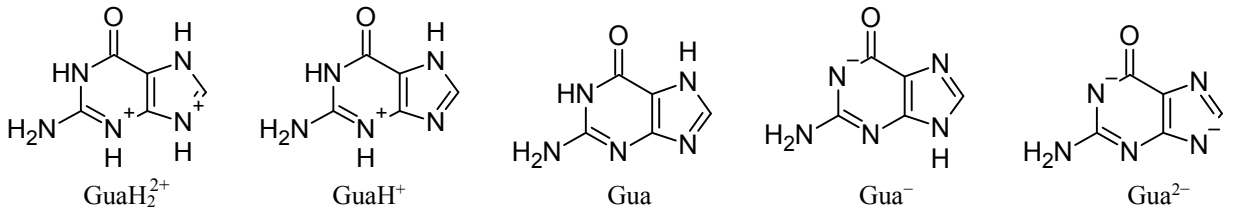

Scheme 9. Different forms of guanine.

Above are presented only the most stable tautomers, either based on the NMR spectra [66] or on quantum chemical calculations [69]. The most stable tautomers of cationic and anionic forms are present in excess of 90%, however the neutral 7H tautomer shown is in equilibrium (70:30) with the 9H one [69]. The dication can be seen only in 10.85 M sulfuric acid, trifluoroacetic acid and fluorosulfuric acid [65]. In my work, a solution of guanine in 65% phosphoric acid was prepared. The spectrum of this solution indicated the presence of only the dicationic form.

All the forms of guanine are in equilibrium with each other in the solution, and if solid guanine is present, also with it (Gua denotes neutral guanine in solution, other notations, as above).

$$\text{Gua(solid)} \rightleftarrows \text{Gua} \rightleftarrows \text{GuaH}^+ - \text{H}^+ \rightleftarrows \text{GuaH}_2^{2+} - 2\text{H}^+ \rightleftarrows \text{Gua}^- + \text{H}^+ \rightleftarrows \text{Gua}^{2-} + 2\text{H}^+ \quad (8)$$

Accordingly, we can equate chemical potentials:

$$\mu^{\ominus}_{\text{solid}} = \mu(\text{Gua}) = \mu(\text{GuaH}^+) - \mu(\text{H}^+) = \mu(\text{GuaH}_2^{2+}) - 2\mu(\text{H}^+) = \mu(\text{Gua}^-) + \mu(\text{H}^+) = \mu(\text{Gua}^{2-}) + 2\mu(\text{H}^+) =$$
$$= \mu^{\ominus}(\text{Gua}) + RT \ln c(\text{Gua}) = \mu^{\ominus}(\text{GuaH}^+) + RT \ln c(\text{GuaH}^+) + RT \cdot \ln(10) \cdot \text{pH} =$$
$$= \mu^{\ominus}(\text{GuaH}_2^{2+}) + RT \ln c(\text{GuaH}_2^{2+}) + 2RT \cdot \ln(10) \cdot \text{pH} =$$
$$= \mu^{\ominus}(\text{Gua}^-) + RT \ln c(\text{Gua}^-) - RT \cdot \ln(10) \cdot \text{pH} = \mu^{\ominus}(\text{Gua}^{2-}) + RT \ln c(\text{Gua}^{2-}) - 2RT \cdot \ln(10) \cdot \text{pH} \quad (9)$$

The values of chemical potentials, and hence, the concentrations of all the species at equilibrium are a function of pH. But, the chemical potential, and, accordingly, the concentration of guanine in the presence of solid guanine must be constant irrespective of pH. Then, I could calculate the concentrations of the other species by using the known values of pK_as, which set the ratios between the respective species and their conjugate bases or acids, and the pH. Obviously, the solubility of guanine is equal to the sum of equilibrium concentrations of all existing forms of guanine in the presence of solid guanine.

$$\text{Guanine solubility} = c(\text{Gua}) + c(\text{GuaH}^+) + c(\text{GuaH}_2^{2+}) + c(\text{Gua}^-) + c(\text{Gua}^{2-}) \quad (10)$$

By using pK_a values, it is possible to calculate the ratio of concentrations of the acid to its conjugate base as a function of pH. The example of pK_{a2} is shown here:

$$\frac{c(\text{GuaH}^+)}{c(\text{Gua})} = 10^{(\text{p}K_{a2} - \text{pH})} \quad (11)$$

Notation	Equilibrium	pK_a	Ref.
pK_{a1}	$\text{GuaH}_2^{2+} \rightleftarrows \text{GuaH}^+ + \text{H}^+$	−1.0 ± 0.2	65
pK_{a2}	$\text{GuaH}^+ \rightleftarrows \text{Gua} + \text{H}^+$	3.3 ± 0.08	66
pK_{a3}	$\text{Gua} \rightleftarrows \text{Gua}^- + \text{H}^+$	9.2 ± 0.08	66
pK_{a4}	$\text{Gua}^- \rightleftarrows \text{Gua}^{2-} + \text{H}^+$	12.3 ± 0.08	66

Table 2. pKa values of acid-base equilibria for guanine and its conjugate acids and bases. Note: the pK_a value is a mean of two values based on NMR and UV spectroscopic studies.

By combining the calculated concentration ratios, it is possible to determine the fractions of guanine and its ionized species in a solution at various pH values, which is shown in Fig. 13. As can be seen, more than 98% guanine in its neutral form is in the middle range, between ca. pH 5 and 7.5. The ranges for other forms are much narrower.

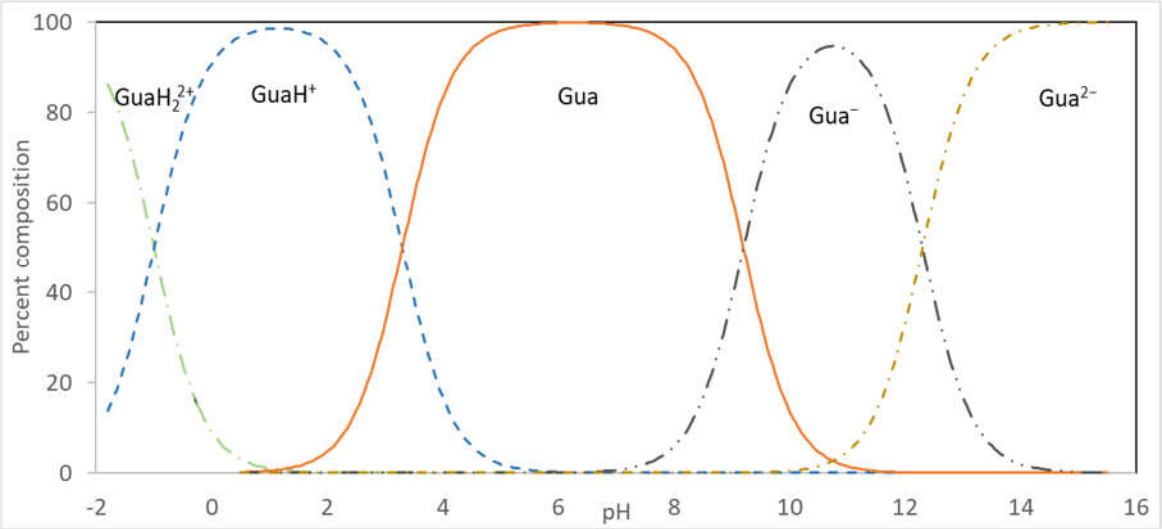

Figure 13. Speciation of guanine solution as a function of pH calculated from the pKa values.

The concentrations of all ionized forms of guanine are related through the pK_a values to the concentration of neutral form, which should be constant over all the pH range.

By knowing this concentration, I was able to calculate the concentration of all the other forms of guanine at a given pH, and hence the solubility, which would be the total concentration of all guanine species present in solution in equilibrium with solid guanine. Also, the deviation between the calculated and experimental values would show any other forms existing in significant amounts, like dimers or quartets. It appeared that the best least squares fit of the total concentration thus calculated to our experimental points gave the value of 25.4 μM for the concentration of neutral guanine. The line exhibited in Fig. 14 was calculated as described above. The inset in this Figure demonstrates how this solubility varies with pH in a wider range. Moreover, you can see in Fig. 14 the overlapping of this curve onto the experimental points published by other researchers [68] demonstrated a nearly ideal agreement in the range between pH 1 and 2. This confirms that there are no significant amounts of other forms present.

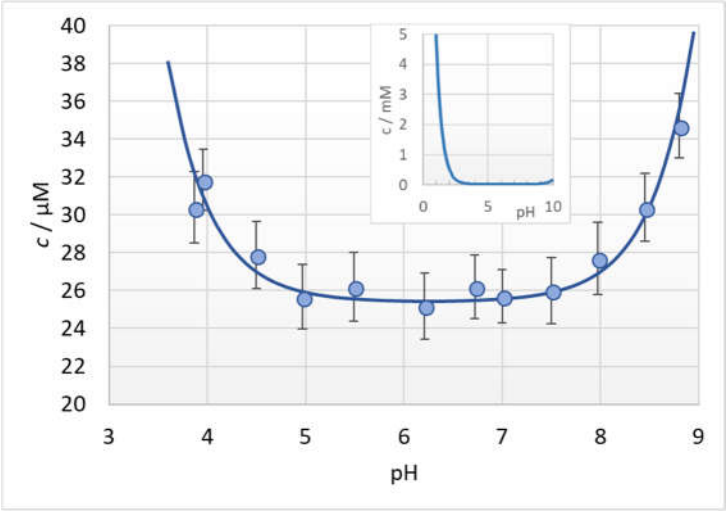

Figure 14. pH dependence of guanine solubility. The line was calculated assuming a constant concentration of neutral guanine equal to 25 µM and summing up the concentrations of its ionised forms calculated from the respective p*K*a values. The inset shows this line over a wide range of pH.

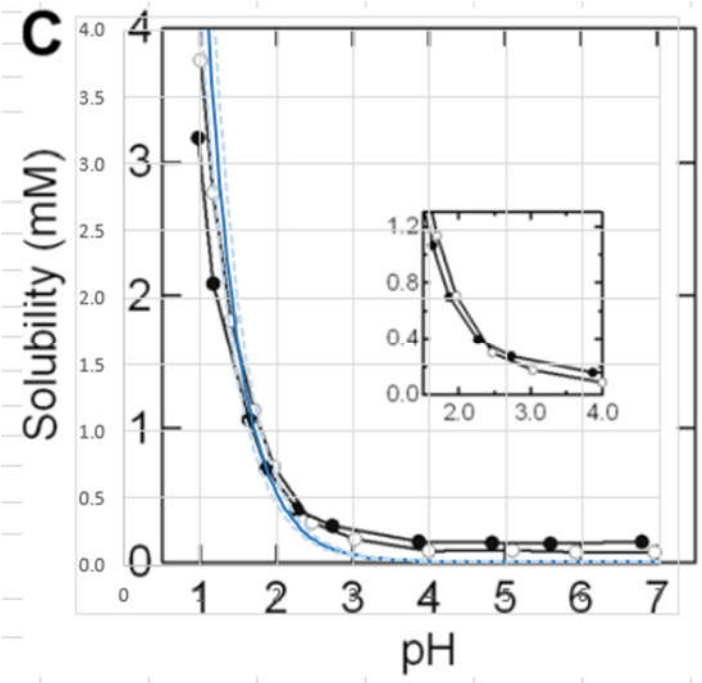

Figure 15. Comparison between our data and what is published by the other authors. Ideal fitting, except for the lowest concentrations (open points refer to pure guanine), dashed lines in our plot denote lower and upper limits.

By examining the crystal structure of the anhydrous guanine [70] or its monohydrate [71], the swelling of guanine upon adding water can be well understood. Both form sheets consisting of hydrogen bonded guanine molecules. The sheets stacked together by applying π-π interactions between offset parallel guanine rings. There are additional water molecules linking the interacting sheets in guanine monohydrate. The interplanar spacing in both crystals is equal to ca. 3.3 Å. N-1

and N-9 are protonated in guanine monohydrate, whereas it is N-1 and N-7 in the anhydrous crystal. The structure of biogenic guanine crystal is just a variant of the anhydrous form [72]. Commercial guanine is anhydrous and it is mainly an amorphous powder. In such a form, it can be expected that water intercalation into this layered structure may occur leading to swelling and eventually to delamination. Sonication would promote this process. I used a simple low energy 100 W ultrasonic bath, which was enough for my work. Guanine molecules would be pulled out by hydration forces from these delamination structures.

Another interesting phenomenon is acidification of solution upon guanine dissolution. Particularly, it is an evident in pure water, with pH dropping below 4. By increasing the amount of guanine powder, the final pH will decrease with the higher concentration of guanine, which is expected that at a lower pH value its solubility is much higher. Even in the buffer solutions with a sufficient concentration such as PBS 0.3 M the pH value decreased. This phenomenon cannot be explained only by the behaviour of guanine. Because, guanine is a weak acid of pK_a 9.2, therefore its aqueous solution will not be very acidic. I assume that the increased solubility of guanine under these conditions is due to the presence of its protonated form, GuH^+. It means that there should be an extra source of acid in guanine powder itself. Only a trace amount of it would be sufficient for 100 mg of powder to change the pH of 10 ml water to 4.0. The formation of the basic oxidation products of guanine, 8-oxoguanine or guanidinohydantion and spiroiminodihydantion is accompanied as a rule by the production of two protons per 2-electron oxidation step [69, 73]. The oxidation products of guanine are also weak acids, comparable to guanine itself, therefore only this acidic by-product of oxidation would be the source of protons required to protonate guanine. The oxidation of guanine does not occur upon dissolution. I confirmed it by applying argon atmosphere, which did not change anything. It is likely that some guanine molecules at the edges of the sheets in the crystal, particularly in its amorphous form, may get oxidized and an acid thus produced remained as an impurity. The amount of it might be negligible for most guanine applications, however they may affect solubility when a large amount of guanine powder is dissolved in a small amount of water.

It has already been mentioned that in many publications on guanine electroanalysis, concentrations as high as 100 μM are applied at pH 7. Generally, these solutions were prepared by dissolving the required amount of guanine. The results show that even at concentrations exceeding the solubility of guanine, the currents were increasing, however, usually there is a deviation from linearity at higher concentrations. When the solutions are freshly prepared, they may contain guanine nanoparticles which should be also electroactive and oxidized at about the same potential as single molecules, and contribute to the voltammetric current [74, 75]. However, their higher masses would make the diffusion coefficient lower, and consequently the expected current response lower, also. It could be concluded from my results that small nanoparticles in such a solution cannot be stable and would undergo aggregation by changing the conditions in time, therefore their presence should be avoided unless their sizes and concentrations are controlled. It is better to use real solutions with concentrations not exceeding the solubility that can be calculated by a method described above.

The results described in this Section were the subject of my publication [76].

Antioxidant evaluation

The final product of the reduction of dioxygen on the surface of carbon electrodes is hydrogen peroxide. Recently, it is proven this process is quite complex and superoxide, $O_2^{\bullet -}$, is actually an intermediate product in this process [77]. By further reduction of superoxide H_2O_2 can be produced. However, this harmful compound can be released by dismutation also. Therefore, I dealt with a complex mixture of ROS that can oxidise guanine to 8-oxoguanine. I developed an electrochemical program including potential hold and scan steps sequences that is possible to detect and quantify 8-oxoguanine electrochemically which is produced by the reduction of dioxygen in a buffer solution containing guanine, the details are presented in the Experimental. Glassy carbon electrodes are applied because they display good activity in both processes. During the electrochemical program, dioxygen is reduced at the potential of −1.00 V (potentials are given vs. Ag/AgCl), initially, then the potential will be stepped to −0.20 V and scanned up to 1.50 V at the scan rate of 0.500 Vs^{-1} (step 5). This scan rate is sufficiently rapid for 8-oxoguanine to be observed. As you can see in Fig. 16, it is proved that 8-oxoguanine was indeed formed upon the oxidation of guanine. Voltammogram of step 2 is recorded before the reduction of dioxygen to check if any amounts of 8-oxoguanine, possibly from the previous cycles, is left on the electrode. The process of dioxygen reduction in step 4, is mainly controlled by diffusion as it is confirmed by the linear plot of charge vs. square root of time, however with a considerable fraction due to double layer charging (following a huge potential step of 2.2 V) and possibly by the reduction of adsorbed oxidation products from the electrode cleaning during step 3.

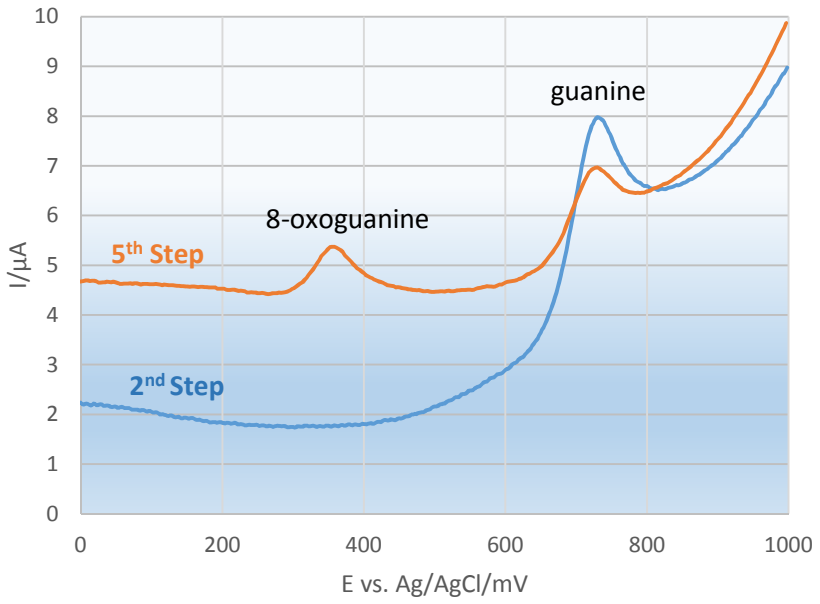

Figure 16. Voltammograms of 2nd and 5th steps recorded in a saturated solution of guanine in phosphate buffer of pH 7. Details on the applied potential hold and scan steps are given in Experimental.

When antioxidants are added to the solution of guanine, they will compete with guanine in the reaction with ROS which are generated by the reduction of dioxygen (step 4), and on this way they

protect guanine against oxidation to 8-oxoguanine. A decrease in the guanine peak current in the subsequent step would prove that. As can be seen from Fig. 17b, upon addition of increasing amounts of catechol as an antioxidant, the height of 8-oxoguanine peak decreased. However, catechol could not inhibit the formation of 8-oxoguanine completely and its presence could still be seen at high concentration of catechol added.

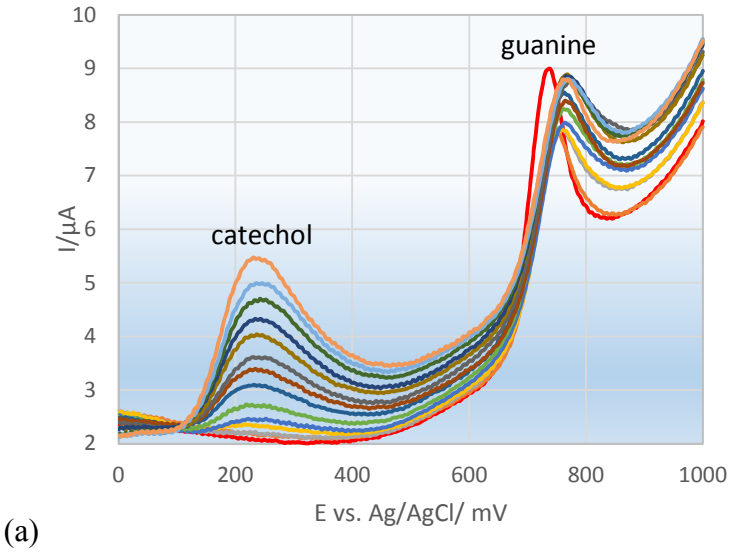

(a)

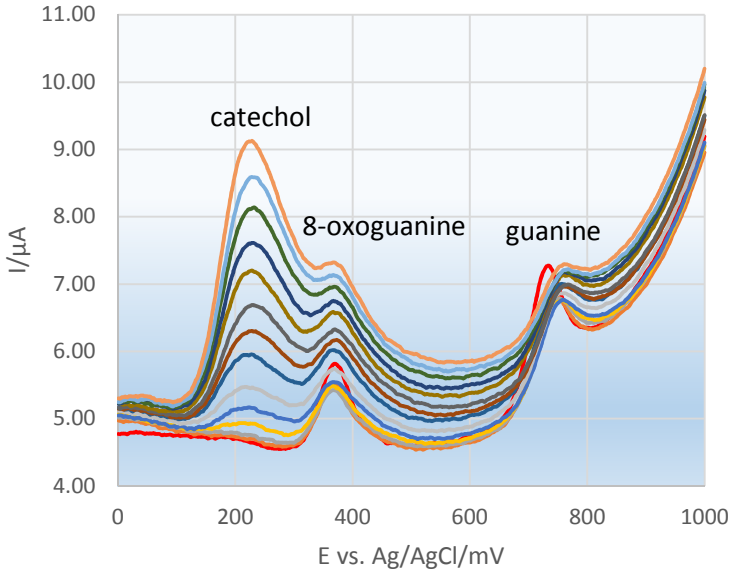

(b)

Figure 17. Voltammograms recorded upon adding increasing amounts of catechol (up to 0.23 mM) to saturated solution of guanine in pH 7 phosphate buffer. The bottom voltammograms were obtained prior to catechol addition (a) Step 2 – no previous dioxygen reduction. No trace of 8-oxoguanine can be seen. (b) Step 5 – directly after dioxygen reduction. 8-Oxoguanine can be seen with its wave decreasing with increasing amounts of added catechol, not totally, but to a limiting value. Significantly higher background (by ca. 3 µA) compared to (a) is due to the reduction of various ROS generated in the dioxygen reduction step and possibly surface oxygenated species on the electrode.

The name and structures of the investigated substances are given below. Simple alcohols are included only for comparison. Alcohols are not usually considered antioxidants, however in my research they exhibited some antioxidant activity.

Methanol

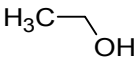

Ethanol

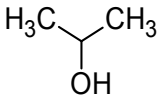

2-Propanol

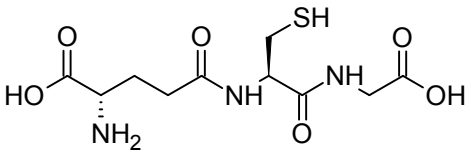

Glutathione

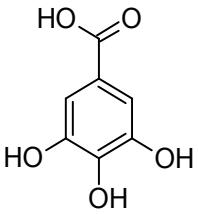

Gallic acid

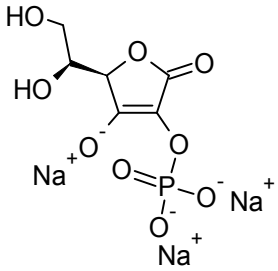

Sodium L-ascorbyl-2-phosphate

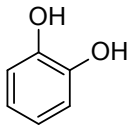

Catechol

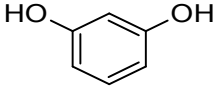

Resorcinol

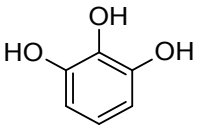

Pyrogallol

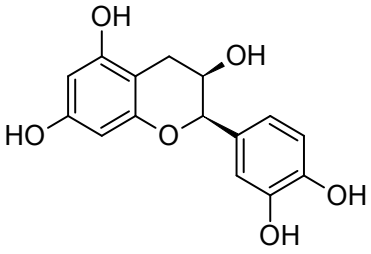

Catechin

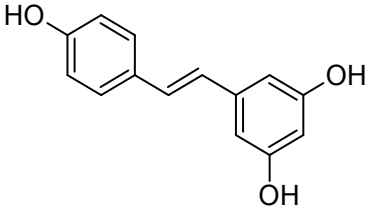

Resveratrol

Scheme 10. The series of antioxidants which were applied in the measurements, by showing their structures.

Behaviour of antioxidants at pH 7

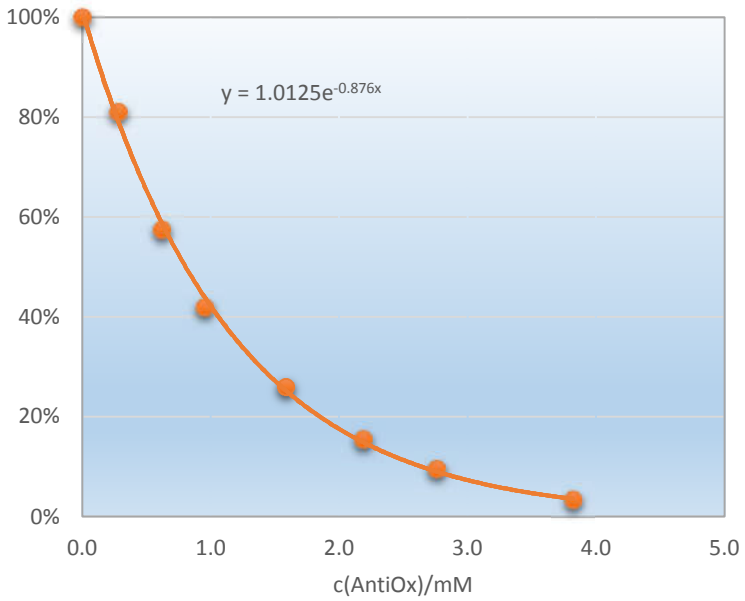

Figure 18. Effect of adding methanol at pH 7. Exponential decay curve for 8-oxoguanine peak current in Step 5, expressed as percent of the peak current obtained for pure saturated guanine solution in phosphate buffer in the absence of methanol. The exponential coefficient in the trend line equation is the decay constant expressed in mM^{-1} (reciprocal of antioxidant (methanol) concentration).

Using methanol yielded a complete vanishing of 8-oxoguanine peak during the experimental work. However, I never think of recommending it as an antioxidant additive for obvious reasons, in fact it is possible to find its antioxidant activity in the literature. (see Fig. 1 in [78]). As can be seen in Fig. 18 methanol exhibits a single-exponential decay all over the concentration range, however, the value of decay constant is below 1 mM^{-1}. It meant methanol antioxidant activity is rather low. Notably, all the simple alcohols under study showed the similar behaviour at pH 7. As can be seen in Fig. 19 ethanol shows more than 70% inhibition effect, however, almost a complete inhibitory effect can be observed by adding 2-propanol (see Fig. 20). Other investigated substances showed different behaviour, however, I assume that at the initial low concentrations the process follows the same mechanism and hence it can be described by using the same equation. I realise that sometimes the concentration range which is selected to fit the trend function is small and in this case it is possible to be matched successfully with the functions of various types. There is another argument supporting the idea of applying the exponential decay function. We observed multiple decay curves in many cases, and because of wider ranges I could prove that it can be fitted with an exponential decay function (see further examples).

The plot of glutathione resembles the single-exponential decay curve, however by closer inspection, it will be revealed that the first step of decay with a coefficient of 32 mM^{-1} ends at about 55% giving about 45% inhibitory effect. Then, a short phase of a slower decay occurs,

which will be levelled off at about 30%. A similar curve was obtained for resorcinol, however in this case a very short phase of a slower decay occurs at about 50% and then it will be levelled off at about 18%. The first step is described by exponential decay coefficient equal to 29 mM^{-1}.

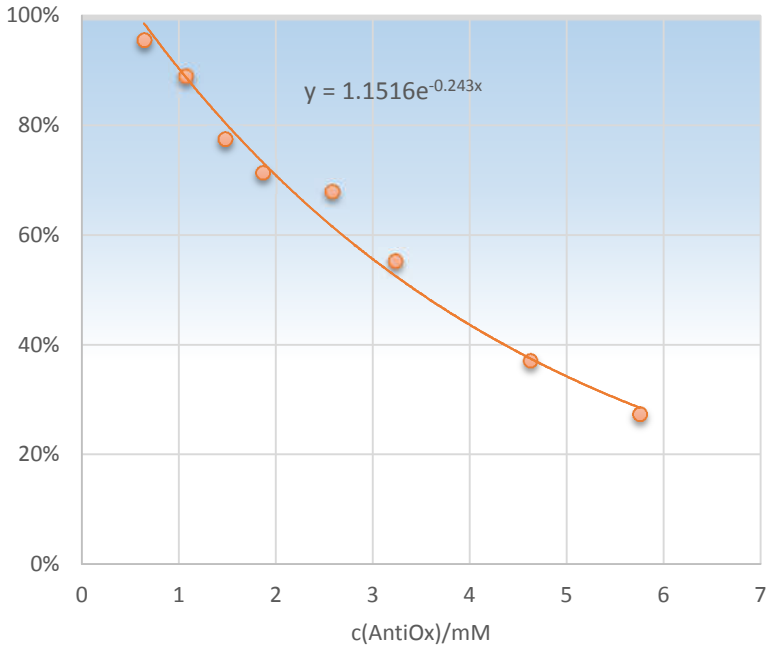

Figure 19. Effect of adding ethanol at pH 7. Conditions as in Fig. 18.

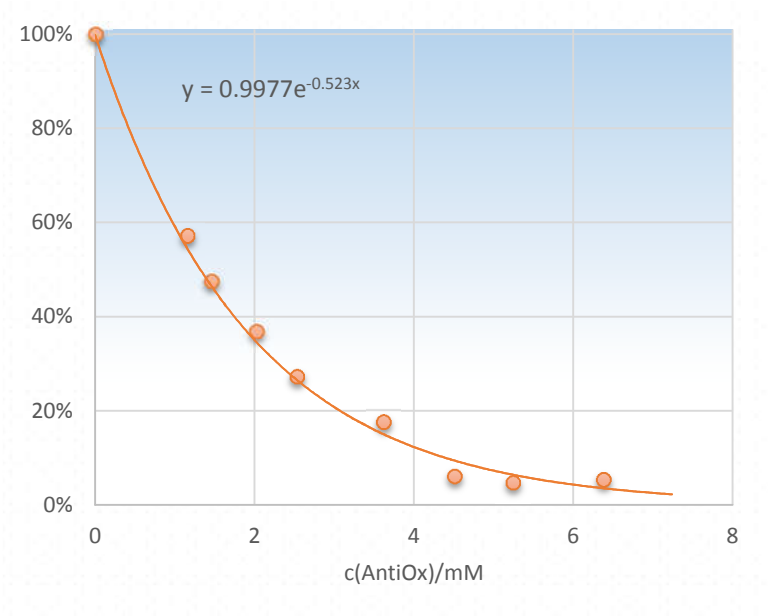

Figure 20. Effect of adding 2-propanol at pH 7. Conditions as in Fig. 18.

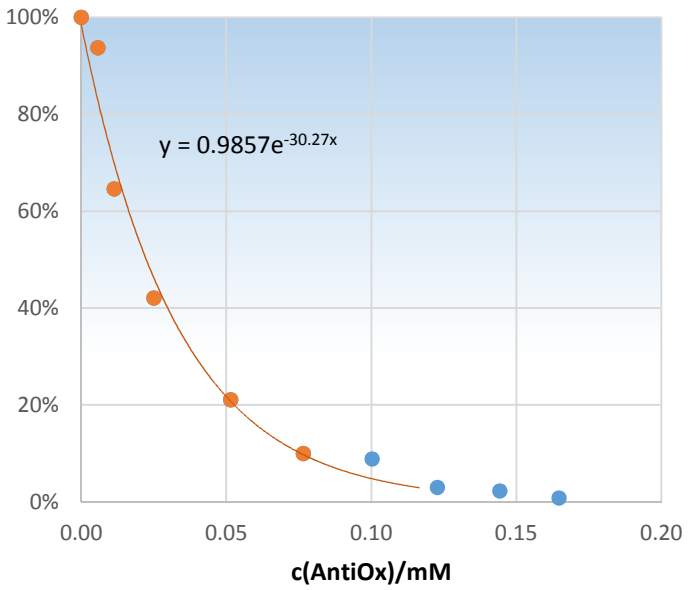

Figure 21. Behaviour of glutathione at pH 7. Conditions at Fig. 18.

Gallic acid displayed the second best antioxidant activity in our research with a decay coefficient of 91.4 mM^{-1} in the first step extending to ca. 0.01 mM concentration (see Fig. 22). At the point which have the highest value of decay coefficient, the height of 8-oxoguanine peak drops to almost 60% compared with its value in the absence of gallic acid. Then, during a slower phase of decay, the third phase leads to a halt at 33% level.

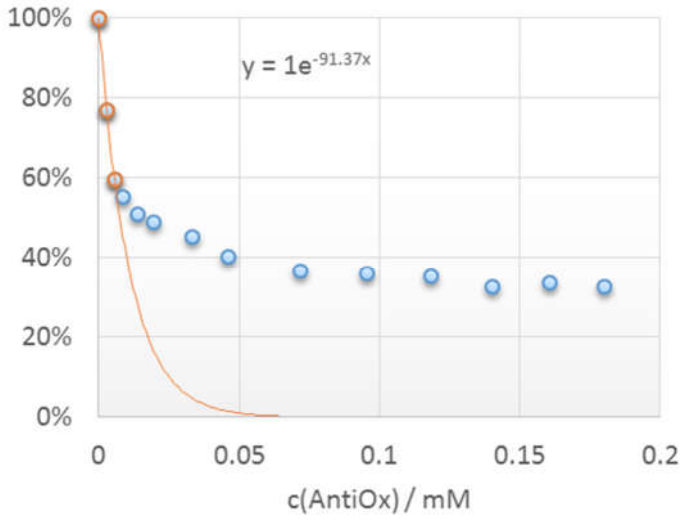

Figure 22.Behaviour of gallic acid at pH 7. Conditions as in Fig. 3. Up to ca. 0.01 mM concentration, very rapid decay is seen, followed by slower steps, and halting at the level of 33%.

I obtained the highest activity by testing resveratrol with a decay coefficient of about 143 mM^{-1}. However, such a high activity ends at ca. 60% by exhibiting 40% inhibition effect at a very

low concentration of 0.003 mM (Fig 23). Then a broad phase with the same activity will appear which is almost independent of concentration, to change into a secondary phase of rapid decay at the concentration ca. 0.035 mM.

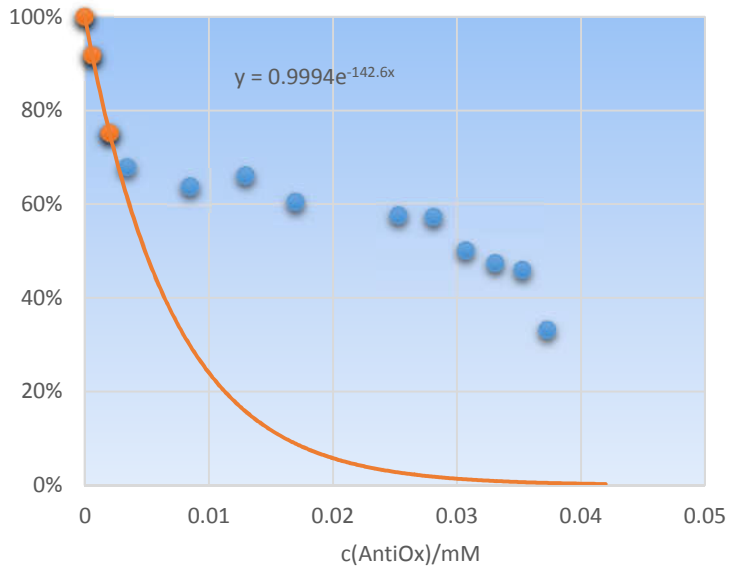

Figure 23. Resveratrol behaviour at pH 7. Conditions as in Fig. 18.

For the case shown in Fig. 17, catechol behaves in a similar way, it means its first phase extends to ca. 0.01 mM, and is characterised by the decay coefficient of 80.97 mM^{-1} (see Fig. 24). A similar pattern can be seen for ascorbyl phosphate but with a decay coefficient only about 6 mM^{-1}, it means its antioxidant activity is very low. Its exponential curve first reach only 60% inhibition at 0.1 mM concentration, and the slow phase ranging to ca. 0.3 mM concentration (see Fig. 25).

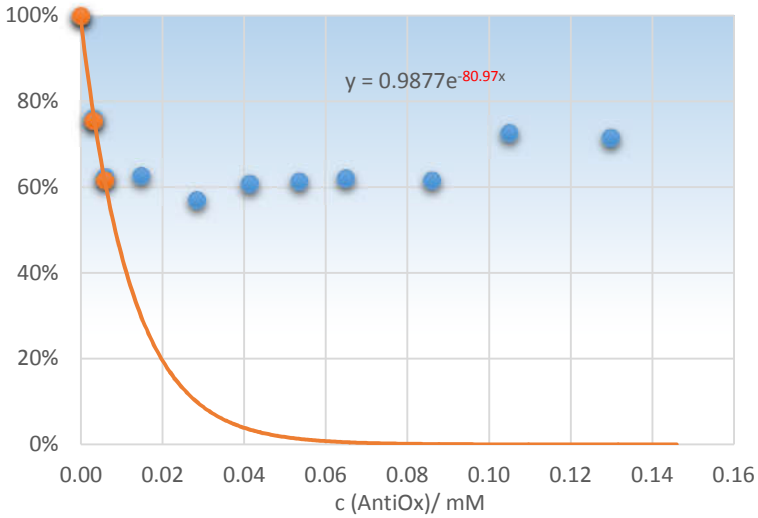

Figure 24. Catechol behaviour at pH 7. Conditions as in Fig. 18.

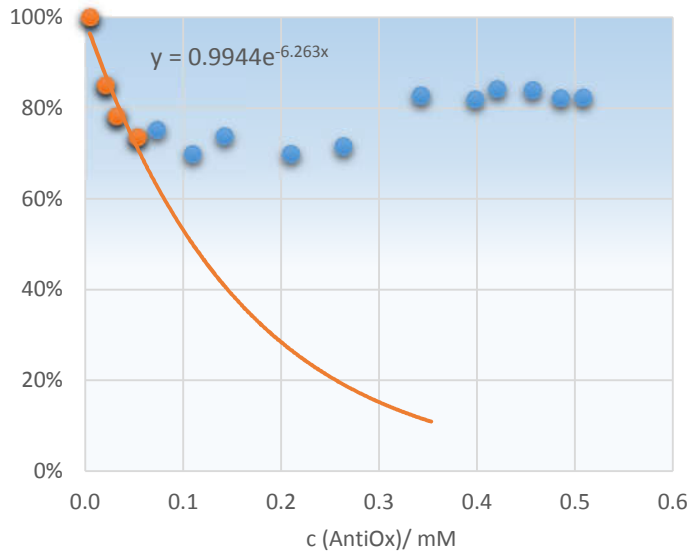

Figure 25. Ascorbyl phosphate behaviour at pH 7. Conditions as in Fig. 18.

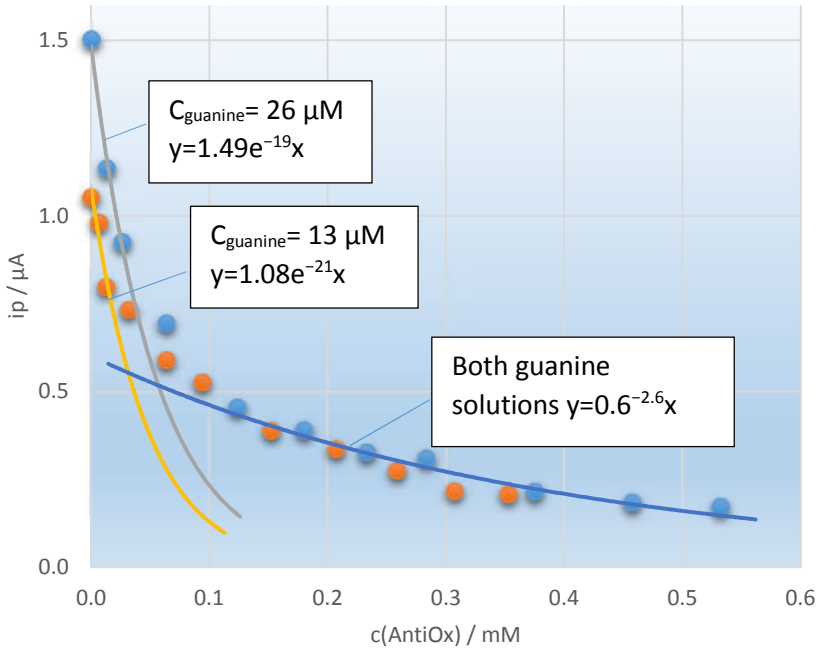

Figure 26. Pyrogallol behaviour at pH 7 and guanine concentration effect. General conditions as in Fig. 18. 8-Oxoguanine peak current as a function of pyrogallol concentration for two different concentrations of guanine.

Pyrogallol demonstrated a double-exponential decay, as it can be seen in Fig. 26. To obtain these results two different concentrations of guanine were used, saturated solution and two times diluted saturated solution in pH 7 phosphate buffer. Interestingly, the decay coefficient for these

two guanine concentrations were almost the same, equal to ca. 20 mM^{-1}. The first rapid decay, in the saturated solution of guanine, occurred up to ca. 0.06 mM concentration and the second one, in the doubly diluted solution, it occurred up to 0.03 mM concentration. The ratio of peak currents for the initial points, in the absence of pyrogallol and in the region of the first decay phase, is equal to 1.4 which is very close to the square root of 2, however, because this result has been obtained from only two points, it is better not to give too much significance for this observation.

Catechin exhibits a similar decay character. It means during the double-exponential curve, first it shows a fast decay with the decay parameter of 38 mM^{-1} up to 0.025 mM concentration and then its decrease slows down (see Fig. 27).

The results of measurements at pH 7 are summarised in Fig. 28. As can be seen in this figure, resveratrol and gallic acid exhibited the highest antioxidant activity, and the lowest antioxidant activity is related to simple alcohols. Alcohols are present only to be compared with the other antioxidants. Another reason for testing alcohols is their perfect inhibitory effect and a single exponential decay. In the case of the other antioxidants, the decay coefficients present in Fig. 28 have been calculated by using the first rapid decay. The t-test confidence intervals (95%) for regression coefficient are very low, ± 3% of the coefficient value for Na ascorbyl phosphate, ±2% for pyrogallol and glutathione, ±1.1% for catechin and less than ±1% for more active antioxidants. These low values may mislead because they are due to the use of logarithmic functions and narrow range of data. The coefficient limits for simple alcohols under study were higher, however, the value of ±0.03 (which correspond to ca. ±3%) for the whole range of 8-oxoguanine percent generation and concentration data means that in this case the fit is really good.

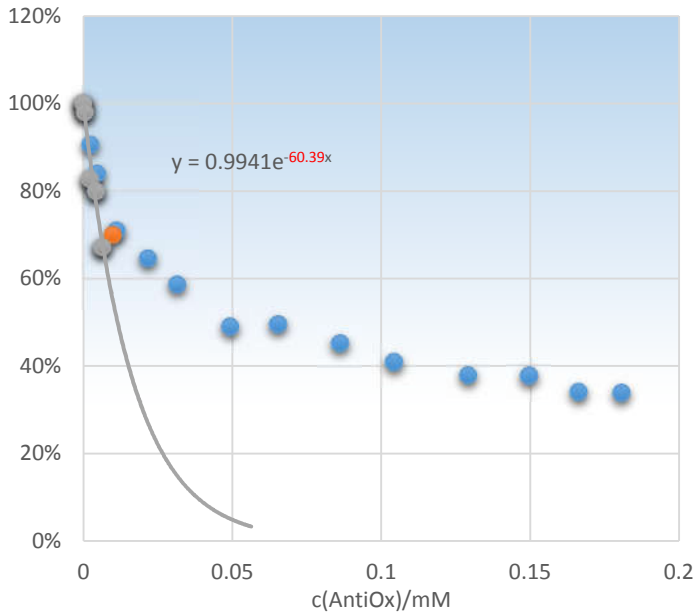

Figure 27. Catechin behaviour at pH 7. Conditions as in Fig. 18.

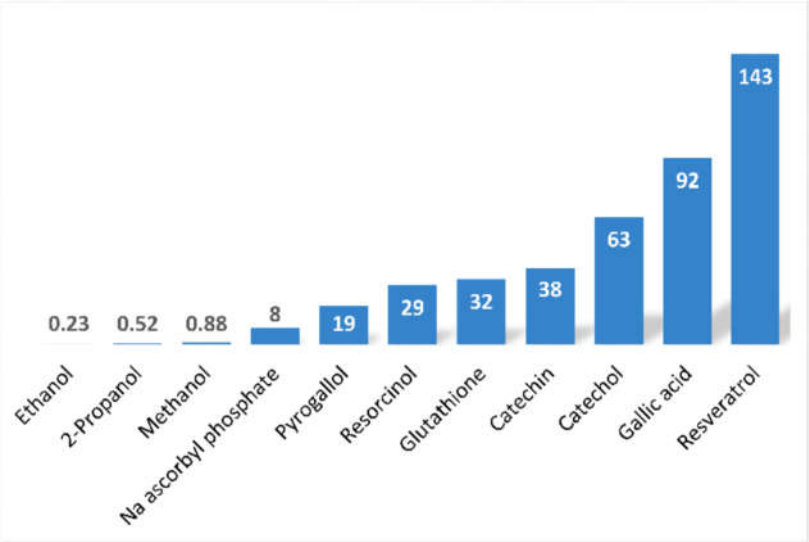

Figure 28. Antioxidative activity coefficients (exponential decay parameters) for investigated substances at pH 7 expressed in mM^{-1}. Where applicable, the decay parameters were used only from the rapid phase at low concentrations.

After the rapid phase of 8-oxoguanine generation with increasing antioxidant concentration, the decay effect weakened, which led to a limiting value of inhibition. Fig. 29 demonstrates these values to which the 8-oxoguanine generation could be reduced in the second step.

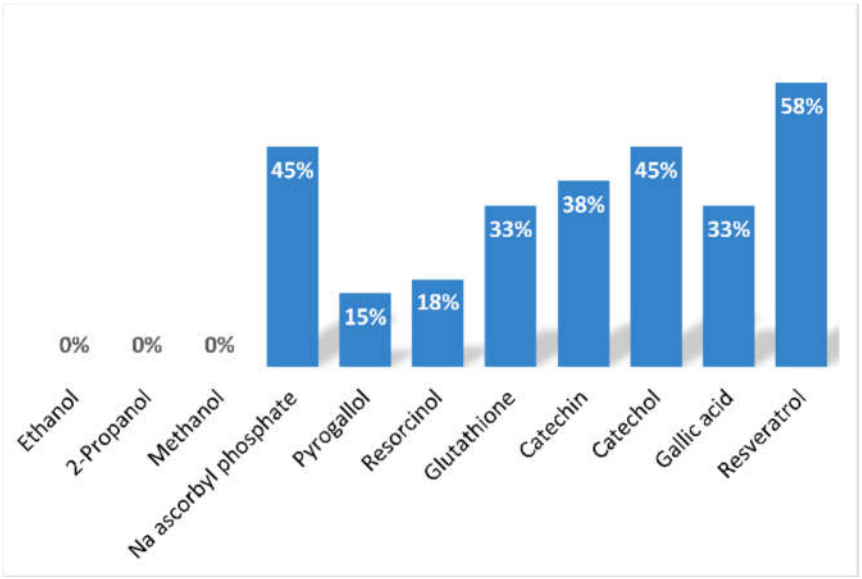

Figure 29. The limiting values of percent 8-oxoguanine formation for studied antioxidants at pH 7. The complement to 100% could be regarded as antioxidant capacity. In some cases, like resveratrol, further reduction in this level could be elicited by adding much higher amounts of the antioxidant.

I noticed that the ability to produce 8-oxoguanine changed with time. I checked this effect in detail for pyrogallol, for concentrations 0.02 and 0.03 mM (close to the end of the first rapid phase, see Fig. 30). The measurements were done at the lower concentration, were giving almost the same

results, during ca. 200 s after adding pyrogallol, then they were rising to catch the steady state, at ca. 20% higher peak current, after 500 s. The results were stable and for ca. 1000 s after adding pyrogallol in 0.03 mM concentration, then they began rising and at this point the second phase started, which exhibited an in-stability for 3000 s. During this phase, measurements were yielding random values in the range of 20% to 30% higher compared with the first measurement after adding pyrogallol. As can be seen in Fig. 30 the changes in the concentrations of guanine and 8-oxoguanine correspond to inverse changes in the concentration of pyrogallol exactly. There are even three peaks which show this relationships very clearly. The first peak at 1762 s exhibits an increase in the amount of guanine and 8-oxoguanine, and at the same moment the amount of pyrogallol decreases. Second peak at 2997 s displays a rise in the concentrations of guanine and 8-oxoguanine on one side and to the opposite side in the case of pyrogallol a dramatic drop in the concentration. The third interesting peak occurred at 3867 s with the opposite changes in the amount of the relevant compounds. These results are not the function of potential (in hold or scan sequences), they are only affected by time, probably due to autoxidation of pyrogallol at the electrode surface and in solution. It means that by autoxidation of pyrogallol in the solution more ROS were produced, therefore more guanine got oxidized and consequently more 8-oxoguanine was produced. It is assumed that the currents which were recorded in Step 4 (reduction at −1.0 V) are virtually the same and were not affected considerably. The plots of charge vs. square root of time illustrated that the slope remained constant in the linear part, however, the intercept increased with time by about 25%, which would correspond to the changes in the peak current of 8-oxoguanine waves which may have occurred accidentally, because I was not able to record the current in the first 100 ms accurately (see Fig. 31). However, the constant slop confirms that the amount of oxygen which is getting reduced on the surface of electrode remained unchanged for all the process. On the other hand the variation of the intercepts may be explained by guanine adsorption that is oxidised on the electrode and affects the amount of the charge. It is notable that at the lower pyrogallol concentration, the charge curves, which were recorded in the absence of pyrogallol, almost overlapped. During step 2 (before reduction of dioxygen, and hence before 8-oxoguanine generation) the height of 8-oxoguanine peak did not change, however the background current increased, and intensity of guanine peaks were rising following the same pattern as the 8-xoguanine peaks in Step 5. This means probably the activity of the electrode towards guanine increased or more guanine was adsorbed on the surface of the electrode. This effect could explain an increase in the intercept values in Anson plots for Step 4 described above. To avoid the instability effects and to obtain reproducible results, in other measurements, consecutive aliquot stock solutions of antioxidants were added in a time period not longer than 60 s and then measurements were done immediately.

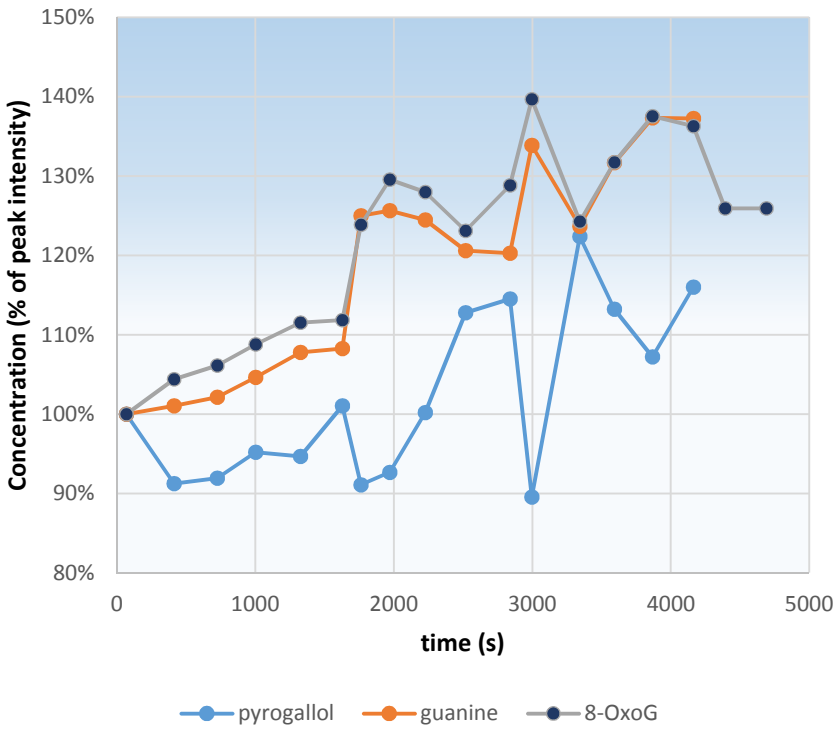

Figure 30. Guanine, 8-oxoguanine and pyrogallol concentration variation with time. Three peaks correspond the opposite behaviour of guanine and 8-oxoguanine with pyrogallol.

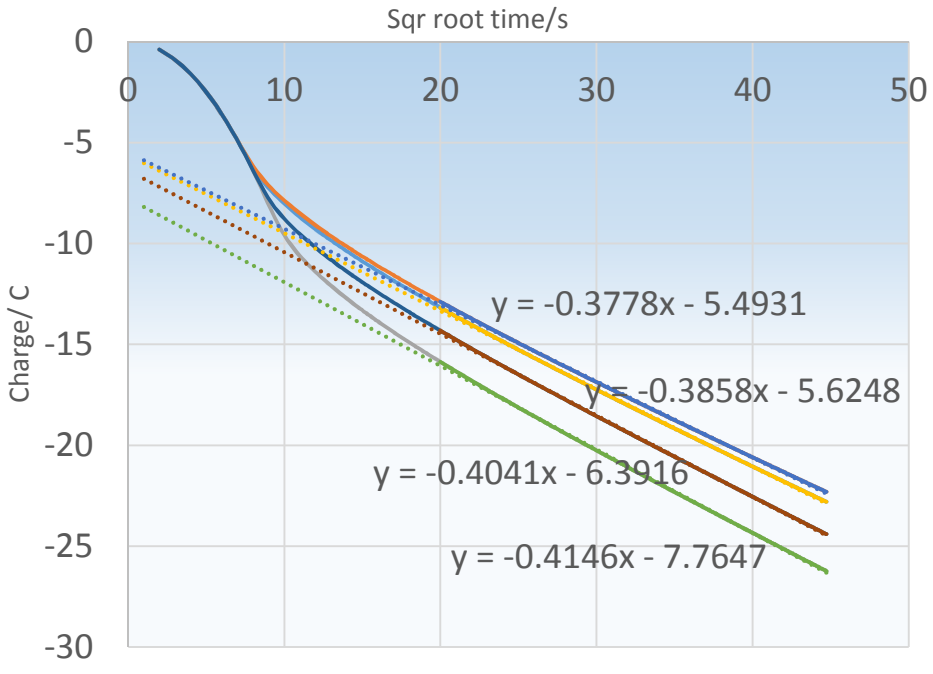

Figure 31. Charge versus square root of time. At the constant concentration of pyrogallol.

I do not have any good rationalization why the curves exhibit the exponential decay. An acceptable opinion would be the competitive reactions of guanine and antioxidants with ROS, both following the second order. Another choice was second order competitive reactions, but with a constant excess amount of ROS. In both of these cases the experimental points should fit an exponential decay function. As it was proven by the linearity of Anson plots (the charges recorded in Step 4), it is known that the formation of superoxide is controlled by diffusion. However, modelling of this process is rather difficult, because the initial product undergoes further reactions yielding various Reactive Oxygen Species. In the case of methanol (see Fig. 18) such a good fit covering all the current range of 8-oxoguanine peak, proves that the fit is correct. About the other antioxidants, the single-exponential decay curve could be seen only at a very low concentration, except for glutathione, for which this range is wider, up to 0.02 mM.

I used the exponential decay constant K as a measure of antioxidant activity in my study. My applied parameter is connected to the very often used IC_{50} parameter, the half maximal inhibitory concentration, it means the concentration which is required to inhibit a process by half. If the inhibitory reaction follows the exponential decay curve then these two parameters will be directly related, $IC_{50}=\ln 2/k$. While for simple alcohols this is correct for the total range of concentration, in the case of other antioxidants, the determination of IC_{50} single point may be incorrect.

In some methods for evaluating the antioxidant activity, the kinetics was used of the reaction between the antioxidant and a free radical as a model (often α,α'-diphenyl-β-picrylhydrazyl radical (DPPH•) or 2,2'-azinobis(3-ethylbenzthiazoline-6-sulphonic acid) radical cation ($ABTS^{\bullet+}$) were applied). These processes did not notably lead to entire disappearance of radicals but to a constant concentration. The level off concentration is also applied as a parameter of antioxidant activity. Some polyphenols, such as catechin, displayed a biphasic kinetic manner, with an initial fast step [79], which was explained by the generation of adducts between polyphenols and $ABTS^{\bullet+}$ radical. This pattern resembles the behaviour observed in my study, where after the fast decay, the increase in the antioxidant concentration did not affect the peak intensity of 8-oxoguanine, particularly, in the case of resveratrol (see Fig. 23).

Behaviour of antioxidants at pH 9

Phenolate anions can be oxidised much easier than neutral phenols, therefore we assume that they may behave differently in the alkaline solutions. That is why we performed our research in phosphate buffer pH 9 also. Polyphenols are oxidised in the alkaline solutions very easily because they react with dioxygen directly which may generate superoxide anion radicals. This process is employed in some methods of antioxidant assessment assays [80]. In my study, to avoid of any changes in the composition of the solution during the experiment, I decided to leave the solution of polyphenol in phosphate buffer pH 9 overnight in the air atmosphere to be oxidised completely and then apply it in my next day measurements. These kinds of measurements carried out in the air atmosphere totally.

As I could expect, simple alcohols exhibited higher antioxidant activity at pH 9 with decay coefficient about 1.0 mM^{-1} (see Fig. 32, 33 and 34). Among them 2-propanol is the most active one. However, glutathione displayed lower activity, with the decay coefficient equal to 3.5 mM^{-1} (see Fig. 35). Gallic acid behaviour at pH 9 is similar to pH 7 but its decay coefficient increased

up to 135 mM^{-1}. The decay character of resorcinol did not change from that at pH 7, only the decay coefficient decreased a little to 23 mM^{-1} (see Fig. 36). Virtually, the result obtained for resveratrol was similar in that its decay coefficient in the first phase dropped to 56 mM^{-1} (see Fig. 37). The other polyphenols such as catechol and catechin, and ascorbyl phosphate showed more dramatic changes (see Fig. 38, 39 and 40). In these cases, I could observe only an increase in the generation of 8-oxoguanine instead of the decay effect. For example in the case of ascorbyl phosphate, this increase in the height of 8-oxoguanine is reaches 160%, and even after a huge excess added (a couple of crystals instead of stock solution), 8-oxoguanine was still produced. For pyrogallol, only after adding the first portion, a small drop could be seen but afterwards after adding subsequent portions the amount of 8-oxoguanine formed increased up to 140% at 0.2 mM pyrogallol concentration. (see Fig. 41).

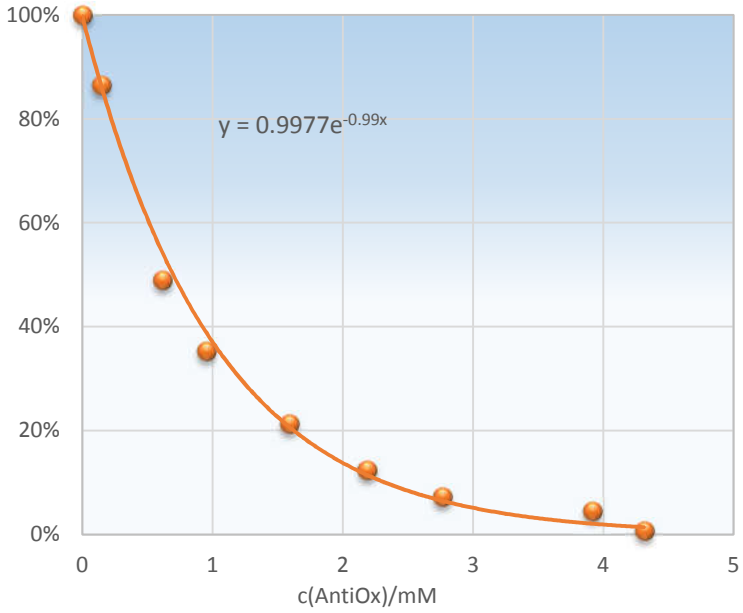

Figure 32. Effect of adding methanol at pH 9. Conditions as in Fig. 18

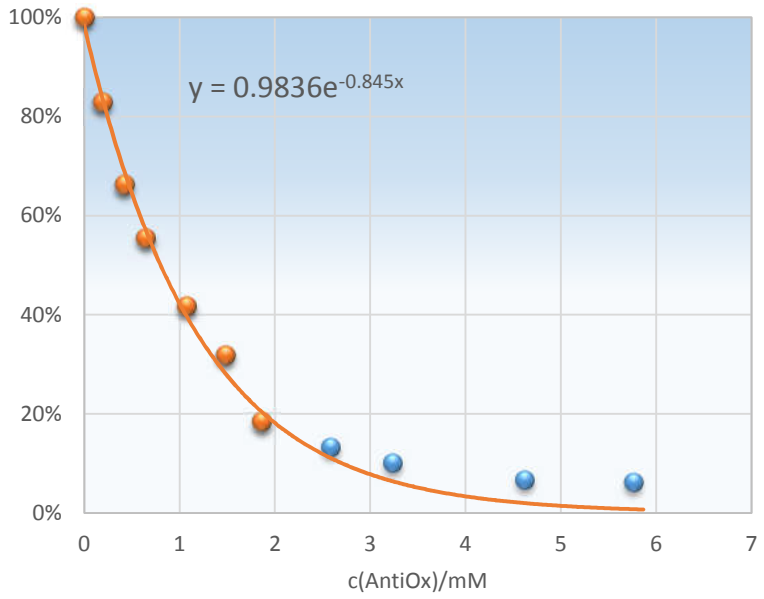

Figure 33. Effect of adding ethanol at pH 9. Conditions as in Fig. 18.

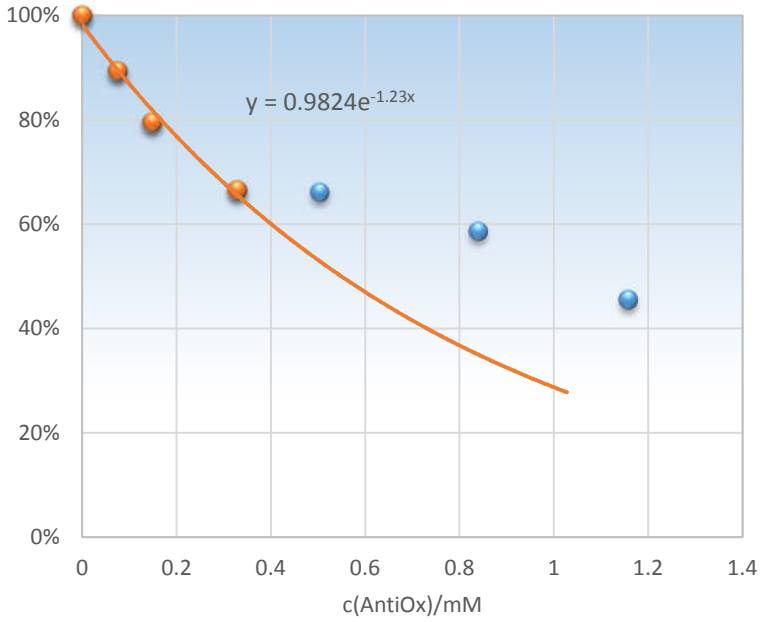

Figure 34. Effect of adding 2-propanol at pH 9. Conditions as in Fig. 18.

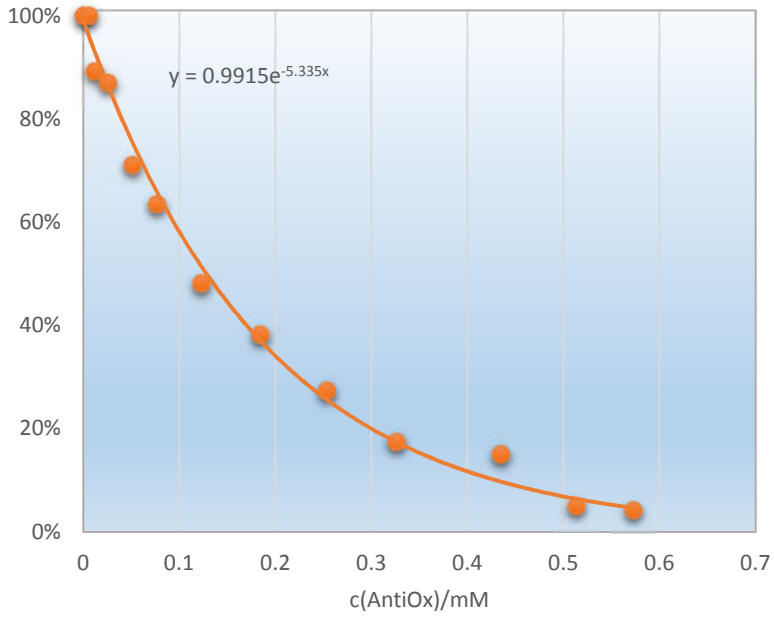

Figure 35. Behaviour of glutothione at pH 9. Conditions as in Fig. 18.

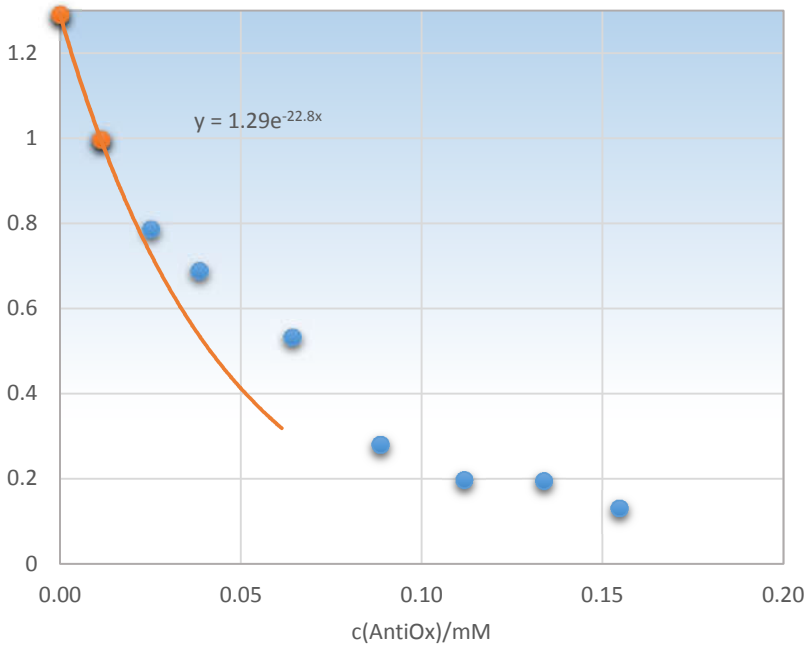

Figure 36. Behaviour of resorcinol at pH 9. Conditions as in Fig. 18.

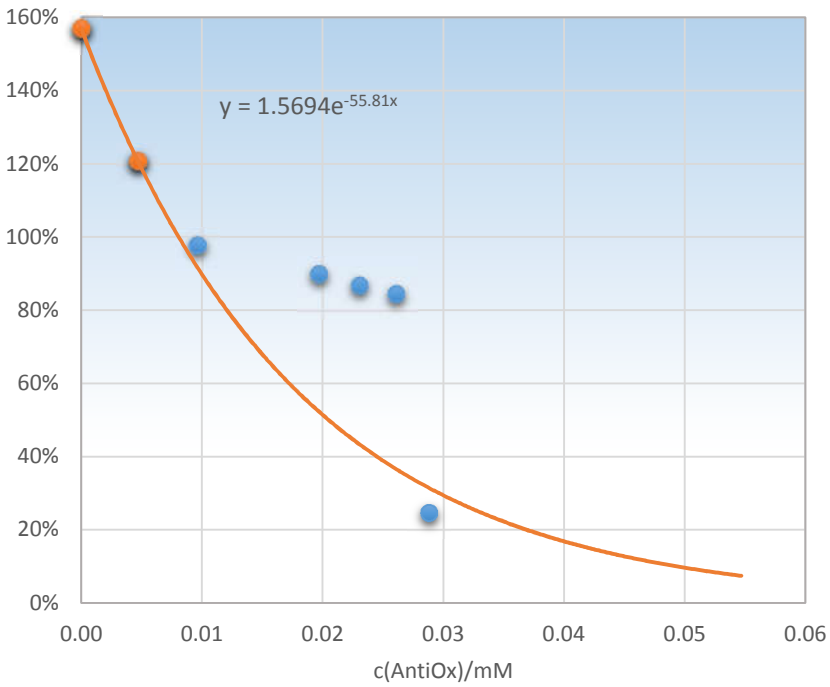

Figure 37. Behaviour of resveratrol at pH 9. Conditions as in Fig. 18.

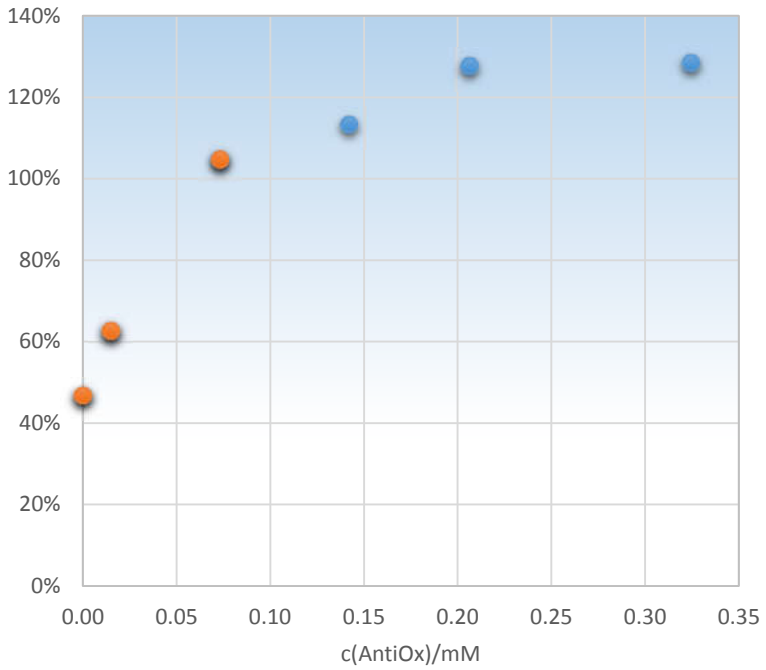

Figure 38. Behaviour of catechol at pH 9. Conditions as in Fig. 18. Instead of decay effect, only pro-oxidative effect can be seen.

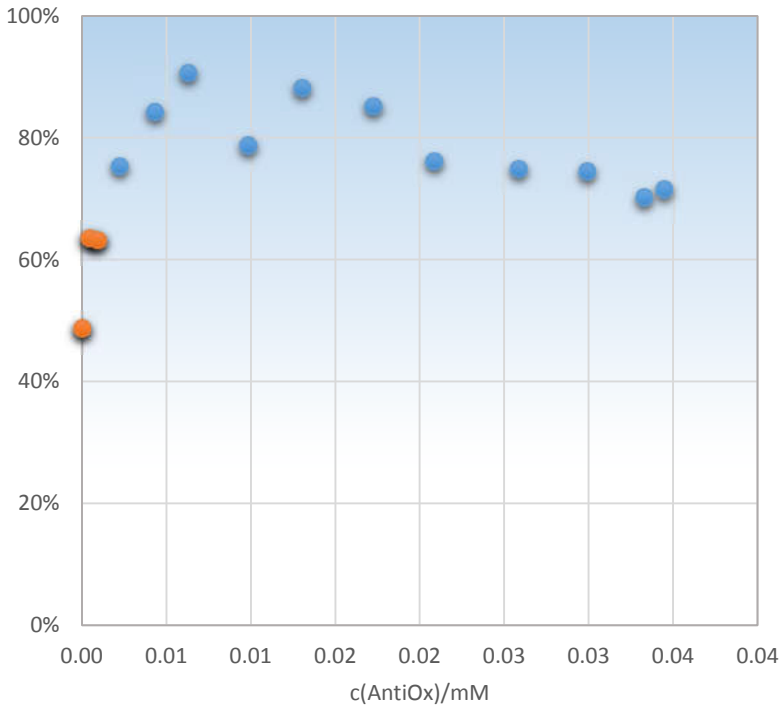

Figure 39. Behaviour of catechin at pH 9. Conditions as in Fig. 18. Instead of decay effect, only pro-oxidative effect can be seen.

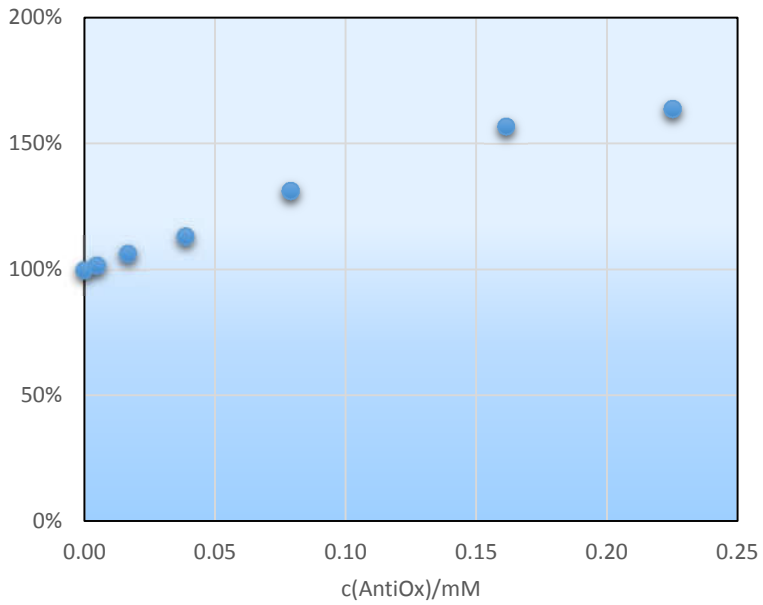

Figure 40. Behaviour of ascorbyl phosphate at pH 9. Conditions as in Fig. 18. Instead of decay effect, only pro-oxidative effect up to 160% can be seen.

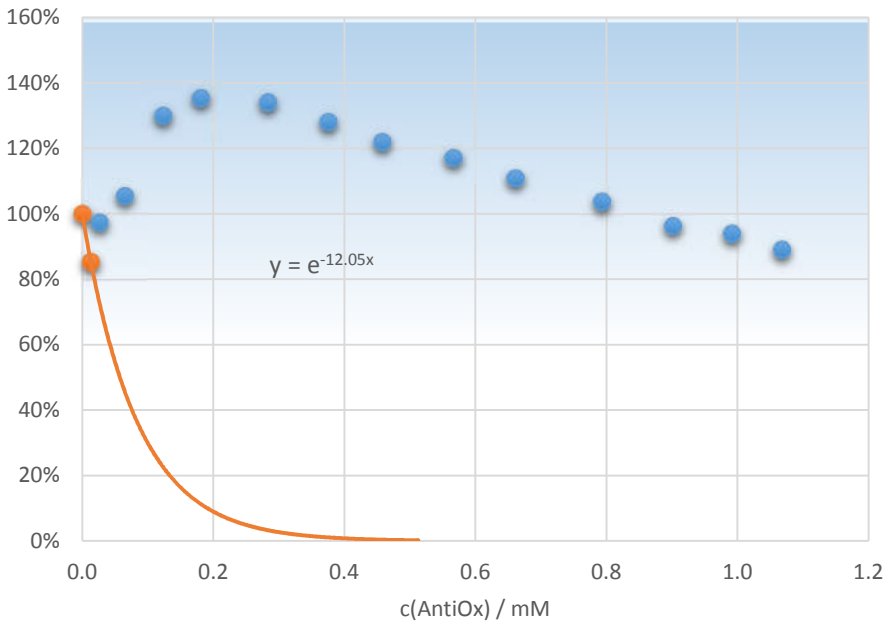

Figure 41. Pro-oxidative activity of pyrogallol at pH 9. Conditions as in Fig. 18. Only the first portion of pyrogallol led to a decrease in 8-oxoguanine production. Then, up to 0.2 mM, the amount of 8-oxoguanine increased to begin slowly falling down.

The pro-oxidative activity, which was observed at pH 9 in the case of some polyphenols and ascorbyl phosphate, may suggest that this pro-oxidative effect can be responsible for weakening the antioxidative activity at a higher concentration of antioxidant at pH 7.

The results described in this Section were the subject of my publication [81].

Electrode modification for guanine analysis

Guanine and its derivatives, like 8-oxoguanine and methylguanine, are important biomarkers of oxidative stress and many diseases. Effective sensors would make early diagnosis possible and that is why their development is so important. Recently, various nanomaterials, nanoparticles and materials with nanocavities, have been employed this end, among them also pyridine-2,6-dicarboxylic acid doped with graphene oxide. I have noticed that the films formed by the oxidation of other pyridinecarboxylic acids on the glassy carbon electrode may exhibit even better characteristics, particularly when inner layers of the film become available after swelling with an organic solvent.

Due to the importance of detecting guanine and the products of this oxidation process such as 8-oxoguanine, I decided to devote the second part of my research to the preparation of a sensitive electroactive system on the surface of the work electrode to be able to detect these compounds in an easier, more efficient and cost effective way.

I have started my work was by repeating some of the literature reports such as electropolymerisation of pyridine-2,6-dicarboxylic acid on the surface of GCE [82]. Then, I decided to try other derivatives of this compound. The results of my measurements are below.

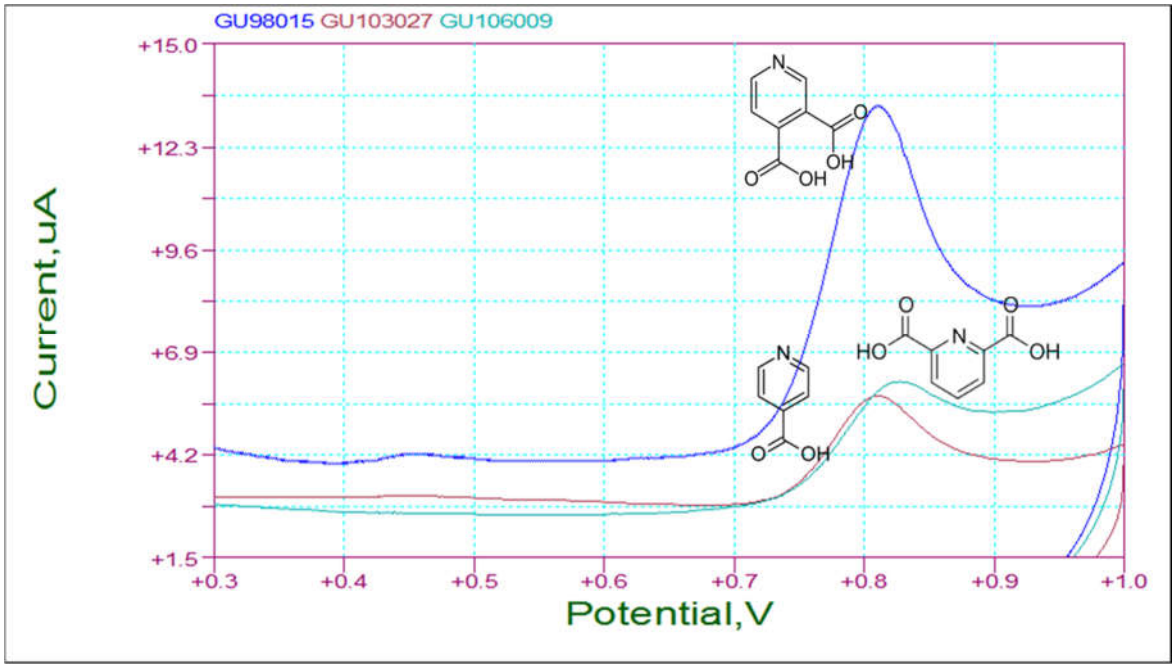

Figure 42. CV. Scan rate= 100 mV/s. 1st Scan. Guanine oxidation peak, using modified GCE by GU98015: Pyridine-3,4-dicarboxylic acid, GU103027: Pyridine-4-carboxylic acid, GU106009: Pyridine-2,6-dicarboxylic acid.

As can be seen in Fig. 42, the most intensive peak was obtained by electropolymerisation of pyridine-3,4-dicarboxylic acid on the surface of a glassy carbon electrode and the intensity of the peak related to the electropolymerisation of pyridine-2,6-dicarboxylic acid and pyridine-4-carboxylic acid are comparable. From this result it is well seen that the best compound for GCE modification, among these three pyridine carboxylic acid derivatives, is pyridine-3,4-dicarboxylic acid.

Afterwards, I wanted to check whether the thickness of the polymer layer affects the efficiency of the modified electrode. Thus, I did another series of measurements by applying different number of cycles during the polymerisation process.

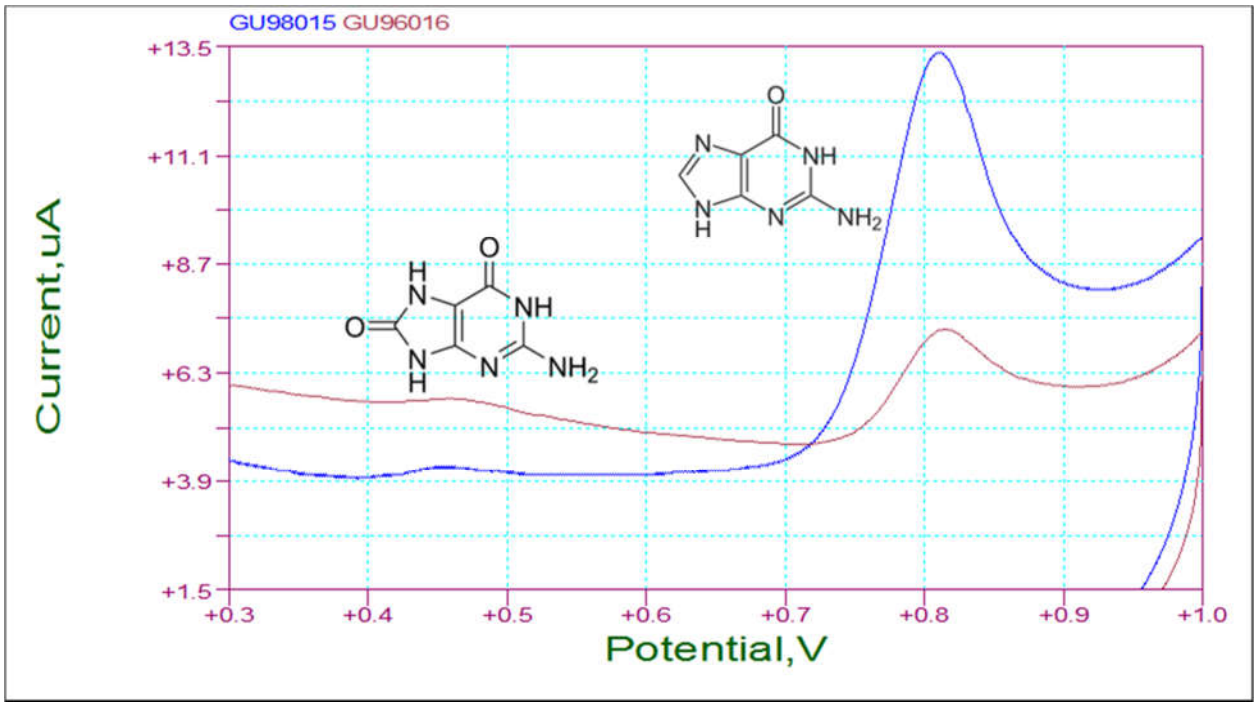

Figure 43. CV scan rate =100 mV/s.1st Scan. Effect of layer thickness. GU98015: Pyridine-3,4- dicarboxylic acid (32 cycles). GU96016: Pyridine-3,4- dicarboxylic acid (12 cycles).

As it can be seen in Fig 43, the thicker polymer layer can detect oxidised guanine several times better by showing a much more intensive oxidation peak. It is probably because the thicker polymer layer provides more space for guanine to penetrate and then get oxidised on the GCE more efficiently.

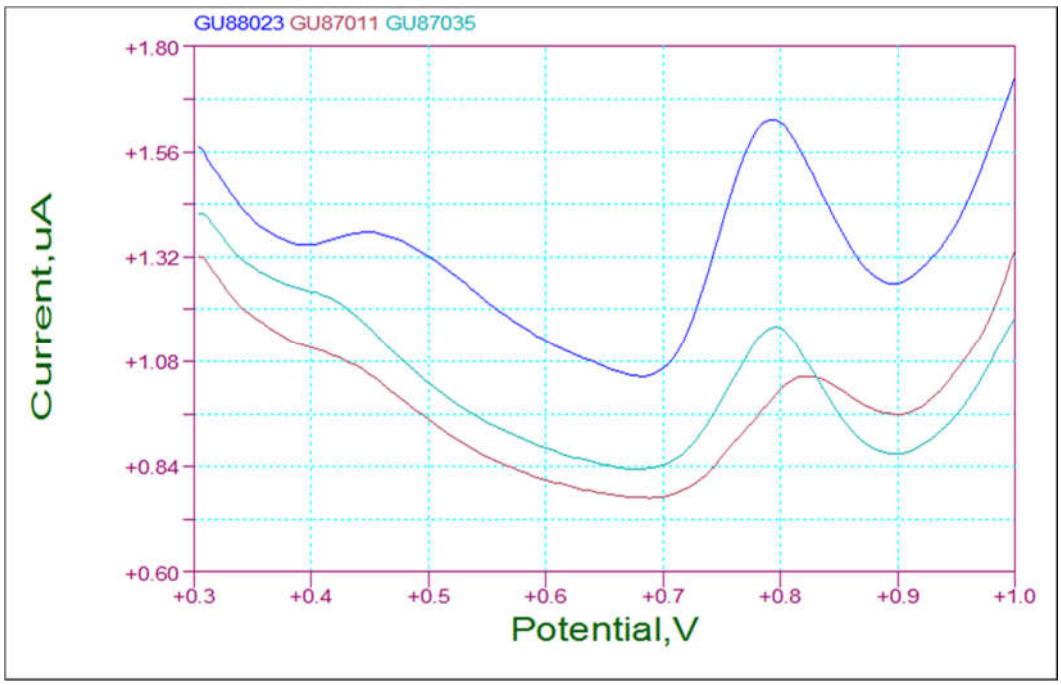

Figure 44. DPV. Guanine dissolved in GU88023: Phosphate buffer solution (KH2PO4(0.2 M)+KOH), GU87011: Phosphate buffer solution (Na_2HPO_4 (1/15 M)+H_3PO_4), GU87035: Phosphate buffer solution (KH2PO4(1/15 M))+KOH).

As can be seen in Fig 44 the presence of potassium cations can increase the electrochemical response of guanine and increasing the concentration of this cation can be more effective. On the other hand, the presence of sodium cations in comparison with potassium cations showed to be not that favourable.

As we know from the literature, guanine molecules in the presence of potassium cations can give quadruplexes by forming hydrogen bonds between four guanine molecules. To prepare such a structure in the presence of potassium cations, more guanine from the solid phase will dissolve into the liquid phase. My measurements could show that this effect is more pronounced in the present of potassium cations and sodium cations are much less effective. Therefore, I preferred to use phosphate buffer of potassium salts in my research.

Then I tried to check the effect of adsorbed porphyrins on the detection of oxidised guanine. In fact I obtained interesting results by applying different kinds of porphyrins (see Fig. 45).

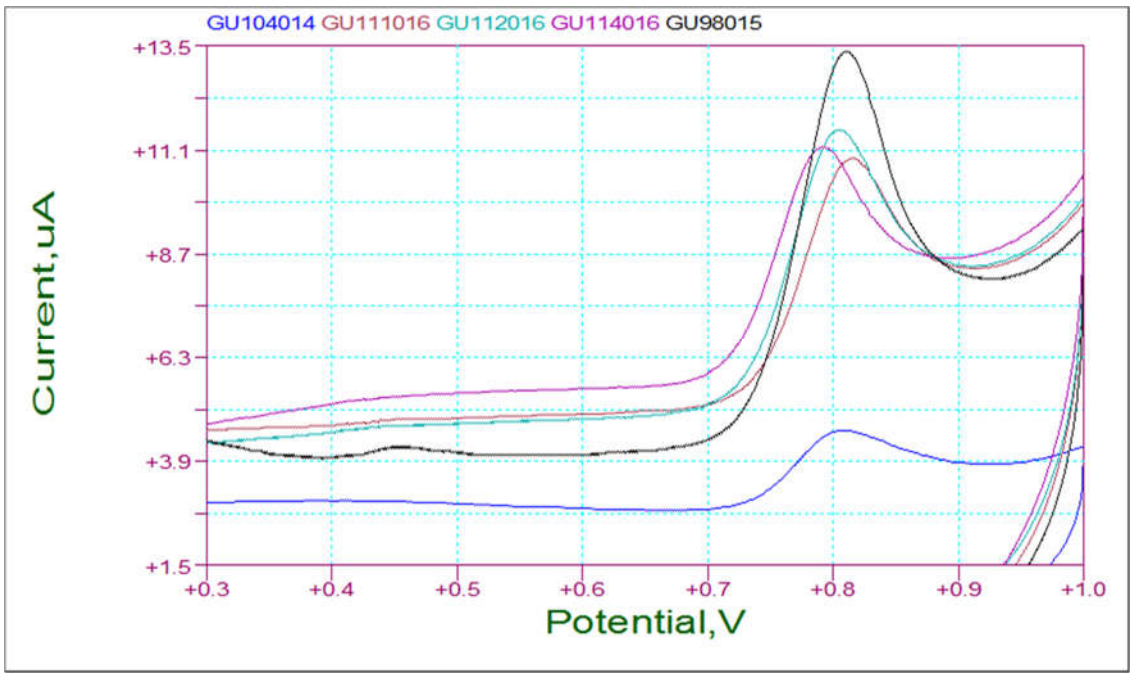

Figure 45. CV. Scan rate: 100 mV/s. 1st Scan. Polymer: Poly-pyridine-3,4-dicarboxylic acid. GU104014: Only Guanine (without any adsorption), GU111016: Guanine (with CoTPP adsorbed), GU112016: Guanine (with H_2-TPP adsorbed), GU114016: Guanine (with ZnTPP adsorbed), Gu98015: Guanine (with FeTPP adsorbed).

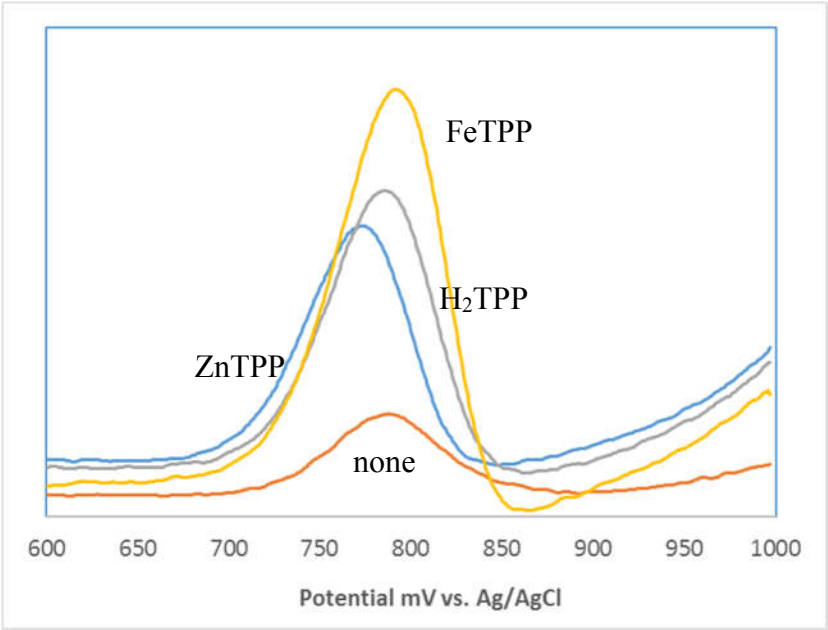

Figure 46. Semiderivatives of voltammograms with a film prepared by oxidation of pyridine-3,4-dicarboxylic acid treated with THF solutions of indicated tetraphenylporphyrins. 'None' denotes the case of no treatment.

As can be seen in Figs. 45 and 46, the best effect is obtained with the electrode modified by iron-porphyrin adsorption. Another interesting thing is that free base porphyrin, H_2TPP, was also effective. It means that contrary to what we thought initially, the interaction of guanine with

porphyrins is not only through the metal centre (in metalloporphyrins) but in this case π-π interactions between the π systems of guanine and porphyrins play a great role.

Because all the porphyrins were used in tetrahydrofuran (THF) solutions, I thought that maybe this solvent itself can affect the detection of guanine by swelling the polymer layer (See Fig. 47).

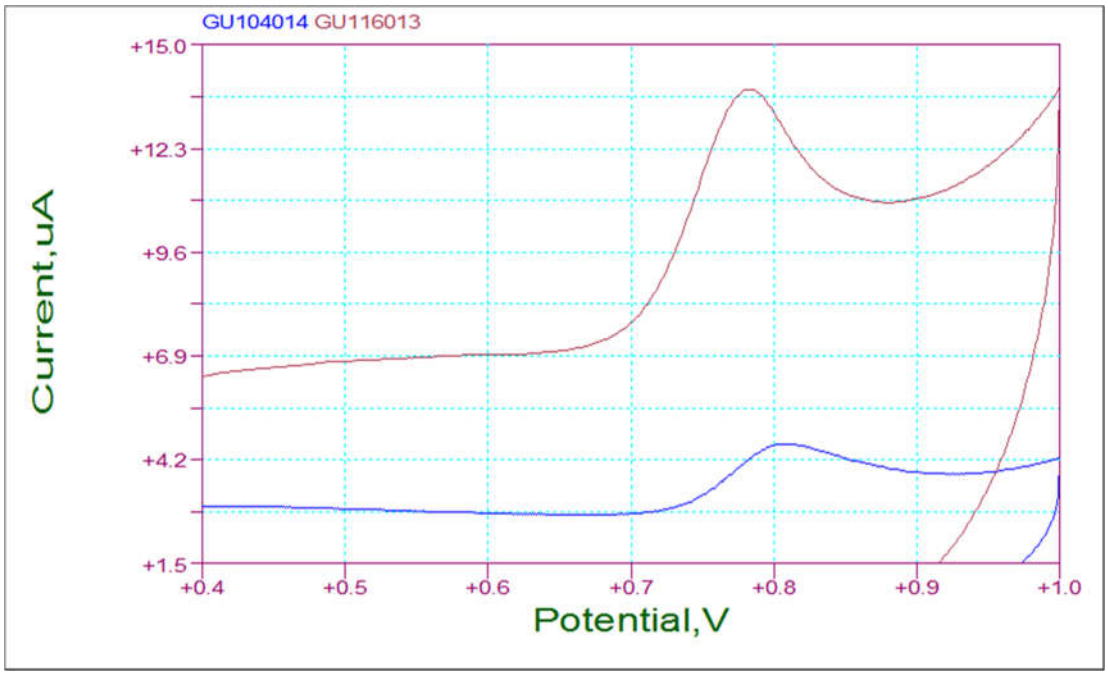

Figure 47. CV. Scan rate: 100 mV/s .1st Scan. GU104014: Only Guanine (without any adsorption), GU116013: by immersing polymerised layer in only THF.

As can be seen in Fig 47, even THF itself can modify the surface of the electrode efficiently. This effect is based only on swelling the polymer layer in the presence of the solvent and offering more space for guanine to be adsorbed on the electrode.

Interestingly, 8-oxoguanine could be seen in the voltammogram of guanine in the case of the electrode modified by iron porphyrin adsorption (see Fig. 48). This means that iron porphyrin itself is able to partly oxidise guanine.

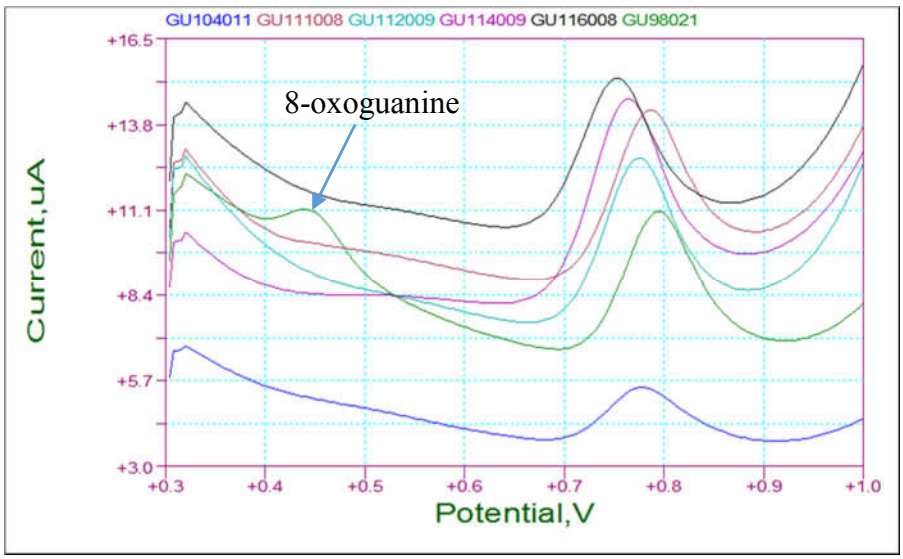

Figure 48. OSWV. Polymer: Poly-pyridine-3,4-dicarboxylic acid. GU104011: Guanine (electrode not modified by porphyrins), GU111008: Guanine (with CoTPP adsorbed), GU112009: (with H_2-TPP adsorbed), GU114009 (with ZnTPP adsorbed), GU116008: modified by immersing polymerised layer in only THF, GU98021: (with FeTPP adsorbed).

Beside commercially available of pyridine carboxylic acid derivatives, I tried some synthesised pyridine carboxylic acid derivatives to modify GCE. The results are presented below.

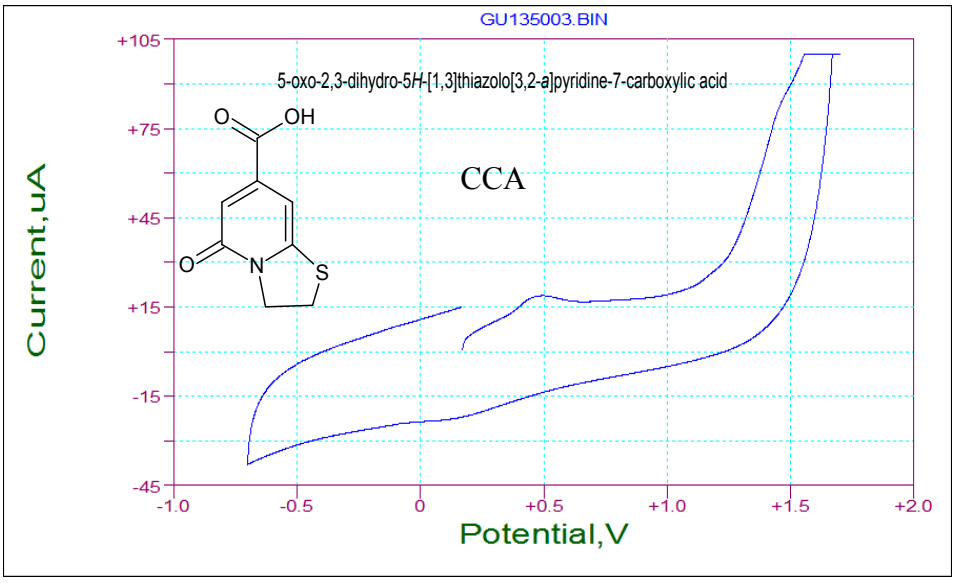

Figure 49. Structure, chemical name (full and symbol) and voltammogram of a synthesised derivative of pyridine carboxylic acid.

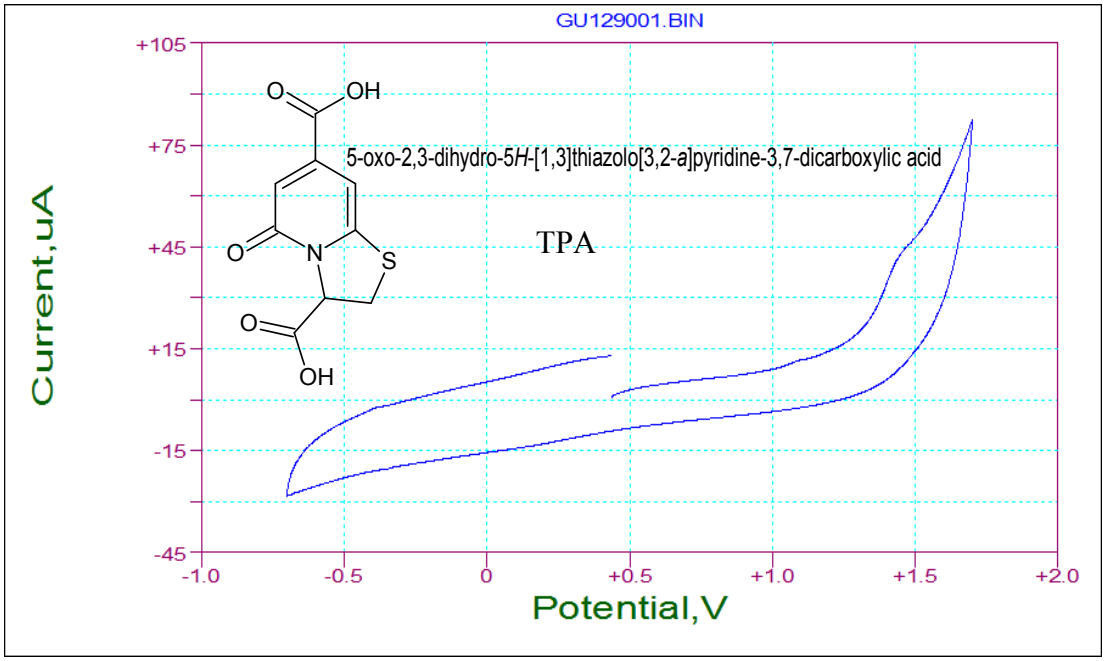

Figure 50. Structure, chemical name (full and symbol) and voltammogram of a synthesised derivative of pyridine carboxylic acid.

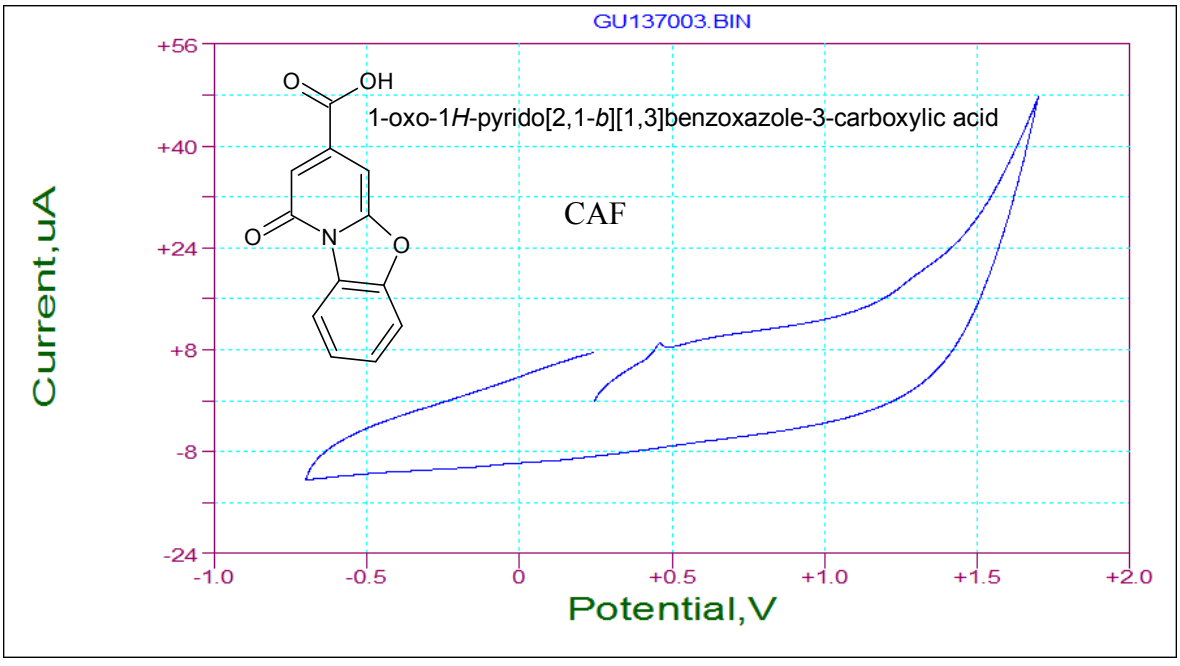

Figure 51. Structure, chemical name (full and symbol) and voltammogram of a synthesised derivative of pyridine carboxylic acid.

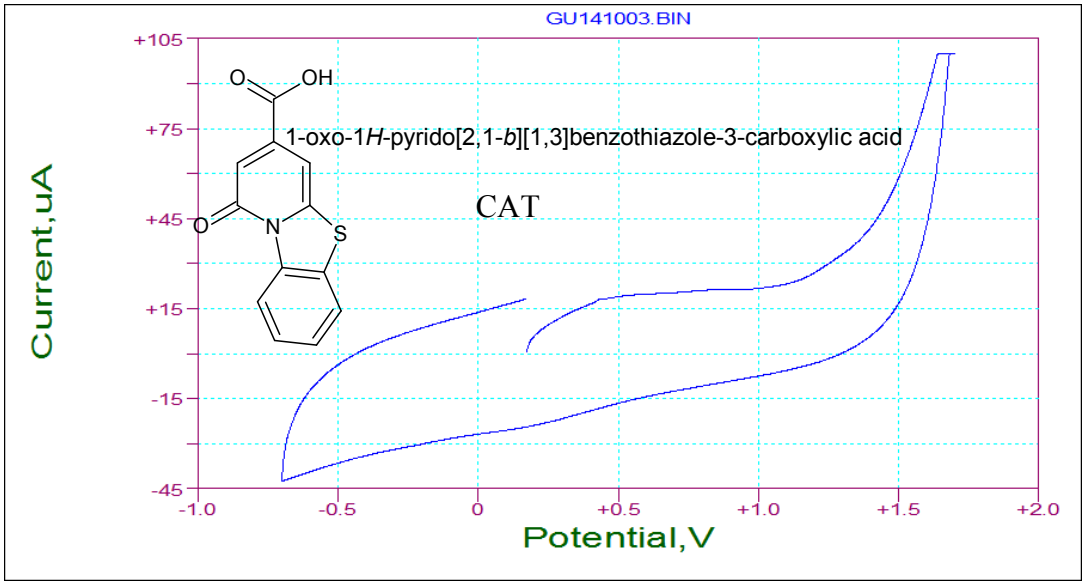

Figure 52. Structure, chemical name (full and symbol) and voltammogram of a synthesised derivative of pyridine carboxylic acid.

Moreover, I used another commercially available compound called citrazinic acid to modify GCE. Its structure and voltammogram are presented below.

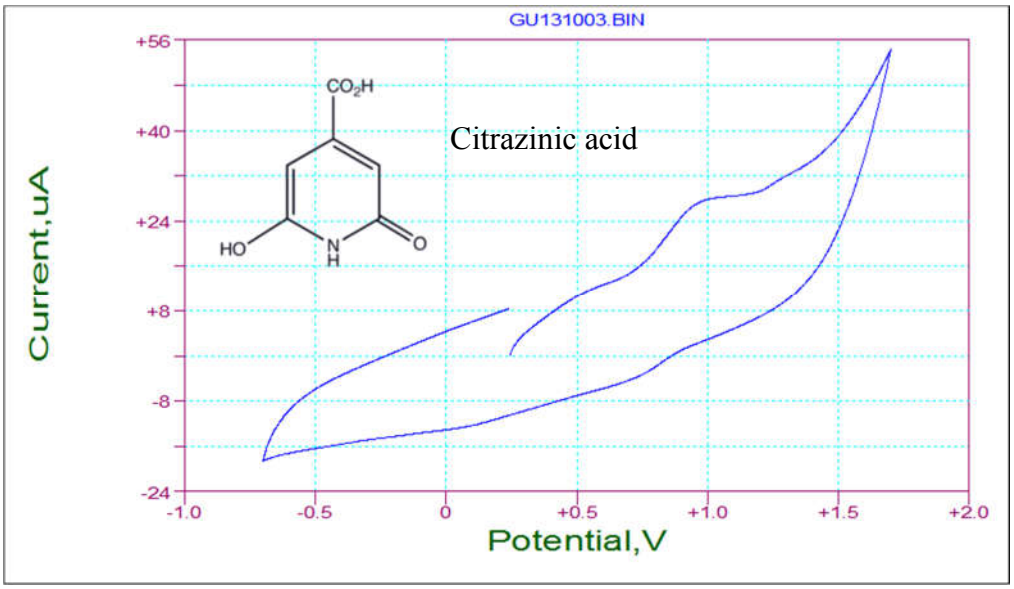

Figure 53. Structure and voltammogram of citrazinic acid in water.

Based on the literature review, this is the first case of citrazinic acid electropolymerisation to modify the surface of GCE. Interestingly, this polymer exhibited the best effect among all the chemical compounds which I electropolimerised to be used for the electrode modification purposes.

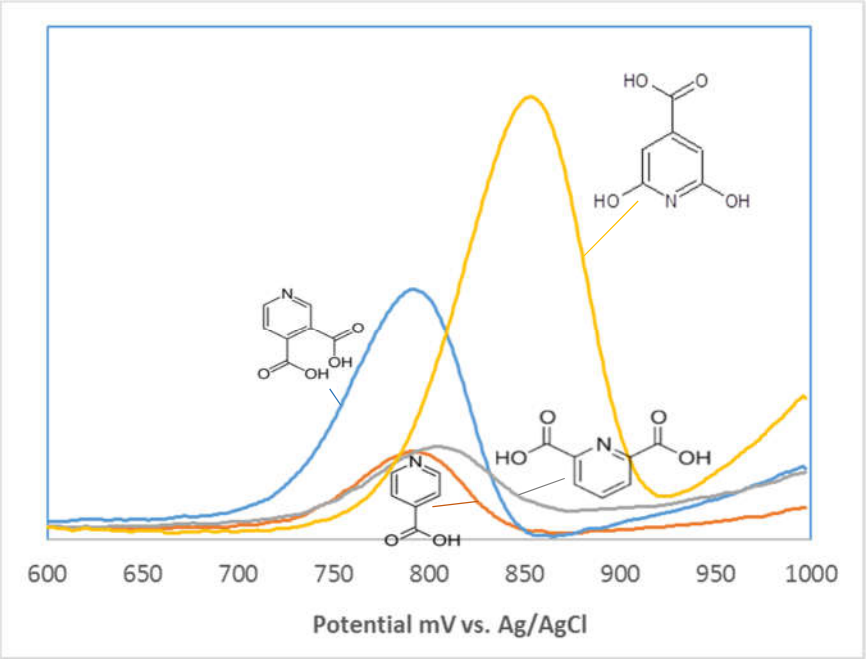

Figure 54. Semiderivatives of voltammograms of 25 µM guanine in phosphate buffer, pH7, on GCE with a layer obtained by oxidation of the shown pyridinecarboxylic acid, followed by treatment with FeTPP in THF. Scan rate 0.1 V s^{-1}.

Guanine electroanalysis on modified electrodes

Effect of scan rate on guanine oxidation

Here, the results of the studies on guanine oxidation process will be presented. The first problem I wanted to clarify was whether oxidation of guanine is a process controlled by diffusion or by adsorption. To this end, I used voltammograms recorded at various scan rates. If the process is controlled by diffusion, then the current is proportional to the square root of scan rate, if it is oxidation or reduction of the species adsorbed then the current is proportional to the scan rate. It is even more convenient to use semiderivatives. In this case, for processes controlled by diffusion semiderivatives of voltammograms recorded at various scan rates should overlap, for processes of adsorbed species, semiderivatives recorded at higher scan rates should be more intense.

To answer this question I varied the scan rate from 20 mV/s to 1000 mV/s and recorded the voltammograms. And then I analysed the behaviour of the intensity of the peaks related to the oxidation of guanine by increasing the scan rate.

Some semiderivatives are presented below. Figures 55 to 57 are the results of the first, second and third cycles respectively. For the first cycle, the higher the scan rate the higher the intensity of the peak related to the oxidation of guanine at about 800 mV. It means that this process during the first cycle is controlled by adsorption. However, it can be seen that during the second and third cycles, the waves of voltammograms recorded at various scan rates overlapped. It means that during the subsequent scans, oxidation of guanine is controlled by diffusion.

The process is more complex in the case of another peak that we can see at about 450 mV, which is most probably related to 8-oxoguanine.

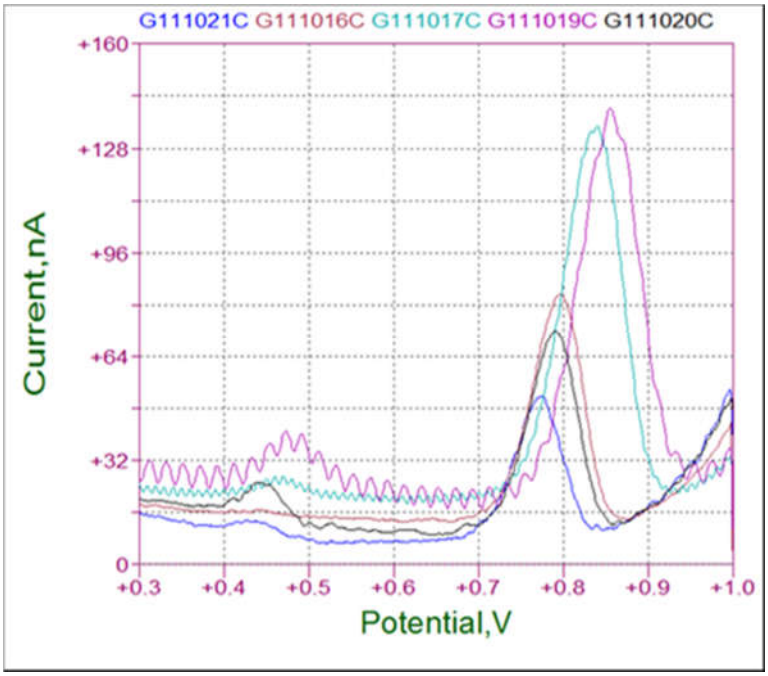

Figure 55. Semiderivatives of the first cycles of voltammograms of guanine oxidation. . GU111016C: scan rate=100 mV/s, GU111017C: scan rate=500 mV/s, GU111019C: scan rate=1000 mV/s, GU111020C: scan rate=50 mV/s, GU111021C: scan rate=20 mV/s.

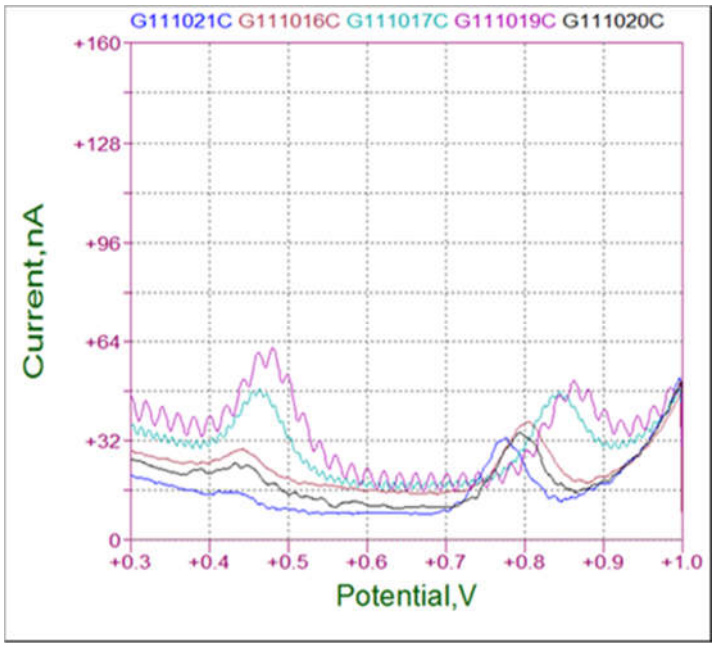

Figure 56. Semiderivatives of second cycles of guanine oxidation. GU111016C: scan rate=100 mV/s, GU111017C: scan rate=500 mV/s, GU111019C: scan rate=1000 mV/s, GU111020C: scan rate=50 mV/s, GU111021C: scan rate=20 mV/s.

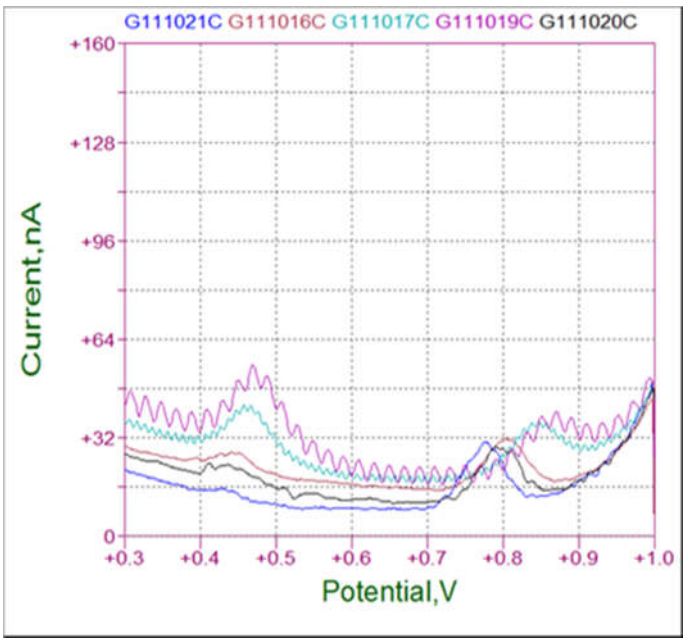

Figure 57. Semiderivatives of third cycles of guanine oxidation.. GU111016C: scan rate=100 mV/s, GU111017C: scan rate=500 mV/s, GU111019C: scan rate=1000 mV/s, GU111020C: scan rate=50 mV/s, GU111021C: scan rate=20 mV/s.

Plotting the intensity of guanine oxidation peaks versus scan rates from another similar series of measurements, I obtained a linear relationship between the current and the scan rate, which can prove that the oxidation of guanine, at least during the first scan, is controlled by adsorption. On the other hand, a simple equation linking the current and charge, $Q = i \cdot t$, shows that if the current is proportional to the scan rate, which means, inversely proportional to the time, then the charge will stay constant all the time. This is very conclusive to prove that the process of guanine oxidation is controlled by adsorption indeed (see Figs. 58 and 59).

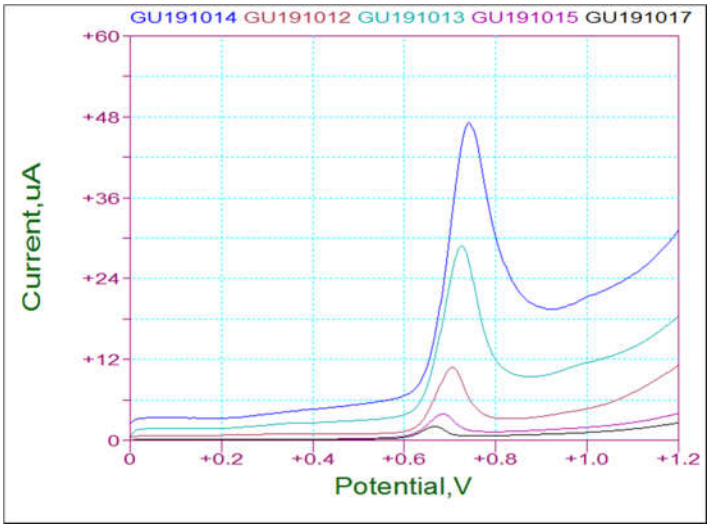

Figure 58. Cyclic Voltammograms 1st Scan. 191012 – 200 mV/s, 191013 – 500 mV/s, 191014 – 1000 mV/s, 191015 – 50 mV/s, 191017 – 20 mV/s.

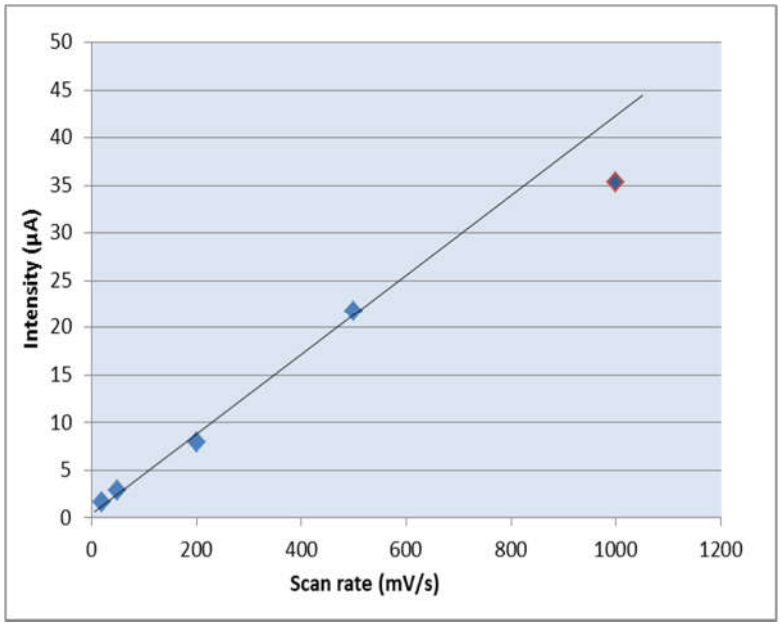

Figure 59. Cyclic Voltammograms 1st Scan. 191012 – 200 mV/s, 191013 – 500 mV/s, 191014 – 1000 mV/s, 191015 – 50 mV/s, 191017 – 20 mV/s.

The limit of detection for TD100

Guanine at a really very low concentration could be detected by using the electrode modified as described above. As it can be seen in the Figs. 60 and 61, there is a nice linear relationship between guanine concentration and current down to 0.08 µM. In this case, the preadsorption time was equal 300 s.

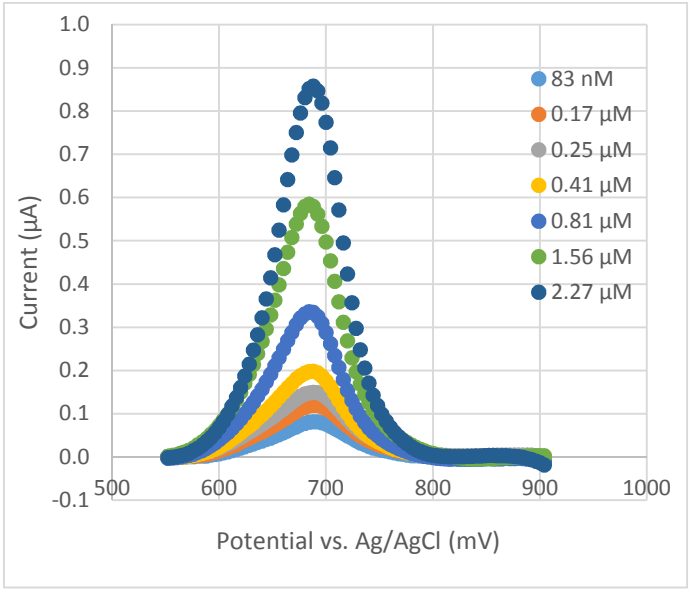

Figure 60. SQWV results. Limit of detection-increasing of current versus guanine concentration.

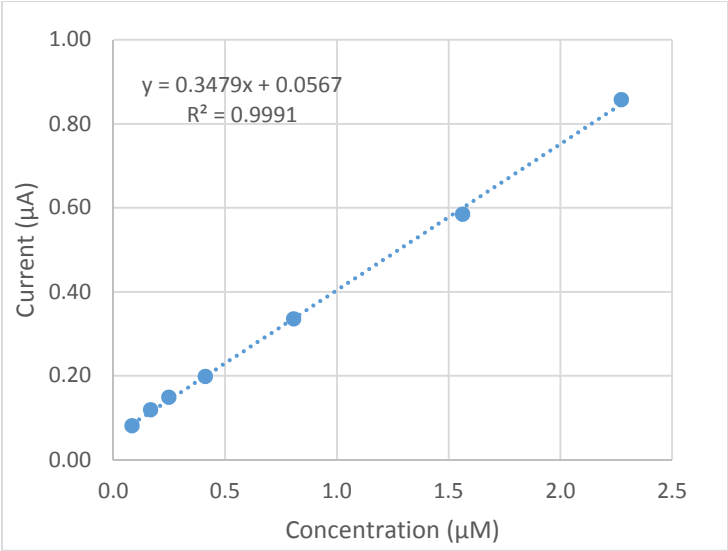

Figure 61. Linear relationship between guanine concentration and current down to 0.08 µM.

However, further experiments with even lower concentrations of guanine have shown that the sensitivity of this polymer is even higher and it can detect guanine at nanomolar concentrations. With a longer preadsorption time of 900 s, the system becomes even more sensitive. As it can be seen in Fig. 63 it is possible to find a linear relationship between current and a range of guanine concentrations, however there are some scattered points which exhibit the surface of this polymer is not uniform. Therefore, despite this extreme sensitivity towards guanine, it is not advised to apply it for quantitative analysis at this really low concentration.

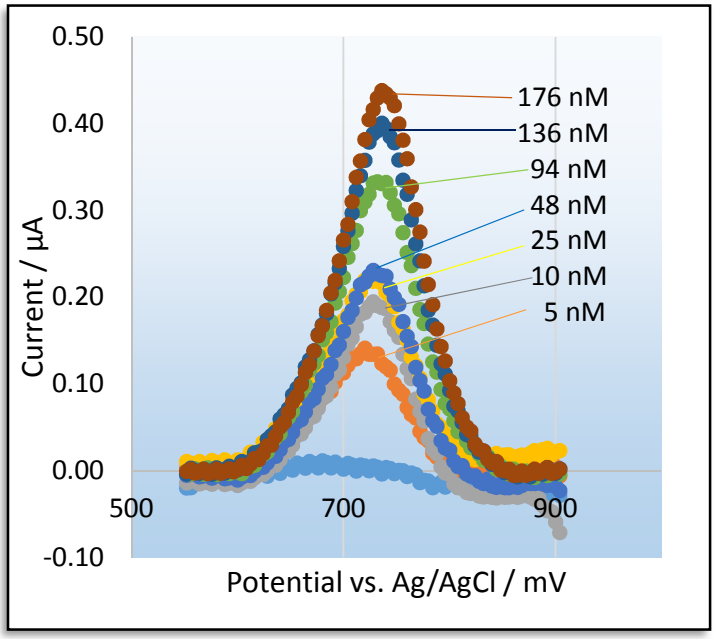

Figure 62. SQWV with subtracted background.

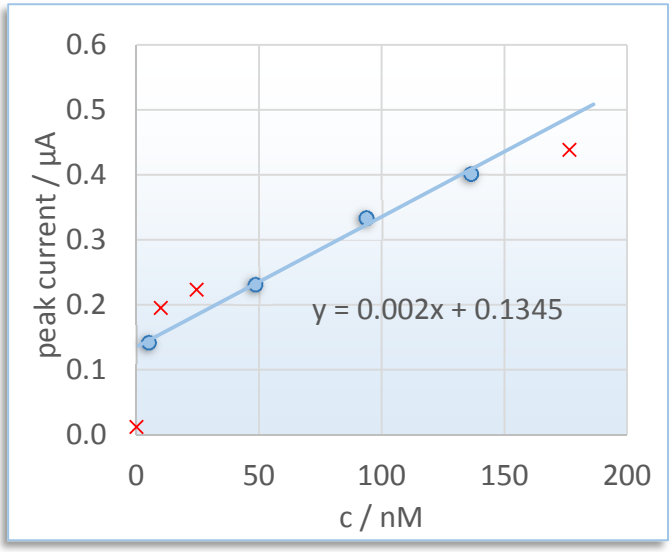

Figure 63. Peak current vs. concentration. Problems at the lowest concentrations. Red crosses denote outliers, not taken for the calculation of the regression equation.

As can be seen in Fig. 64, the modified GCE is sensitive to pollution of the cell and electrodes by guanine, which always disturbs the measurements and is almost impossible to avoid. The signal at for 1 nM is comparable to the blank voltammogram, prior to adding guanine. Interestingly, the signal for 2 nM is much more intense, which shows this modified electrode to be really very sensitive, but not yielding very reproducible responses for extremely low concentrations of guanine

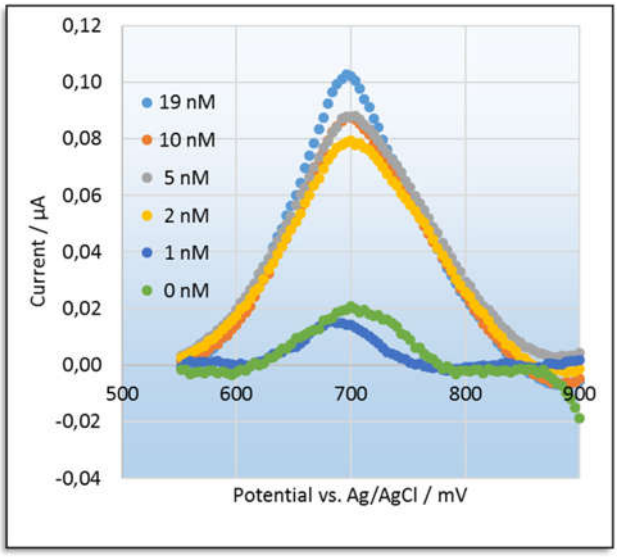

Figure 64. SQWV with subtracted background.

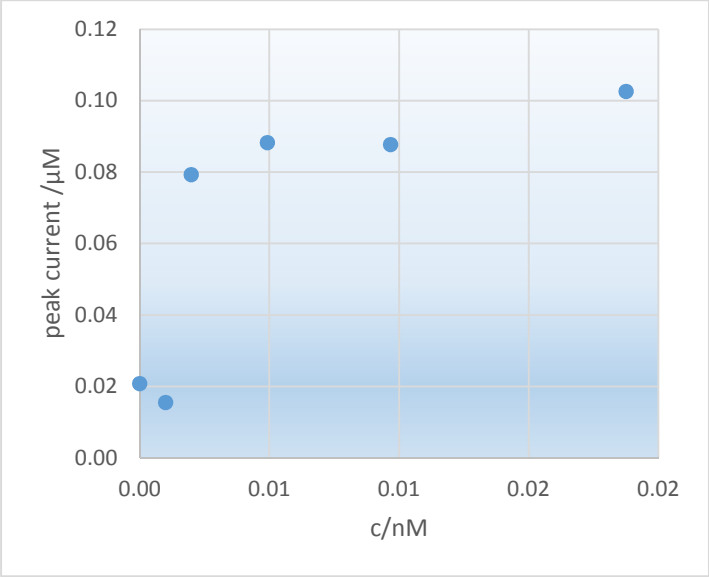

Figure 65. Peak current vs. concentration. Problems at the lowest concentrations.

Other products of guanine oxidation

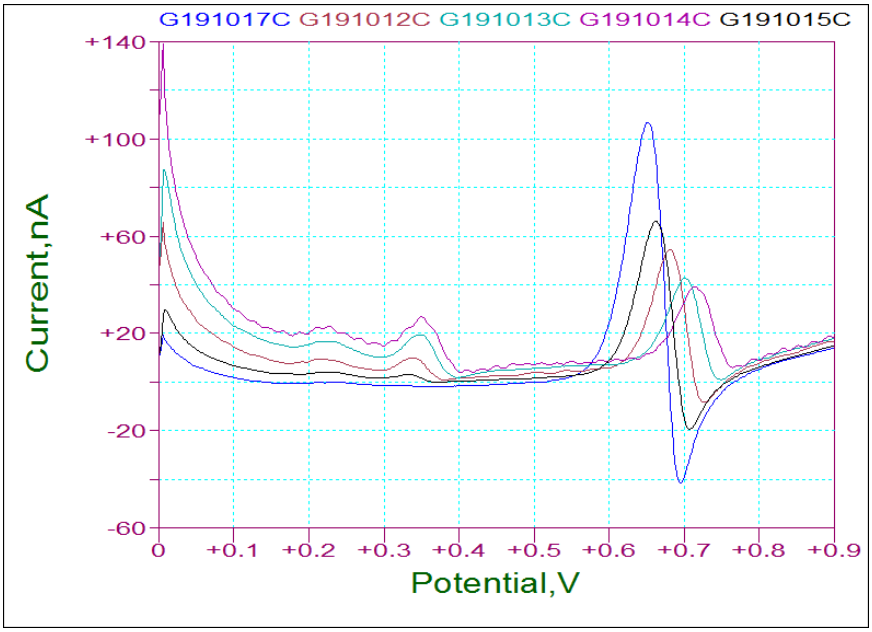

Figure 66. Semiderivatives 2nd Scan. 191012 – 200 mV/s; …13 – 500 mV/s; …14 – 1000 mV/s; …15 – 50 mV/s; … 17 – 20 mV/s.

In Fig. 66, we can see that except for guanine, two other products of guanine oxidation can be detected by using the modified GCE. One of them, at about 350 mV, can be due to 8-oxoguanine but even another transient appeared at about 250 mV. Interestingly, these two transients are converted to guanine, mostly at the lower scan rate, when there is enough time for this process. This measurement was run on the surface of modified GCE by applying the polymer obtained by

the electropolymerisation of citrazinic acid and by adsorption of iron porphyrin. This result can prove that layer modifying the electrode efficiently converts the harmful products of oxidation of guanine to guanine. And on this way it can really help to remove the dangerous effects of guanine oxidation.

Chronocoulometric results

In chronocoulometry, for processes controlled by diffusion, we have according to the Cottrell equation:

$$Q_t = \frac{2nFAD_0^{1/2}C_0}{\pi^{1/2}} t^{1/2}$$

where n is number of electrons, F is the Faraday constant, 96,485 C/mol, A is the area of the (planar) electrode in cm^2, D_0 is the diffusion coefficient for species j in cm^2/s, C_0 is initial concentration of the reducible analyte j in mol/cm^3 and t is time in s.

In a plot of charge versus square root of time, the slope can give us information about the diffusion controlled process, and the intercept can give us information about the charge used for adsorbed species. And according to:

$$Q_{total} = Q_{dl} + Q_{pol} + Q_{ads} + Q_{diff}$$

The total charge is equal to the sum of charges used for double layer charging, modifying polymer layer charging, adsorbed species oxidation, and the charge used for the oxidation of species diffusing from the bulk of solution. Examples are shown in Figs. 67 a and b.

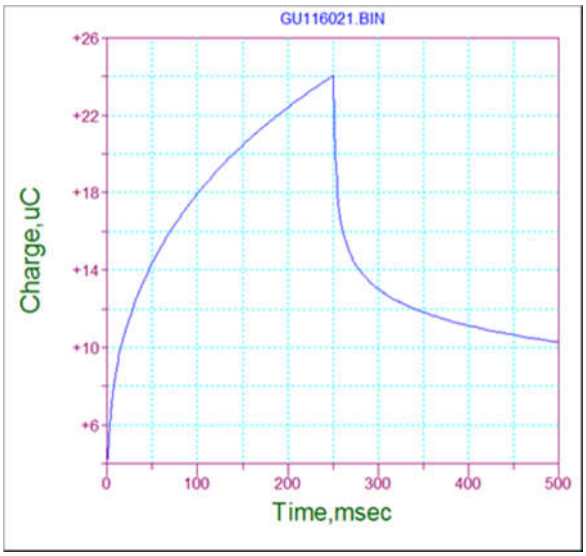

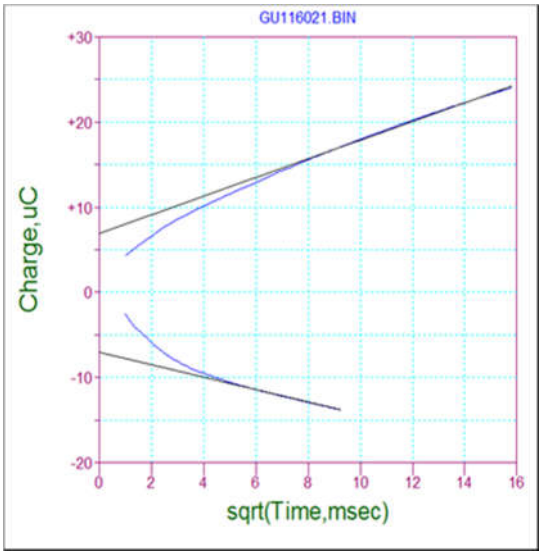

Forward step:
Slp = +1.093e-006
Int = +6.951e-006

Reverse step:
Slp = -7.277e-007
Int = -7.068e-006

Figure 67. a) Charge versus time and b) Charge versus square rout of time in guanine oxidation process.

Using the chronocoulometric measurements, it is possible to calculate the capacity of the polymer layer applied onto the surface of electrode. As an example I calculated the capacity of the polymer layer on the surface of GCE when this electrode was covered by the polymer obtained by electropolymerisation of pyridine-3,4-dicarboxylic acid, and cobalt tetrapyridyl porphyrin (CoTPP) solution in THF was used in the adsorption step (see Figs. 68 and Table 3).

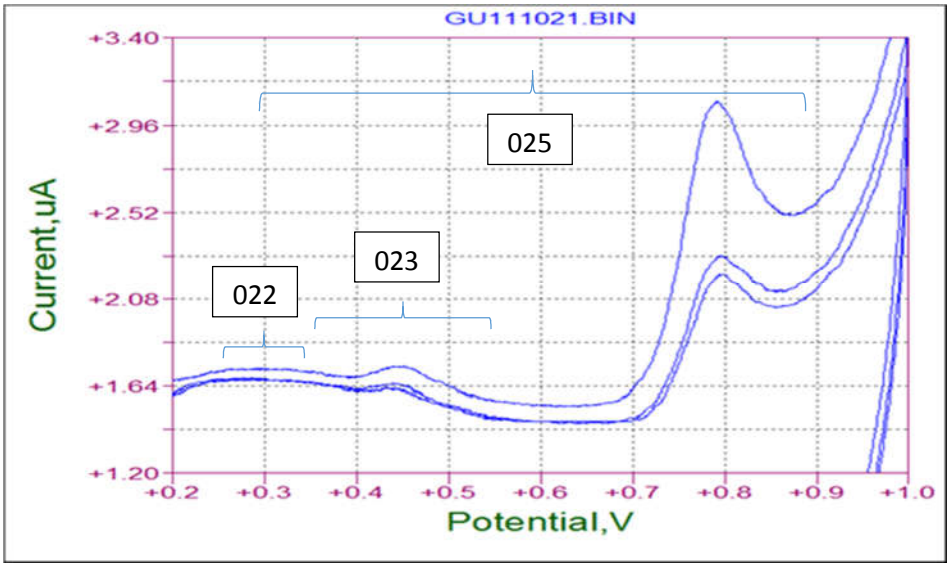

Figure 68. CV. Scan rate= 20 mV/s. Guanine oxidation and 8-oxoguanine peaks at the GCE modified by polymerisation of pyridine-3,4-dicarboxylic acid and CoTPP adsorption from its THF solution. The numbers and ranges refer to chronocoulometric measurements from Table 3.

#	from / mV	to / mV	Forward			Reverse		
			Slp	Int/µC	Nett Q/µC	Slp	Int/µC	Nett Q
022	249	349	0,0834	1,497	C=14.97µF	0,1020	1,380	C=13.8µF
023	258	558	0,2463	4,659	0.17	0,2742	4,164	0.02
025	290	890	0,7513	10,07	1.09	0,5678	8,328	0.05

Table 3. Chronocoulometric results obtained from guanine oxidation on modified GCE; voltammograms shown in Fig. 68. Nett charge (Nett Q) for chronocoulograms #023 and 025 were calculated by subtracting the charge used for double layer and polymer charging from the intercept (see text below).

The capacity of the polymer layer and the double layer in solution calculated from the intercept for #022 is close to 15 µF, which is very high with respect to the surface area of GCE of only 5 mm^2. As it is almost the same for the reverse step, it can be assumed that the polymer behaves as a capacitor and is charged and discharged reversibly. Assuming that it may behave in the same way all over the applied potentials, the charged used for charging the polymer in subsequent measurements, #023 and 025 can be calculated. The nett charge (Nett Q) is a difference between the intercept and the charge used for the polymer charging. As can be seen, 8-oxoguanine (at ca.

0.45 V) and guanine (at ca. 0.8 V) are oxidised in their adsorbed form. The nett charge close to zero in the reverse step means that these processes are irreversible.

During another chronocoulometric probe, in which guanine and adenine both are present in the cell solution, I divided the voltammogram of the oxidation process of these two bases into three regions. And then, I considered the chronocoulometric results into these three regions (see Fig. 69).

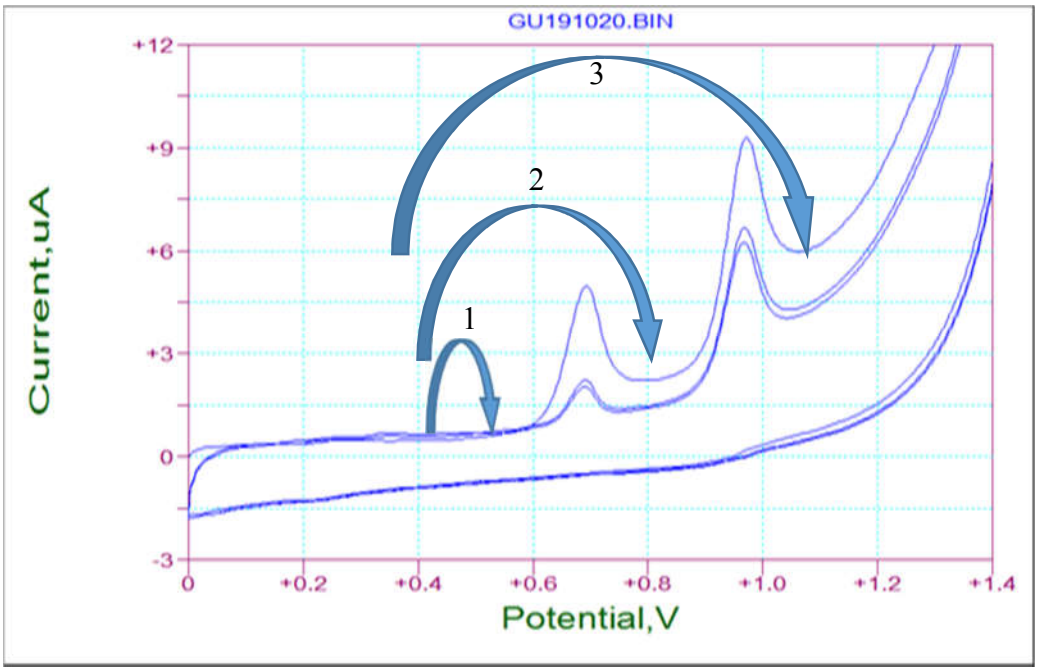

Figure 69. Scan rate= 100 mV/s. Guanine and adenine oxidation on GCE modified by polymerisation of citrazinic acid and FeTPP adsorption from its THF solution.

Region number 1: Polymer and double layer Oxidation

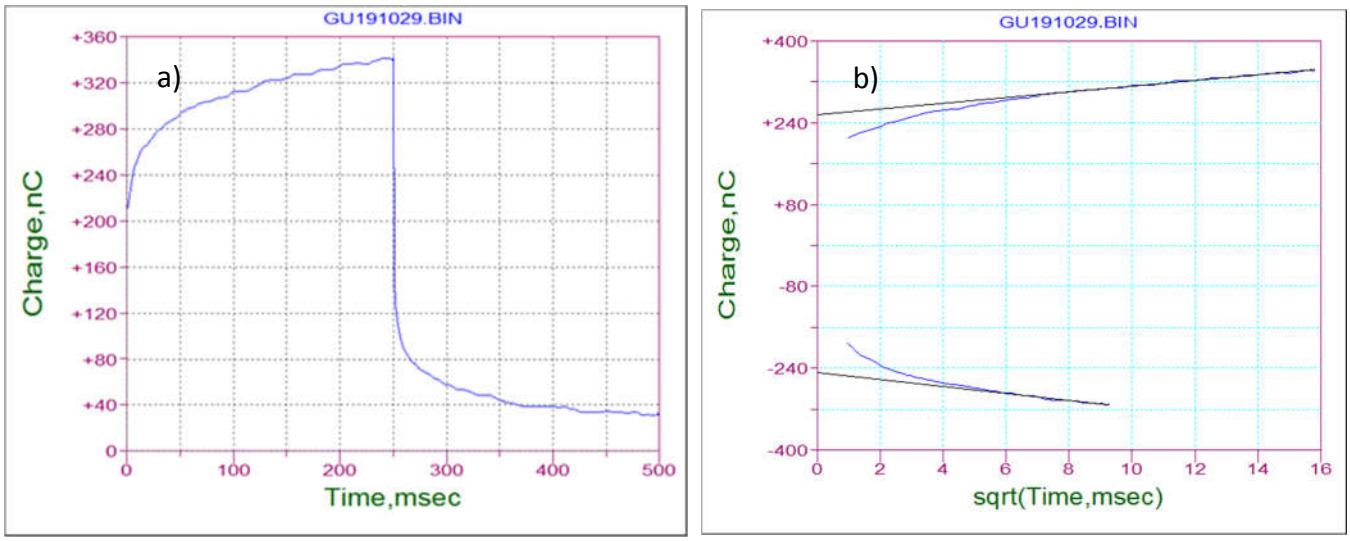

Figure 70. a) Charge versus time, b) Charge versus the square root of time; 1st region.

Initial E=435mV, Final E=540	
Forward step:	Reverse step:
Slp = +5.492e-009	Slp = -6.962e-009
Int = +2.564e-007	Int = -2.475e-007
Cor = +0.9969	Cor = -0.9826

Table 4. Chronocoulometric data of the 1st region.

First region included only the polymer and double layer charging. As we can see in Table. 4 the intercepts of forward (oxidation) and reverse (reduction) steps are almost the same. It means the amount of the charge which is consumed for forward and reverse steps is almost the same. This is the expected result. The diffusion currents are small, which is seen in Fig. 70 b. This time the capacity was 2.5 µF, which is lower than in the previously described case, but the polymer layer was thinner. However, it is still high regarding the polymer layer size.

Region number2: Polymer and Guanine Oxidation

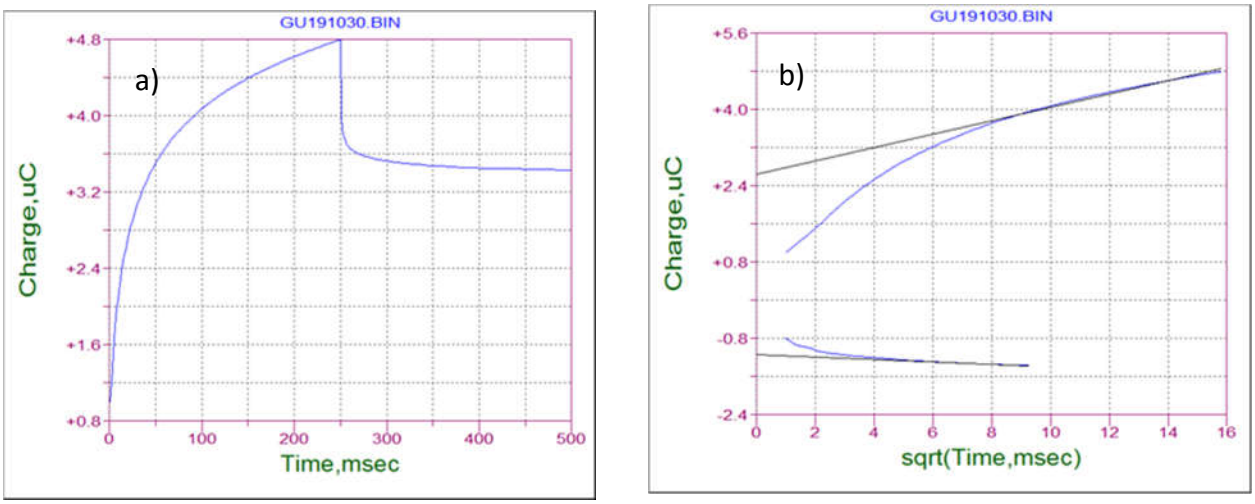

Figure 71. a) Charge versus time, b) Charge versus the square root of time; 2nd region.

IE=408 mV, FE=790 mV

Forward step:	Reverse step:
Slp = +1.403e-007	Slp = -2.413e-008
Int = +2.641e-006	Int = -1.148e-006
Cor = +0.9940	Cor = -0.9933

Table 5. Chronocoulometric data of 2nd region.

As we can see in Table. 5 the intercept of the forward step is about 1.5 µC higher than for the reverse step. This means that guanine oxidation in its adsorbed state is irreversible. It can also be seen comparing Figs. 71b and 70b. Again, as before, the intercept for the reverse step is close to the expected charge of the polymer charging (2.5 µF · (0.790 – 0.408) V = 0.955 µC). That would leave 1.69 µC for guanine oxidation.

Region number3: Polymer, Guanine and Adenine oxidation

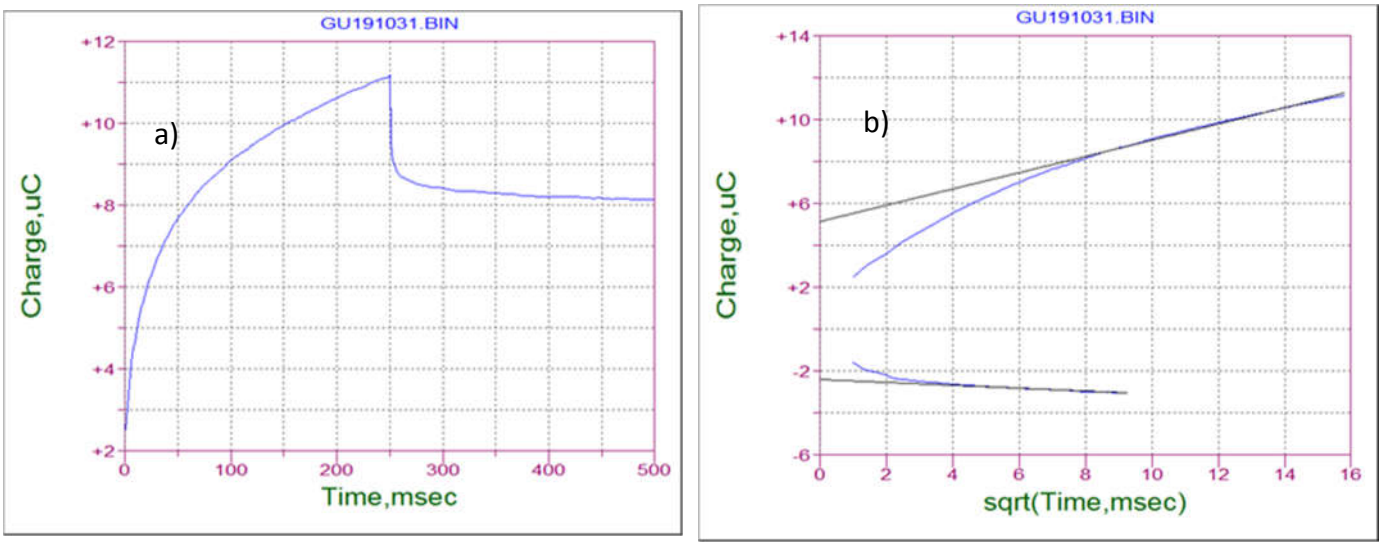

Figure 72. a) Charge versus time, b) Charge versus the square root of time; 3rd region.

IE=378 mV, FE=1050 mV	
Forward step:	**Reverse step:**
Slp = +3.857e-007	Slp = -7.067e-008
Int = +5.174e-006	Int = -2.390e-006
Cor = +0.9975	Cor = -0.9902

Table 6. Chronocoulometric data of 3rd region.

As we can see in Table. 6, the intercept of the forward step is about 3 μC larger than for the reverse step. It means that the amount of the charge which is consumed for the oxidation process during the forward step is about 3 μC more than the amount of the charge which is consumed for the reduction process during the reverse step. If, again, we deduct the charge used for polymer charging (2.5 μF · (1.050 – 0.378) V = 1.68 μC) and that used for guanine oxidation (1.69 μC), then the charge used for adenine oxidation will be 1.8 μC, almost the same as for guanine oxidation. This means that guanine and adenine behave similarly. They are both oxidised irreversibly in their adsorbed state.

Spectroscopic studies of citrazinic acid and its polymer

The polymer used to successfully modify the electrode deserved further characterisation, as also its interaction with guanine. I have started my studies with Uv-vis spectroscopy of citrazinic acid (see Fig. 73). The spectrum was recorded in alkaline solution because of higher solubility of guanine.

As it can be seen in Fig. 74, by adding guanine to the aqueous solution of citrazinic acid no important changes were observed in the spectrum but in the differential spectrum in Fig. 75 indicates shifts in the wavelengths, so something happens to guanine.

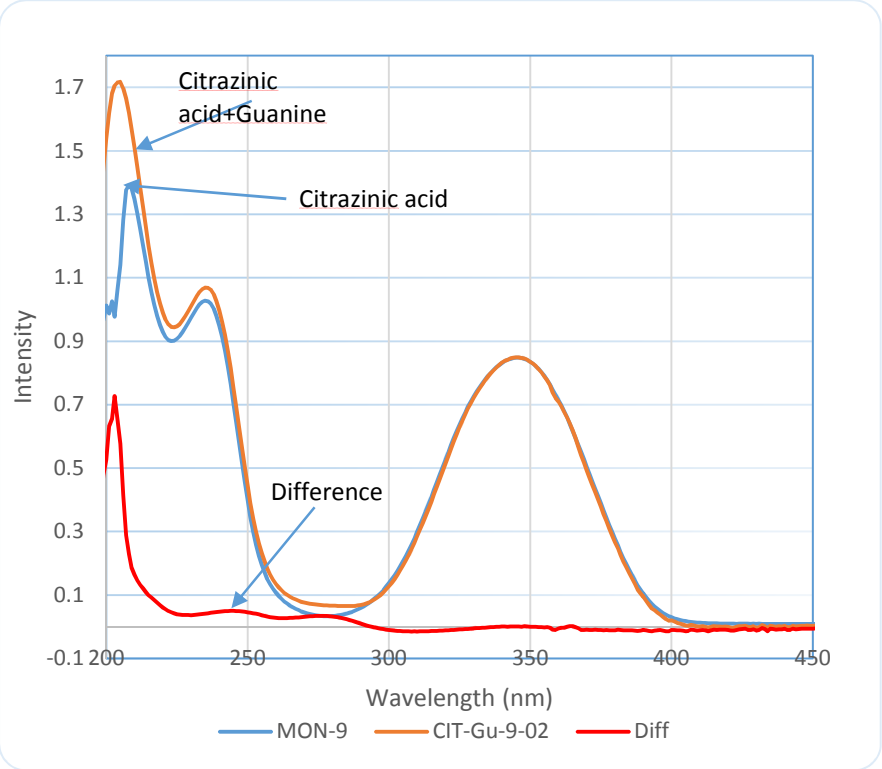

Figure 73. Uv-vis spectra of citrazinic acid itself and after adding guanine in phosphate buffer solution (KH2PO4+KOH, pH=9).

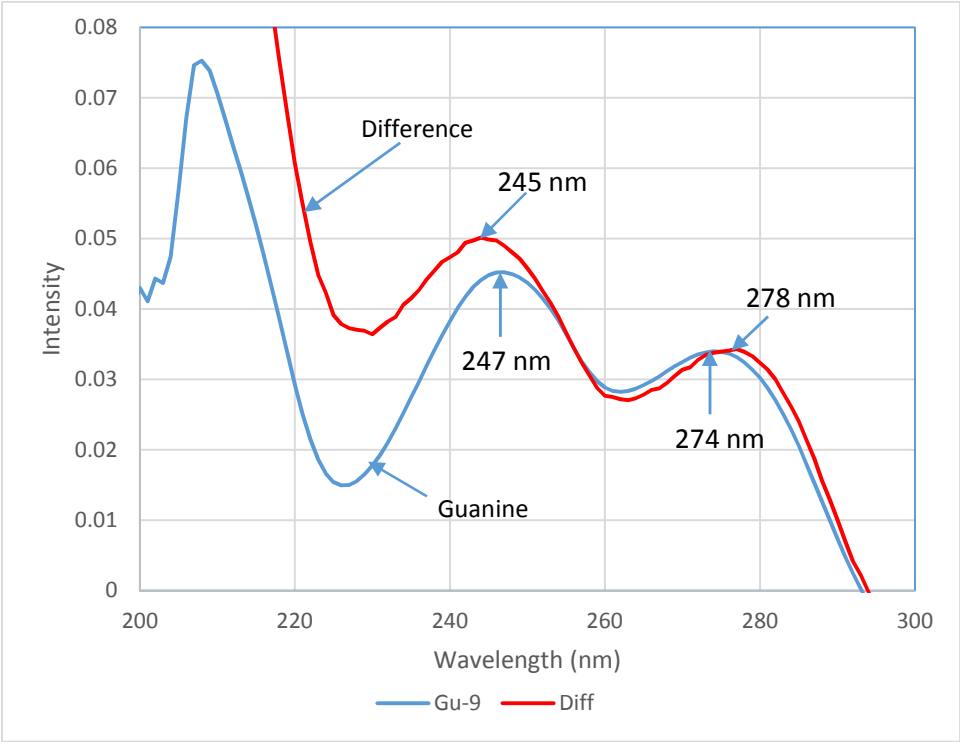

Figure 74. Effect of Guanine on the citrazinic acid spectrum. Diff is the differential spectrum from Fig. 73 expanded. Here, it is compared with the spectrum of guanine.

Moreover, to check this effect in detail, I subtracted the spectrum of guanine from the differential spectrum and then compared it with guanine itself. A new band appeared at 282 nm, as can be seen in Fig. 75.

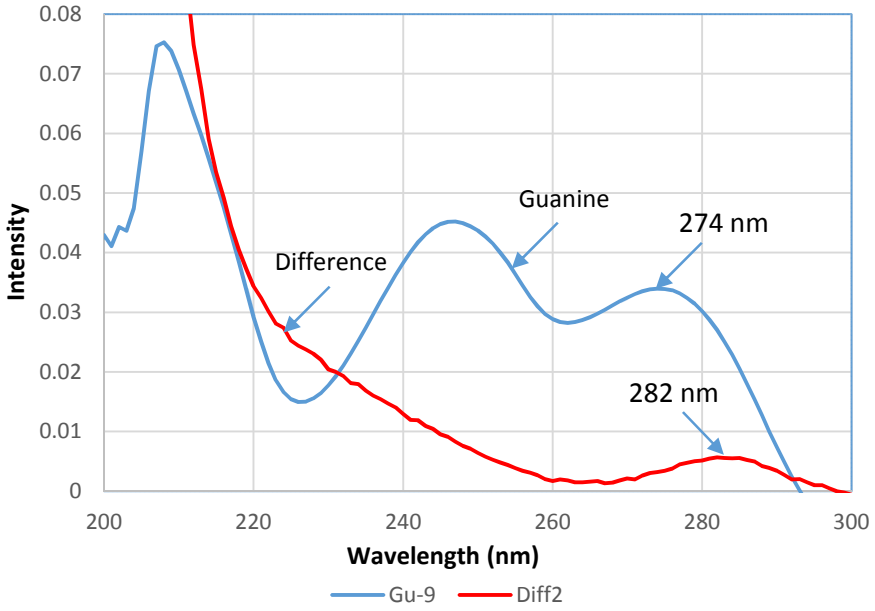

Figure 75. Doubly differential spectrum obtained by subtracting guanine spectrum from the differential spectrum of Fig. 74. A new band is seen.

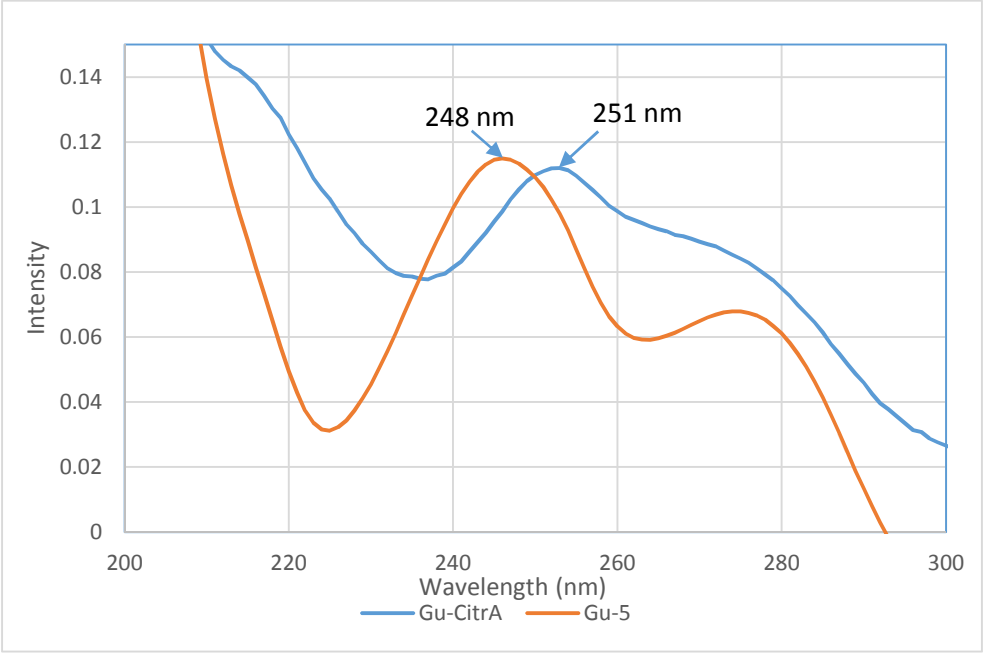

Figure 76. Comparison of the spectrum of citrazinic acid in the presence of guanine with guanine itself in the phosphate buffer solution pH 5.

I could see some changes in the spectrum of citrazinic acid affected by guanine at pH 5, too (see Fig. 76).

For unknown reasons, I could not see any effects at pH 7 (see Fig. 77).

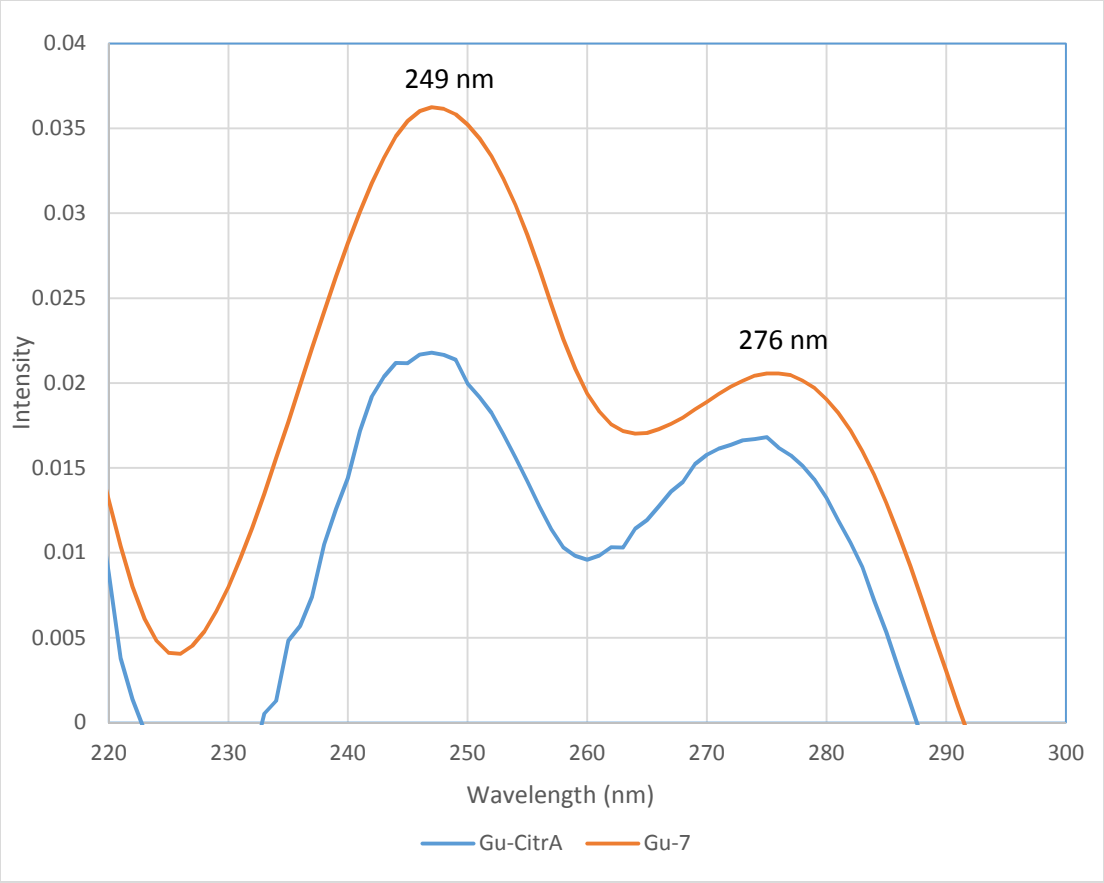

Figure 77. No changes could be seen on the spectrum of citrazinic acid by adding guanine at pH 7.

Then, I tried fluorescence spectroscopy for studying citrazinic acid and its polymer and I found interesting results (see Fig. 78). As it can be seen in Fig. 78, fluorescence of citrazinic acid monomer is slightly quenched in the presence of guanine. On the other hand, guanine increases fluorescence of the citrazinic acid polymer. This effect can prove that guanine prefers to interact with polymer than monomer and because of this it will interact with the polymer in the mixture of monomer and polymer more efficiently. Interestingly, at higher concentrations of citrazinic acid, the addition of guanine may even enhance the intensity of fluorescence, as can be seen in Fig. 79.

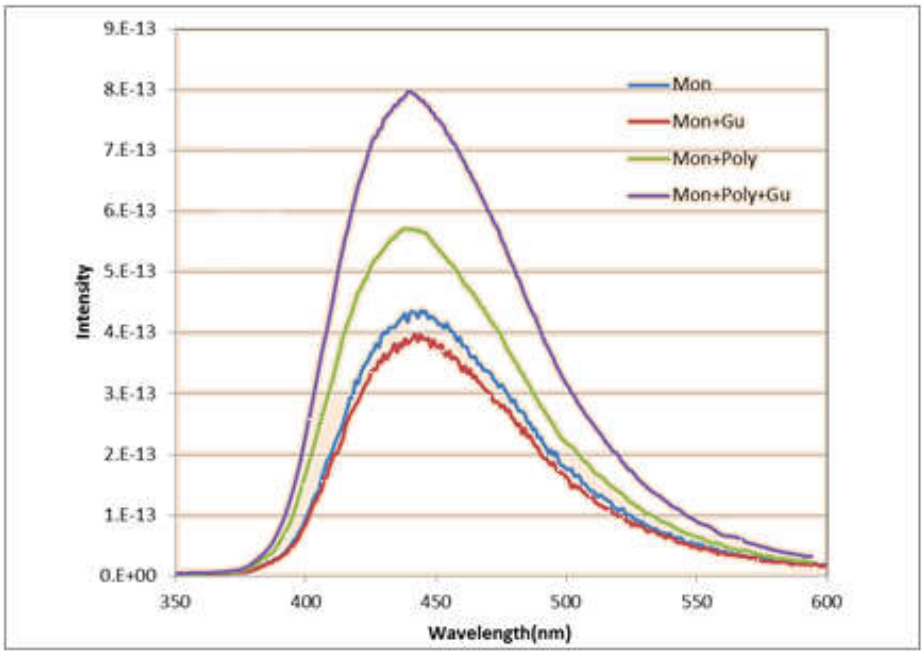

Figure 78. Fluorescence spectra of citrazinic acid as the monomer, polymer and monomer in the absence and presence of guanine in water.

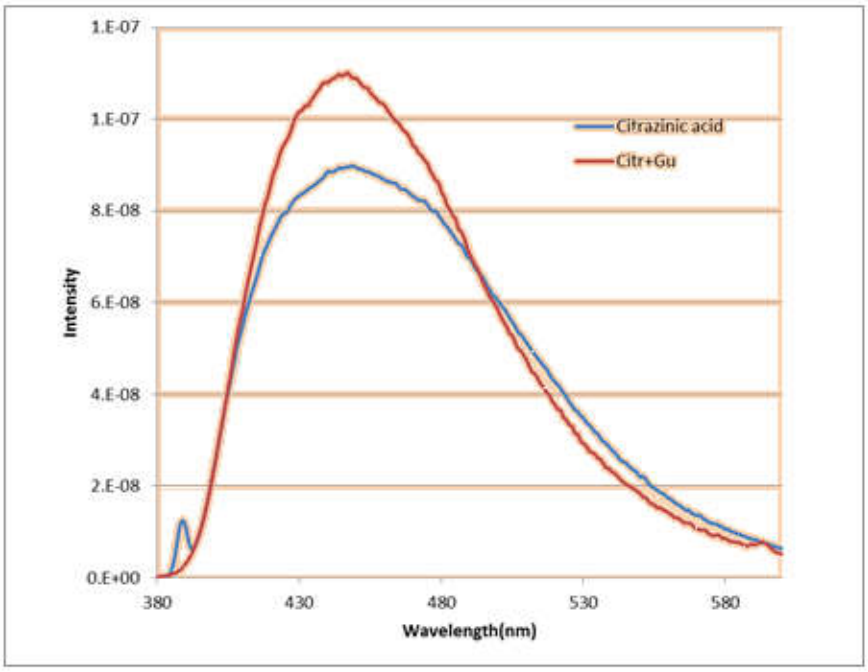

Figure 79. Fluorescence spctra of citrazinic acid in phosphate buffer solution pH 7 in the absence and presence of guanine.

I subtracted the spectrum of citrazinic acid from the spectrum of citrazinic acid in the presence of guanine. The result showed a new band (see Fig. 80).

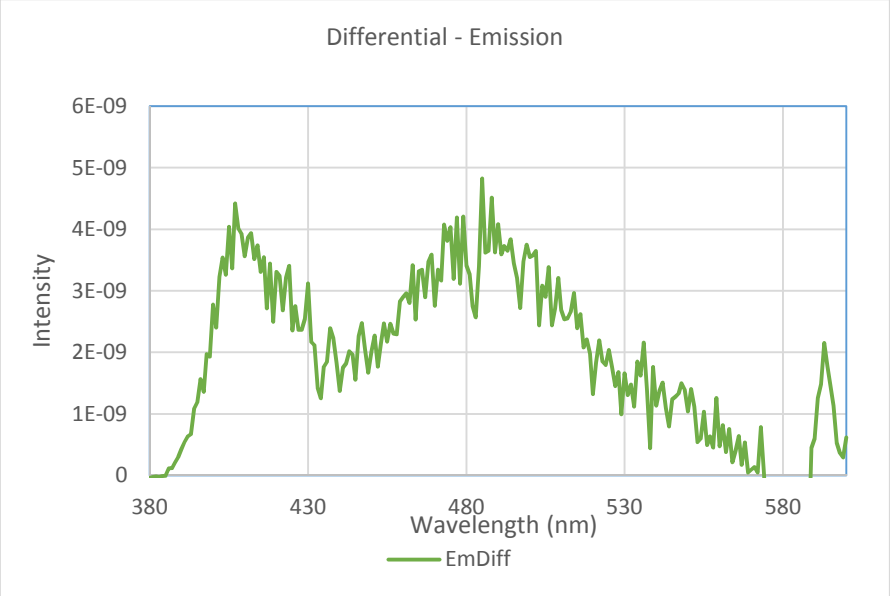

Figure 80. The new band obtained by subtracting the spectrum of citrazinic acid from the spectrum of this acid in the presence of guanine at pH 7.

To be sure that this peak is not related to guanine itself, I compared the emission of guanine using various excitation wavelengths. As we can see in Fig. 81 its fluorescence is very low and only noise can be seen.

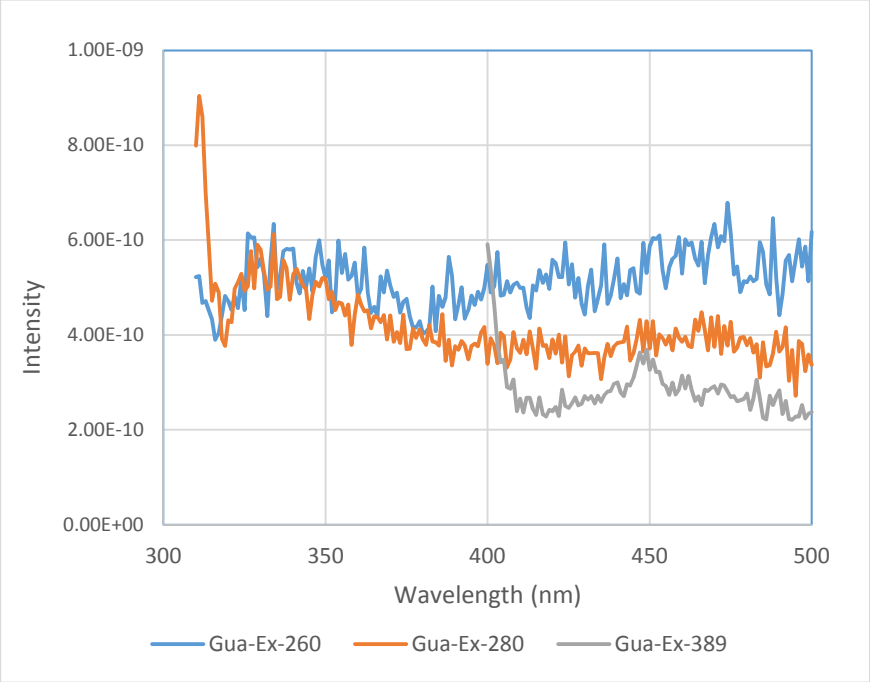

Figure 81. Emission of guanine in 260 nm, 280 nm and 389 nm excitation wavelengths.

We can see the result of this kind in the measurement at pH 5 in Fig. 82. As we can see in Fig. 83 by subtracting of two spectra a new band appeared. But still it can prove that guanine affects the fluorescence of citrazinic acid.

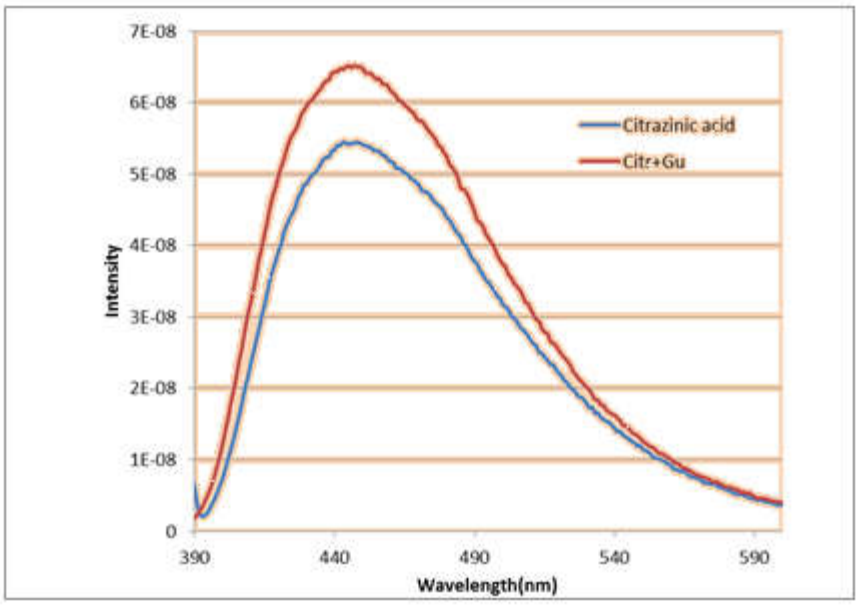

Figure 82. Fluorescence spectra of citrazinic acid in the absence and presence of guanine at pH 5.

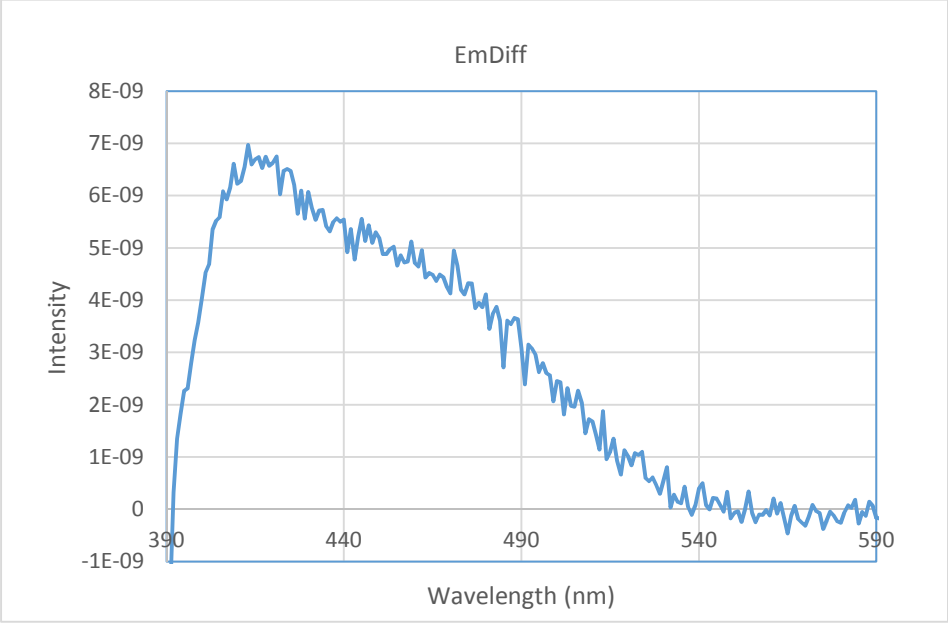

Figure 83. The band obtained by subtracting of the spectrum of citrazinic acid from the spectrum of this acid in the presence of guanine at pH 5.

I have got at pH 9 almost the similar results to those obtained at pH 7 in this series of measurements (see Fig. 84 and 85).

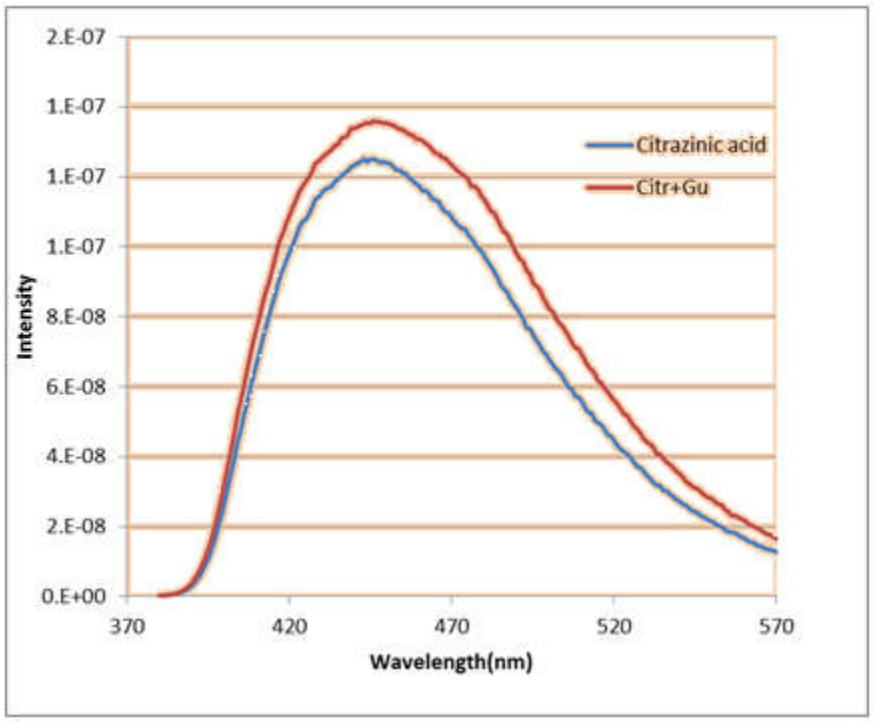

Figure 84. Fluorescence spectra of citrazinic acid in the absence and presence of guanine at pH 9.

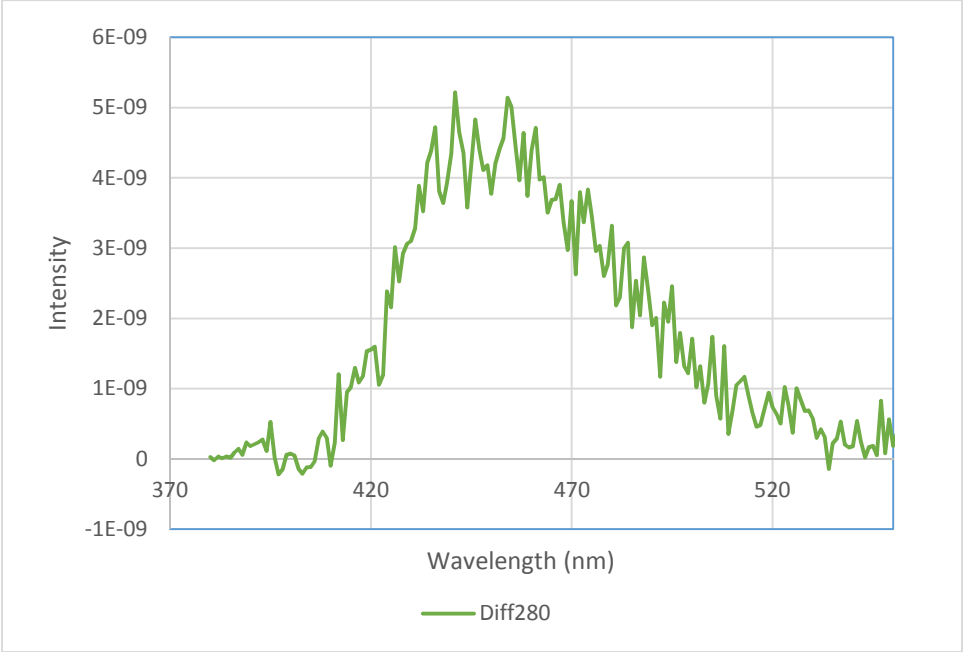

Figure 85. The new peak obtained by subtracting of the spectrum of citrazinic acid from the spectrum of this acid in the presence of guanine at pH 9.

I did this kind of measurement in the case of polymer obtained by electropolymerisation of citrazinic acid. In Fig. 86, you can see the Uv-vis spectrum of this polymer in water. I kept this solution in the presence of an excess amount of solid guanine for a couple of days. Then, after centrifuging off the excess guanine, I recorded the Uv-vis spectrum of this solution. You can see the result on Fig. 87. By subtracting these two spectra two new bands in 314 nm and 321 nm were observed which are completely in a new place compared with the peak of polymer in 354 nm.

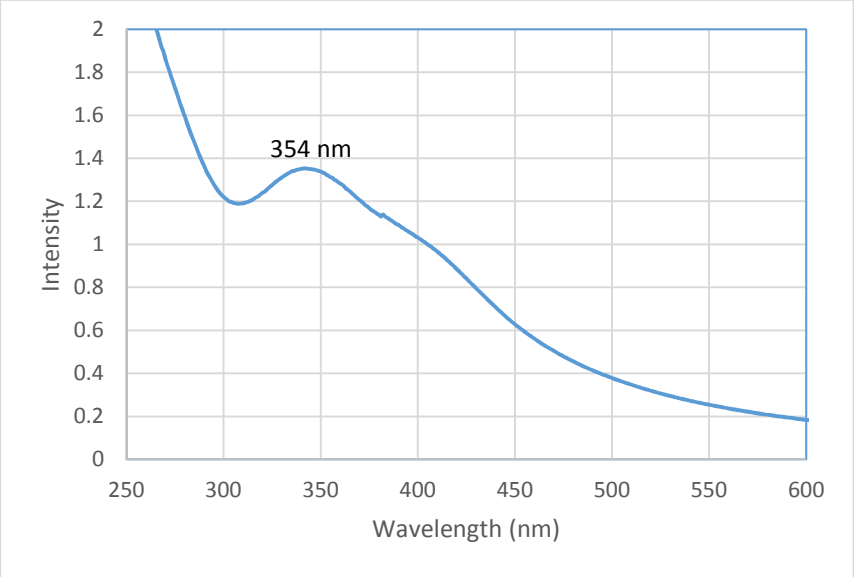

Figure 86. Uv-Vis spectrum of citrazinic acid polymer in water.

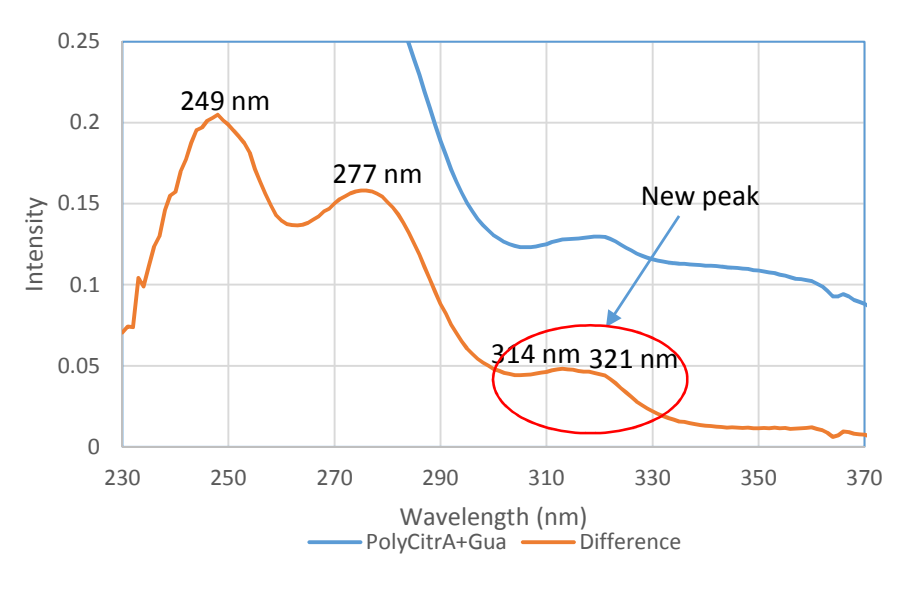

Figure 87. The new bands obtained by subtracting the spectrum of polymer in the absence and presence of guanine.

I recorded the fluorescence spectra of this polymer at different pHs as I did for the monomer. I obtained very similar results for all three pH values and I could see that guanine affects the fluorescence spectra of polymer all the time. As an example, I show here this effect at pH 9.

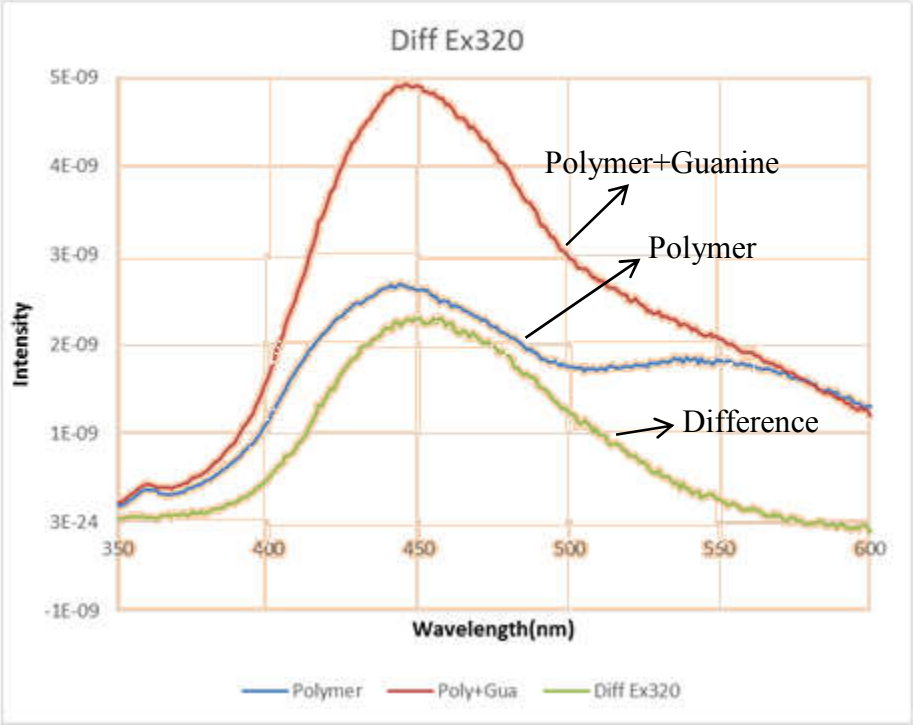

Figure 88. Fluorescence spectra of polymer in the absence and presence of guanine. And the difference between these two spectra at pH 9.

As can be seen in Fig. 88, after adding guanine to the solution of polymer the intensity of this peak is increased. Moreover, subtracting these two spectra exhibited a new band.

All these measurements demonstrate that guanine interacts with citrazinic acid and its polymer efficiently.

Polymer obtained from citrazinic acid (TD100)

Modification of the electrode by electropolymerisation of citrazinic acid gave us the best result. Therefore, it was really worth to study this polymer and understand the type of interaction between this polymer and guanine.

To get the molecular weight distribution, gel permeation chromatography was used, the result of which proves that it is a polymer with the molecular weight of 10000 g/ mol.

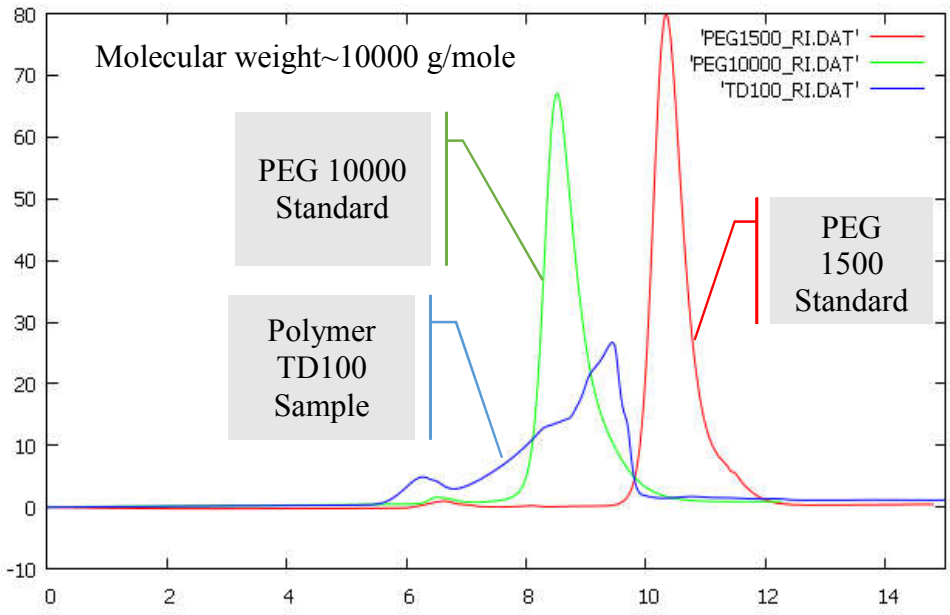

Figure 89. Gel permeation chromatography of polymer obtained from citrazinic acid.

Moreover, magnetic susceptibility measurements demonstrated that this polymer is paramagnetic. This was the reason why it was not possible to get any NMR spectra. It means that unfortunately, it is not possible to characterize the structure of this polymer by using ordinary spectroscopic methods. Below you can find the results of magnetic susceptibility measurements.

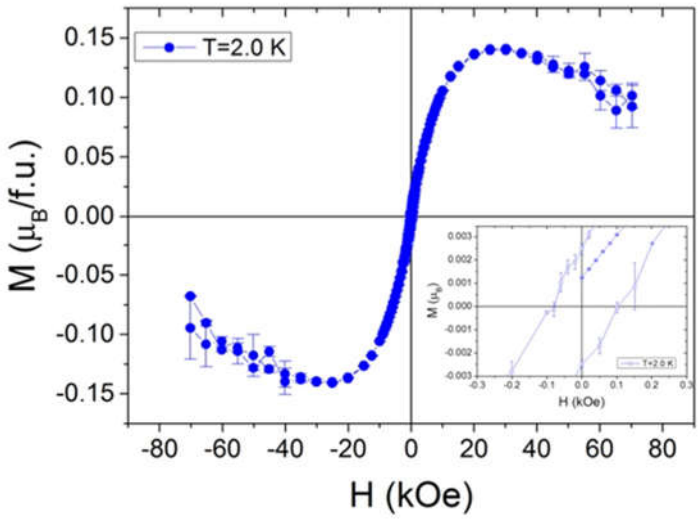

Figure 90. Isothermal magnetization in 2.0 K. Insert points out the value of coercive field of about 90 Oe. The lines are only guides for eyes.

The shape of isothermal magnetization suggests that the studied compound does not behave as a simple paramagnetic material. Also the coercive field of about 90 Oe suggest some kind of interaction between magnetic moments.

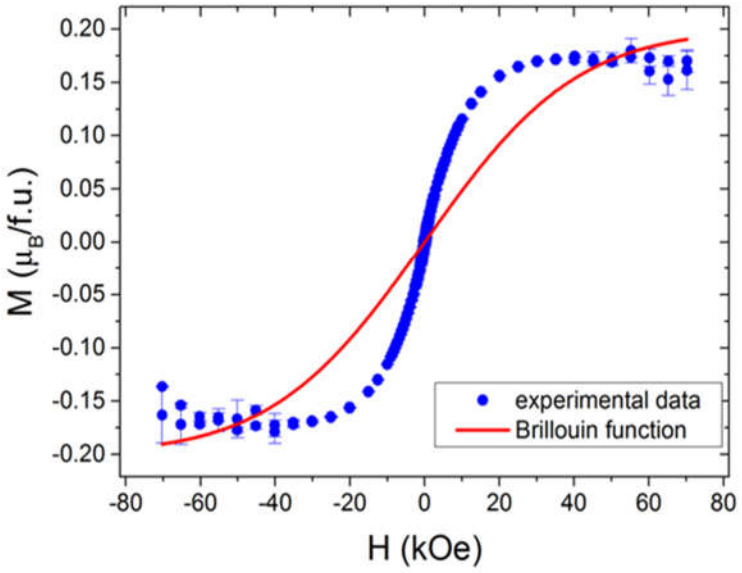

Figure 91. Isothermal magnetization in 2.0K with subtracted diamagnetic contribution (blue circles). The red line represent the Brillouin function for spin 1/2, g=2.0 and with assumption that there is one delocalized electron for each 5 formula unit.

As can be seen in Fig. 91 the isothermal magnetization (blue line) does not fit the Brillouin function (red line). This is another proof that this polymer is not a simple paramagnetic compound. However, we can say that this polymer is a complex antiferromagnetic compound.

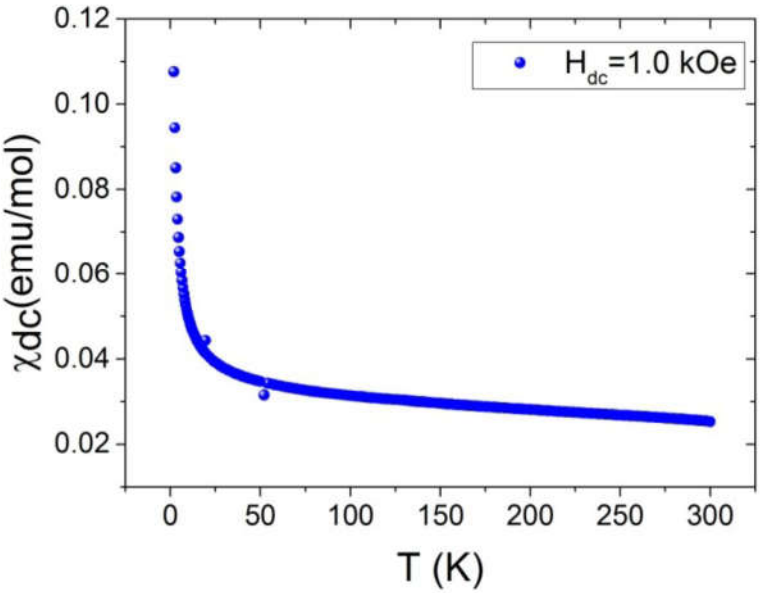

Figure 92. Dc susceptibility as a function of temperature in constant field of 1000 Oe.

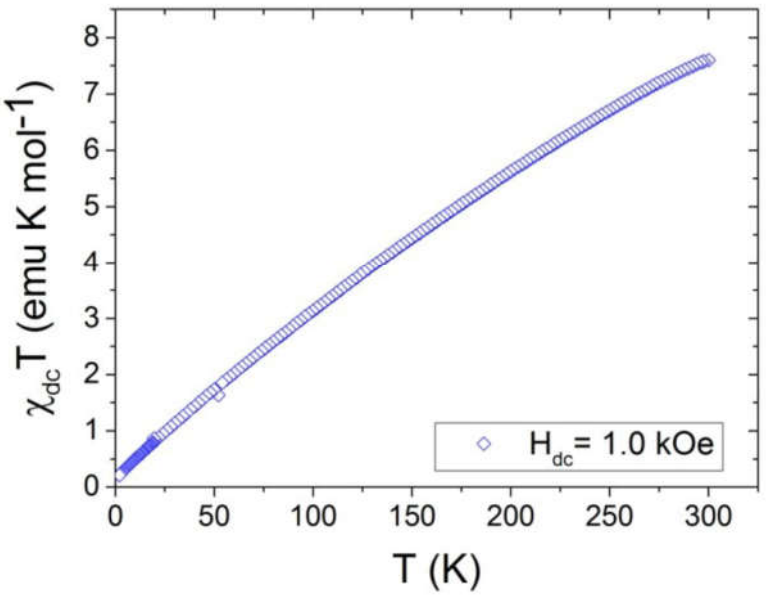

Figure 93. The temperature dependence of χT product.

Another proof that TD100 is not a simple paramagnetic material is the χT product as a function of temperature (Fig. 93). This curve is almost a straight line pointing to 0 for the lowest temperature and as the temperature increases also the χT signal is growing. Further research of magnetic properties and structure is needed to characterized more carefully the TD100 compound.

Furthermore, elemental analysis was also done for TD100 polymer. The results of this measurements are presented in Table. 7.

Elements	1st Analysis	2nd Analysis	Mean Values	Number of Moles
C	9.66%	9.44%	9.55%	4.7
N	2.39%	2.39%	2.39%	1
H	1.92%	1.79%	1.86%	10.8
Summation and the obtained formula	-	-	13.80%	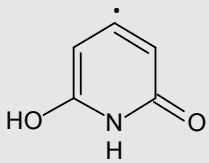 C_5NH_4• (+7H)

Table 7. Elemental analysis of TD100.

I could obtain a valuable result from the elemental analysis of TD100. And it is the number of carbon atoms per one nitrogen atom, assumed to be in one mer of this polymer. As can be seen in Table. 7 this value is close to 5. This result proves that citrazinic acid, upon electropolymerization, will be decarboxylated. Therefore, I can assume the radical structure which is shown in Table forming a mer unit of this polymer.

Electropolymerisation was carried out in a phosphate buffer solution, so it was quite possible that phosphate ions attached to the polymer and got included into its structure. To check this I tried phosphate ion chromatography analysis. The results are included in Table. 8.

	Percentage	Molar mass (g/mole)	(Radical + K_2HPO_4)*	(*+Phosphate)**	(**+Phosphate)***	(***+Water)****	(****+Water)
Total Phosphate	**34%**	94.97	-	-	-	-	-
K_2HPO_4	62.36%	174.18	-	-	-	-	-
Citrazinic acid($C_6H_5NO_4$)	-	155.11	-	-	-	-	-
PO_4		94.97136					
COO	-	44.0098	-	-	-	-	-
Radical	-	110.0923	-	-	-	-	-
C	-	60.055	21.1%	15.8%	12.7%	12.20%	11.77%
N	-	14.00674	4.9%	3.7%	3.0%	2.85%	2.75%
H	-	6.04764	2.1%	1.6%	1.3%	1.64%	1.98%

Table 8. Phosphate ion chromatography analysis results.

The total amount of phosphate which I obtained from this analysis was only 34%, which is not enough to balance the elemental analysis results that showed that the total amount of organic groups is makes only 13.8% of the total mass of the sample. Therefore, I assumed that this phosphate group can be in the form of dipotassium hydrogen phosphate (K_2HPO_4) with some water molecules included into the structure of polymer. Attempts to balance these results are shown in the right columns in Table 8. Unfortunately, the results are not satisfactory. As the polymer is

extremely hygroscopic, it cannot be excluded that the samples provided for elemental analysis and ion chromatography contained different amounts of water, despite having been carefully dried.

Acidity determination

For the first time, I calculated pK_a for citrazinic acid and the polymer obtained by electropolymerisation of this acid. See the results below.

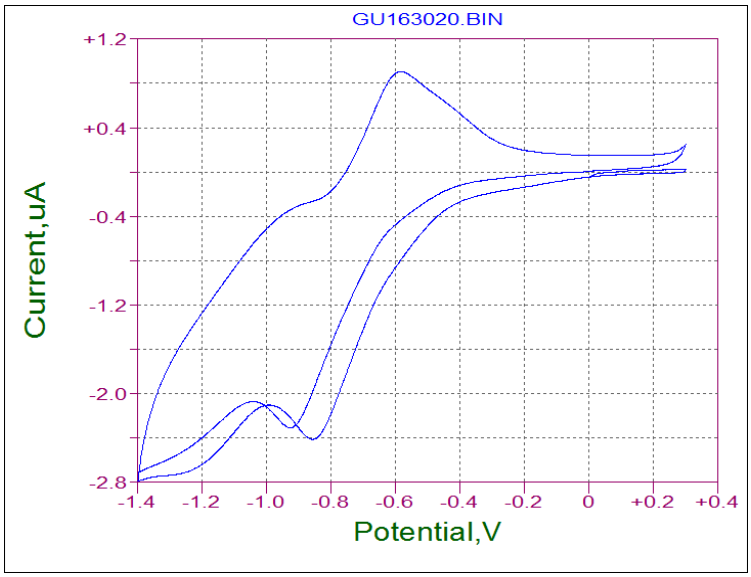

Figure 94. Cyclic voltammograms of citrazinic acid in DMF on Pt electrode.

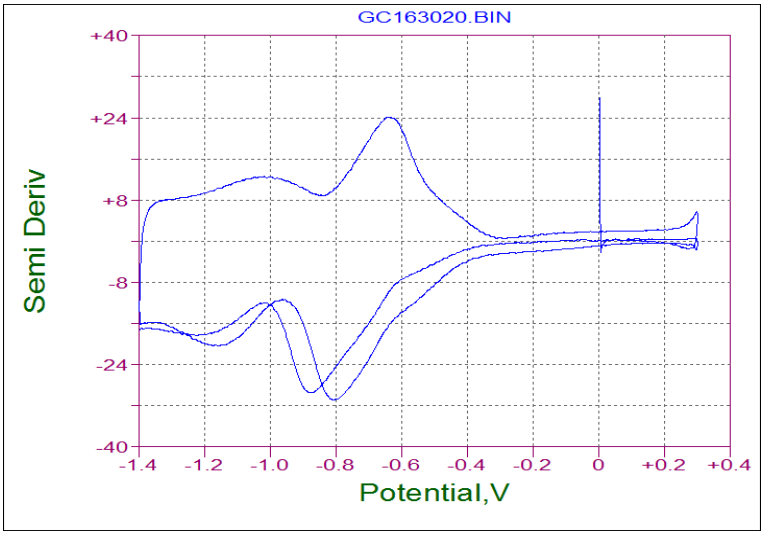

Figure 95. Semiderivatives of the voltammograms in Fig. 94.

	1	2	3
$E_{1/2}$(V, vs. AgCl/Ag)	-1.02	-0.641	-0.476
pK_a	16.6	11.7	8.8

Table 9. pKa values of citrazinic acid in DMF.

There are three distinct processes observed. Most probably three different tautomers showing different values of pK_a are present in the solution.

In the case of the polymer, there is only one process seen.

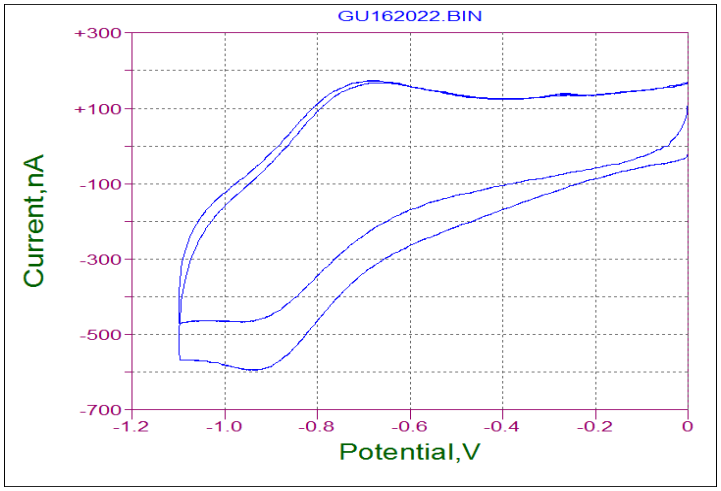

Figure 96. Cyclic voltammograms of polymer in DMF on Pt electrode.

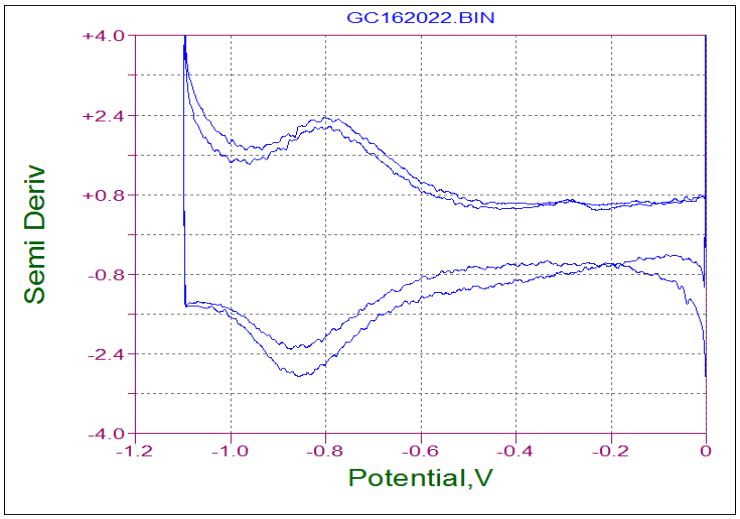

Figure 97. Semiderivatives of the voltammograms in Fig. 96.

$E_{1/2}$(V, vs. AgCl/Ag)	-1.320
pK_a	12.8

Table 10. pKa value of polymer in DMF.

All the calculations were done based on the literature [52].

Acid	pK_a	Chlorophenols	pK_a
Aniline hydrochloride	5.11	Pentachlorophenol	8.5
Oxalic acid	7.5	2,3,6-Trichlorophenol	10.5
Malonic acid	7.5	2,4,5-Trichlorophenol	12.2
Salicylic acid	8.2	2-Chlorophenol	14.4
Succinic acid	10.2	3,4-Dichlorophenol	15.4
Triethylamine hydrochloride	10.2	4-Chlorophenol	17.9
Benzoic acid	12.2	2,3-Dichlorophenol	17.9
Acetic acid	13.4	2,3,4,6-Tetrachlorophenol	8.9
		Tetrachlorocatechol	8.5

Table 11. p*K*a values of a couple of acids in DMF for comparison [52].

As it can be seen in Table. 11, the third pK_a calculated value of citrazinic acid is close to the pK_a for salicylic acid and pentachlorophenol and the pK_a value for the polymer is close to this parameter for benzoic acid. These values will be expected given their similar structures.

The interaction between TD100 and guanine

As we know, guanine base pair in nature is cytosine. Moreover, we know that guanine and cytosine in DNA helix connect to each other by using triple hydrogen bonds. On the other hand, the structure of citrazinic acid really resembles the structure of cytosine. It means that citrazinic acid, like cytosine, should be capable of forming three hydrogen bonds (see Fig. 98). Therefore, I thought why not? The type of this effective interaction between TD100 and guanine can be due to hydrogen bonds.

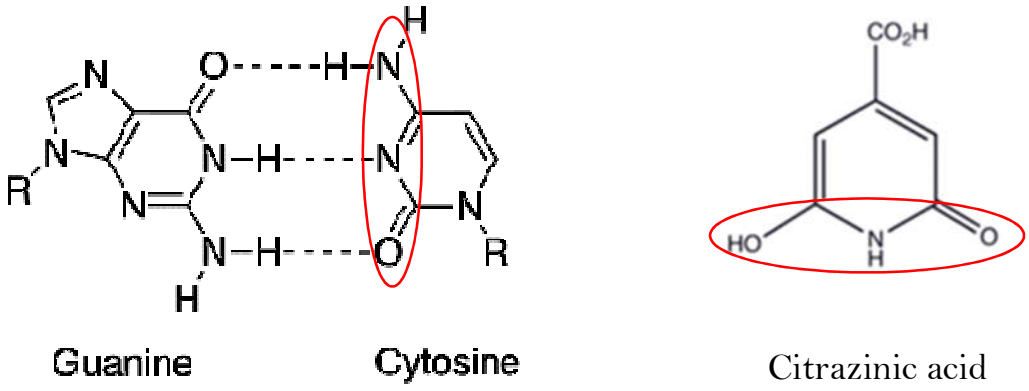

Figure 98. Guanine-cytosine pair and citrazinic acid structures.

To prove my hypothesis, I did some measurements by using platinum electrode. Citrazinic acid shows two reduction waves at the Pt electrode (see Figs. 99 and 100) that cannot be seen at GCE. This means that they are due to the reduction of acidic hydrogens.

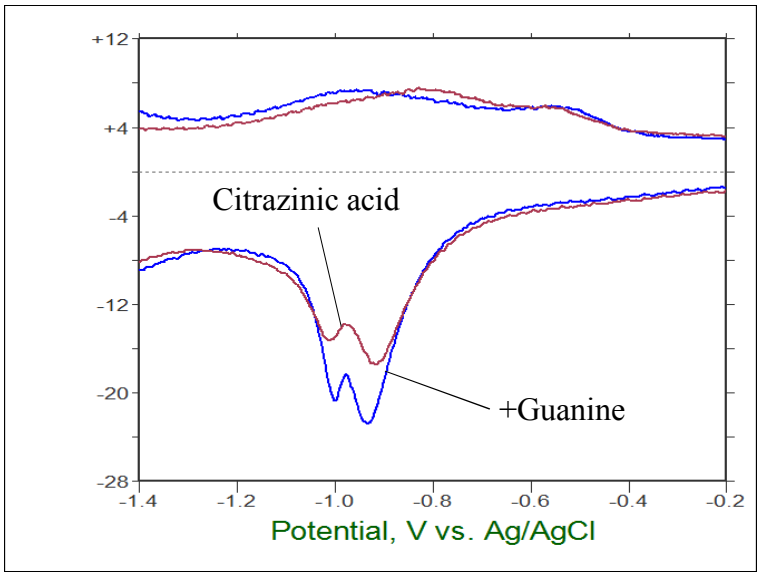

Figure 99. Semiderivatives of voltammograms of citrazinic acid, without and with guanine added in DMF at Pt. Scan rate 0.02 V s^{-1}.

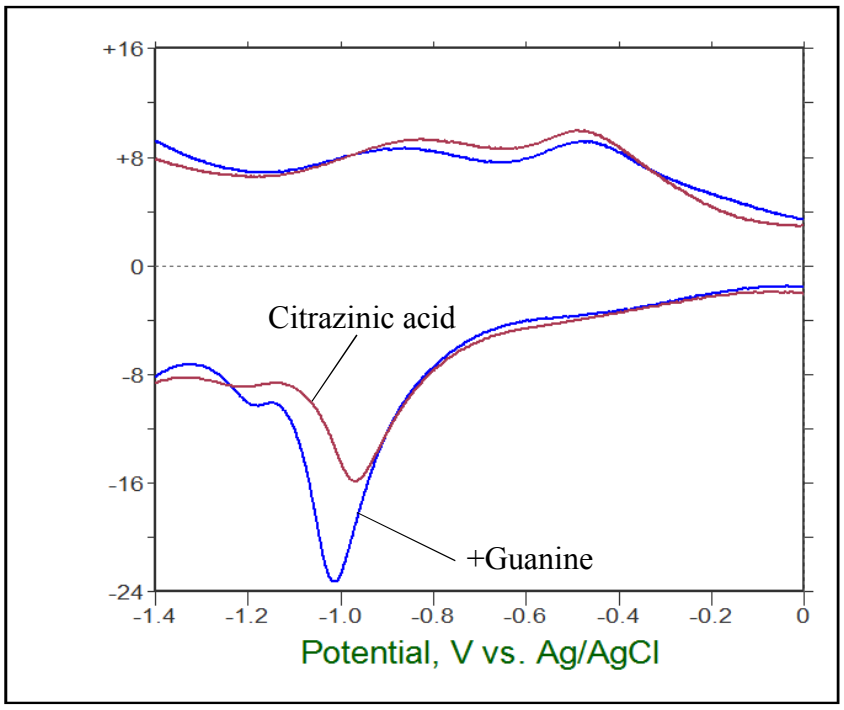

Figure 100. Semiderivatives of voltammograms at a scan rate 0.2 V s^{-1}.

The second reduction wave is shifted to more cathodic potentials at higher scan rates and becomes significantly wider (compare Figs. 99 and 100). Adding guanine that has an acidic

hydrogen that can be reduced at about the same potential as the first hydrogen of citrazinic acid, increases the intensity of both waves at the lower scan rate, without shifting the potentials. At higher scan rates, however, even the first reduction wave for the mixture of citrazinic acid and guanine is slightly shifted to more cathodic potentials compared with the wave for pure citrazinic acid. There are even bigger differences concerning the second wave, that is more intense and shifted to less cathodic potentials. The pattern is complex and requires more data to be convincingly explained. However, it is clear that it is due to specific H-bond interactions of guanine with citrazinic acid.

To prove that this effect can be observed especially in the solution of guanine and citrazinic acid, I prepared another experiment by adding piperazine to the solution of citrazinic acid and then acidified the solution by introducing hydrochloric acid gas. As you can see in Fig. 101, the pattern of interaction between piperazine and citrazinic acid is totally different from guanine, because of the steric effect in the structure of piperazine, this base can interact with citrazinic acid only with one hydrogen bond while as I showed before, guanine is capable of making three hydrogen bonds with citrazinic acid which is more effective.

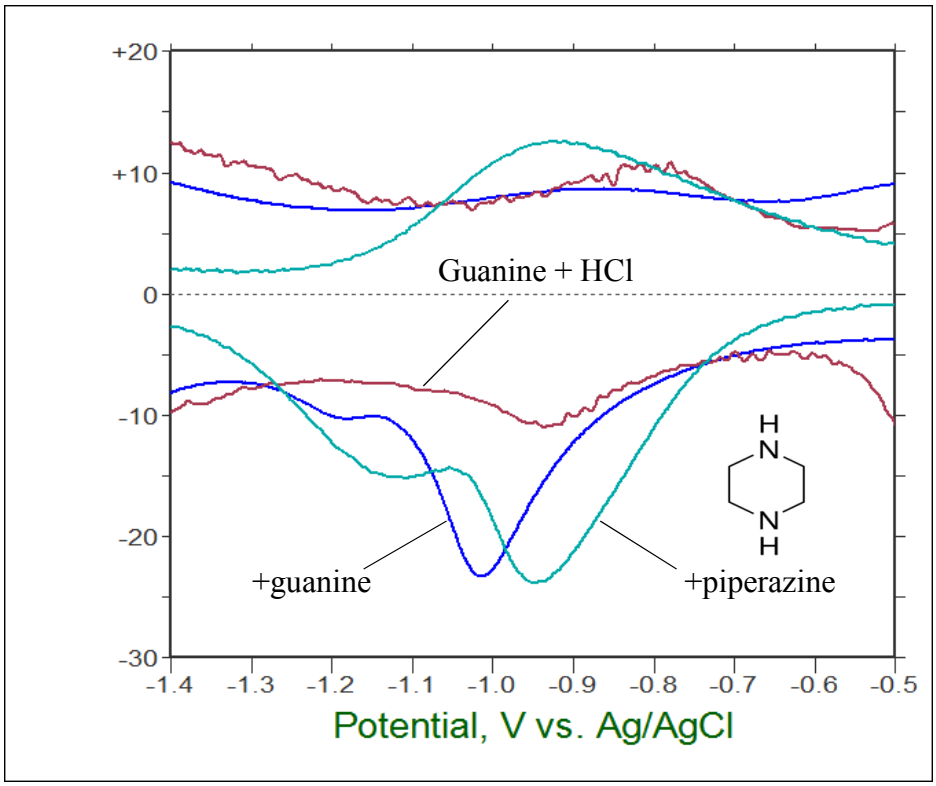

Figure 101. Comparison of semiderivatives of voltammograms of indicated mixtures in DMF at Pt. Scan rate 0.2 V s^{-1}.

AFM measurements

The interaction of the polymer with guanine was also probed with Atomic Force Microscopy. The addition of guanine changes the morphology of polymer obtained from citrazinic acid (TD100) films as random elongated and elevated structures appeared in topography images. The topographical differences can be described quantitatively using coefficients: Root Mean Square (RMS), Skewness (Skw) and Kurtosis (Kur). The skewness coefficient is a measure for the degree of symmetry in the variable distribution (equals 1 for a symmetric distribution) while kurtosis is a measure for the degree of flatness in the variable distribution. The RMS gives information on roughness of the surface. The coefficients calculated for images presented in Fig. 102 a and Fig. 102 b give RMS values of 0.501 nm and 1.169 nm, respectively. Skw of pure polymer film is 0.942 while Skw obtained for polymer and guanine film topography image equals to 3.110. Kurtosis equals to 9.88 and 23.90, respectively. Contrast in lateral force image of the mixture of polymer and guanine sample suggests presence of areas of different friction properties.

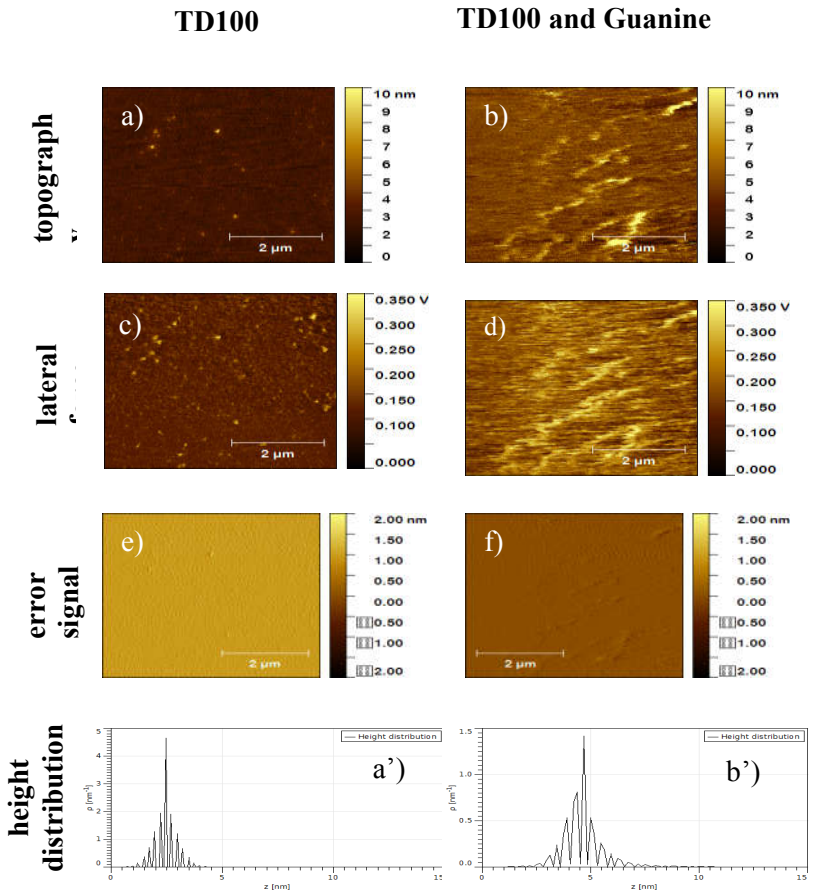

Figure 102. Representative surface topography images of citrazinic acid layer (a) and citrazinic acid admixed with guanine film (b). Lateral force (c, d) and error signal (e, f) images of investigated samples. Additionally, pixel height distributions are presented in (a') and (b').

Conclusions

Guanine solubility

The method described makes it possible to calculate the solubility of guanine depending on the pH of solution. It appeared and was confirmed by agreement with the literature data for acidic solutions that the solubility is simply equal to the sum of concentrations of all guanine species present in solution in equilibrium with solid guanine. The concentrations of individual species, either ionised or protonated forms of guanine could be calculated using known values of the respective pK_as and assuming a pH independent concentration of the neutral guanine, which is in equilibrium with solid guanine, and constant over all the pH range.

Dissolution of guanine powder gives rise to the formation of nanoparticles, of 20 to 100 nm size that undergo enlargement in time to form stable particles of ca. 800 nm size. The presence of these particles is not evident and apparently it was the main reason of obtaining too high solubility data.

The most probable cause of acidification of guanine solutions and the secondary reason behind problems with reproducibility in solubility determination is the presence of acidic impurities in commercial guanine powder. As a advise, it is better to use properly small quantities of guanine for dissolution and not too diluted buffer solutions.

Antioxidant evaluation

A novel electrochemical method based on a sequence of successive potential hold and scan steps proved to be useful in evaluation of the antioxidant activity meant as the ability to inhibit the generation of 8-oxoguanine in the reaction with in situ formed Reactive Oxygen Species. This method can measure pro-oxidative activity of antioxidants, too.

Simple alcohols exhibited weak antioxidant activity and did not show any antioxidant activity. The 8-oxoguanine production vs. antioxidant concentration shows exponential decay character. For simple alcohols this is a single-exponential decay down to a complete inhibition of 8-oxoguanine generation. Glutathione shows a similar behaviour. The exponential coefficient, k, can be used as a measure of antioxidant activity. This value is related directly to the often applied parameter, IC50 (or EC50), by a simple relation IC50 = ln2/k. By proving that the dependence follows the exponential decay and by knowing the decay parameter, it is possible to calculate the inhibition degree at a given concentration of the antioxidant.

The study of other antioxidants at pH 7 exhibited multi-exponential decay character. Generally, at low antioxidant concentrations, antioxidative activity was much more efficient. Then, at higher concentrations, the efficiency dropped much, sometimes even several times. In some cases, the curve virtually levelled off, resembling the radical scavenging situation by achieving a steady state where the activity is not affected by increasing antioxidant concentration any more.

A high decay parameter indicates better antioxidant activity. In my study, at pH 7, gallic acid and resveratrol showed the best antioxidant activity. However, resveratrol reached virtually a steady state at ca. 40% inhibition level at a very low, 3 μM, concentration.

Many of antioxidants under my study such as polyphenols showed even pro-oxidative activity at pH 9. Catechol, catechin and ascorbyl phosphate demonstrated an increase in the generation of 8-oxoguanine up to 160% compared to the situation in the absence of these compounds. In other cases, like pyrogallol, for lower concentrations, some antioxidant activity was observed but much lower than that at pH 7, but it turned to high pro-oxidative activity at higher concentrations.

According to the literature, guanosine or deoxyguanosine, which are the guanine forms in the nucleotides in RNA and DNA, respectively, are oxidised at the potential not much different from that of guanine to form 8-oxoguanosine or 8-oxodeoxyguanosine. Therefore, I can suggest the above method to be applied to detect guanosine or deoxyguanosine oxidation products, too. Even, I assume that this method can be used for monitoring the RNA/DNA damage caused by oxidative stress.

Guanine electroanalysis and electrode modification

A series of pyridine carboxylic acids was used to modify the glassy carbon electrode with the goal to make it more sensitive towards guanine oxidation. The best results were obtained by polymerising electrochemically citrazinic acid, followed by adsorption of iron tetraphenylporphyrin from its solution in tetrahydrofuran. This polymer attaches strongly to the surface of GCE and actively adsorbs guanine.

It was found that adsorption of metalloporphyrins increases the efficiency of guanine oxidation process. Even free base tetraphenylporphyrin showed this effect. It could be thus concluded that π-π interaction has a significant role in the binding of guanine. Tetrahydrofuran which is used as the solvent for the porphyrin solutions, can itself modify the GCE by swelling the polymer layer. The type and thickness of the polymer layer affects the oxidation of guanine on modified GCE.

The modified electrode adsorbs very efficiently guanine and can be used for trace analysis of this compound even at 5 nM concentration with the use of square wave voltammetry. At lower concentrations, 2 nM, the signal is still but there may be problems with reproducibility.

Guanine oxidation yields two transient products that give oxidation waves in the second scan, but only at higher scan rates. One of these transients was already identified as 8-oxoguanine. Surprisingly, these two transients relatively slowly convert back to guanine on the polymer used for electrode modification.

The electrical capacity of the polymer layer is very high with respect to the size of it (surface area ~5 mm^2), and it even increases after adsorption of porphyrins.

Guanine oxidation process is controlled by adsorption in the 1st scan and by diffusion during the subsequent scans.

The interaction between the electroactive polymer layer and guanine is based on the formation of multiple H-bonds, which was proven by comparing this effect with other bases, like piperazine, capable of forming just one H-bond.

Uv-vis absorption and emission spectroscopy showed interaction between citrazinic acid and its polymer with guanine by the formation of new bands in mixed solutions.

The polymer formed by electrooxidation of citrazinic acid has a molecular weight of ca. 10 000 g/mol. This electroactive system is a complex antiferromagnetic compound. We assume that the structure of this polymer is based on the radical $C_5NH_4O_2$ formed by decarboxylation of citrazinic acid. It is highly hygroscopic, soluble in water, and even after careful drying contains water and phosphates.

Three pK_a values were determined for citrazinic acid and just one for the polymer obtained by electrooxidation of citrazinic acid, by using $E_{1/2}$ values for acidic proton reduction on the Pt electrode in DMF.

AFM measurements showed that guanine can change the topography of TD100 by increasing the roughness, flatness and symmetry coefficients of the under study surface.

Reference

[1] S. Tadepalli, J. M. Slocik, M. K. Gupta, R. R. Naik, S. Singamaneni, Chem. Rev. 117 (2017) 12705–12763.
[2] D. Gur, B. A. Palmer, S. Weiner, L. Addadi, Adv. Funct. Mater. 27 (2017) 1603514.
[3] B. A. Palmer, G. J. Taylor, V. Brumfeld, D. Gur, M. Shemesh, N. Elad, A. Osherov, D. Oron, S. Weiner, L. Addadi, Science 358 (2017) 1172–1175.
[4] D. Gur, M. Pierantoni, N. E. Dov, A. Hirsh, Y. Feldman, S. Weiner, L. Addadi, Cryst. Growth Des. 16 (2016) 4975−4980.
[5] A. Hirsch, D. Gur, I. Polishchuk, D. Levy, B. Pokroy, A. J. Cruz-Cabeza, L. Addadi, L. Kronik, L. Leiserowitz, Chem. Mater. 27 (2015) 8289–8297.
[6] H. B. Singh, K. A. Bharati, Enumeration of dyes, in: *Handbook of Natural Dyes and Pigments*; Woodhead Publishing India, (2014) pp. 33–260.
[7] M. Iwasaka, Y. Miyashita, Y. Mizukawa, K. Suzuki, T. Toyota, T. Sugawara, Appl. Phys. Express 6 (2013) 037002.
[8] H. DeVoe, S. P. Wasik, J. Solution Chem. 13 (1984) 51–60.
[9] H.-J. Hinz, Ed. *Thermodynamic Data for Biochemistry and Biotechnology*; Springer-Verlag, Berlin, 1986.
[10] A. Hirano, H. Tokunaga, M. Tokunaga, T. Arakawa, K. Shiraki, Arch. Biochem. Biophys. 497 (2010) 90–96.
[11] Q. Li, C. Batchelor-McAuley, R. G. Compton, J. Phys. Chem. B 114 (2010) 7423–7428.
[12] T. H. Li, W. Li. Jia, H. S. Wang, R.M. Liu, Biosens. Bioelectronics 22 (2007) 1245–1250.
[13] A. M. Nowicka, A. Kowalczyk, S. Sęk, Z. Stojek, Anal. Chem. 85 (2013) 355−361.
[14] R. Apak, M. Özyürek, K. Güçlü, E. Çapanoğlu, J. Agric. Food Chem. 64(2016) 1046−1070.
[15] C. Tong, C. Shuo-Bin, T. Jia-Li, W. Bo, W. Yu-Qing, Zh. Yan, W. Jing, W. Zeng-Qing, Zh. Ze-Peng, O. Tian-Miao, Zh. Yong, T. Jia-Heng, H. Zhi-Shu, J. Med. Chem. 61 (2018) 3436-3453.
[16] S. C. B. Oliveira, A. M. Oliveira-Brett, J. Electroanal. Chem. 648 (2010) 60–66. 2010.
[17] A. T. Dharmaraja, J. Med. Chem. 60 (2017) 3221–3240.
[18] P.T. Henderson, J. C. Delaney, J. G. Muller, W. L. Neeley, S. R. Tannenbaum, C. J. Burrows, J. M. Essigmann, Biochemistry 42 (2003) 9257-9262.
[19] P. G. Slade, M. K. Hailer, B. D. Martin, K. D. Sugden, Chem. Res. Toxicol. 18 (2005) 1140–1149.
[20] E. M. Norabuena, S. B. Williams, M. A. Klureza, L. J. Goehring, B. Gruessner, M. L. Radhakrishnan, E. R. Jamieson, M. E. Núñez, Biochemistry 55 (2016) 2411−2421.
[21] M. Faraggi, F. Broitman, J. B. Trent, M. H. Klapper, J. Phys. Chem. 100 (1996) 14751–14761.
[22] E. E. Ferapontova, Electrochim. Acta 49 (2004) 1751–1759.
[23] A. M. Oliveira-Brett, V. Diculescu, J. A. P. Piedade, Bioelectrochemistry 55 (2002) 61–62.
[24] E. E. Ferapontova, E. DomÌnguez, Electroanalysis 15 (2003) 629-634.
[25] U. Mohan, S. Kaushik, U. C. Banerjee, Open Biotechnol. J. 5 (2011) 21-27.
[26] A. Barberis, Y. Spissu, G. Bazzu, A. Fadda, E. Azara, D. Sanna, M. Schirra, P. A. Serra, Anal. Chem. 86 (2014) 8727−8734.
[27] A. J. Blasco, A. G. Crevillén, M. C. González, A. Escarpa, Electroanalysis 19 (2007) 2275–2286.
[28] X. Li, J. Agric. Food Chem. 60 (2012) 6418–6424.
[29] S. A. Pshenichnyuk, A. Modelli, E. F. Lazneva, A. S. Komolov, J. Phys. Chem. A 120 (2016) 2667–2676.
[30] M. P. Bradshawa, P. D. Prenzlera, G. R. Scollary, Electroanalysis 14 (2002) 546-550.
[31] S. A. Pshenichnyuk, A. S. Komolov, J. Phys. Chem. Lett. 6 (2015) 1104−1110.
[32] S. Eghbaliferiz, M. Iranshahi, Phytother. Res. 30 (2016) 1379–1391.
[33] E. Kim, Y. Liu, C. J. Baker, R. Owens, S. Xiao, W. E. Bentley, G. F. Payne, Biomacromolecules 12 (2011) 880–888.

[34] E. Kim, Y. Liu, W. T. Leverage, J.-J. Yin, I. M. White, W. E. Bentley, G. F. Payne, Biomacromolecules 15 (2014) 1653–1662.
[35] A. H. Kamel, F. T. C. Moreira, C. Delerue-Matos, M. G. F. Sales, Biosens. Bioelectronics 24 (2008) 591–599.
[36] R. Apak, M. Özyürek, K. Güçlü, E. Çapanoğlu, J. Agric. Food Chem. 64 (2016) 997–1027.
[37] L.D. Mello, L.T. Kubota, Talanta. 72 (2007) 335–348.
[38] E. Kim, Y. Liu, W. T. Leverage, J. J. Yin, I. M. White, W. E. Bentley, G. F. Payne, Biomacromolecules 15 (2014) 1653−1662.
[39] A. Rene, M. L. Abasq, D. Hauchard, P. Hapiot, Anal. Chem. 82 (2010) 8703-8710.
[40] A. H. Kamel1, F. T.C. Moreira, C. D. Matos, M. G. F. Sales, Biosens. Bioelectronics 24 (2008) 591–599.
[41] E. Suresh, K. Sundaram, B. Kavitha, N. Senthil Kumar, Int. J. Pharm. Res. 8 (2016) 44-48.
[42] H. Yin, Y. Zhouc, Q. Ma, S. Ai, P. Ju, L. Zhu, L. Lu, Process Biochem. 45 (2010) 1707–1712.
[43] E. R. Apaydın, G. Saglikoglu, S. Yilmaz, M. Yildiz, Int. J. Electrochem. Sci. 10 (2015) 1904 – 1915.
[44] F. Solano, New J. Sci. 2014 (2014) 1-28.
[45] A. D. Schweitzer, E. Revskaya, P. Chu, V. Pazo, M. Friedman, J. D. Nosanchuk, S. Cahill, S. Frases, A.Casadevall, E. Dadachova, Int. J. Radiation Oncology Biol. Phys. 78 (2010) 1-9.
[46] S. Anandhakumar, J. Mathiyarasu, K. L. N. Phani, V. Yegnaraman, Am. J. Anal. Chem. 2 (2011) 470-474.
[47] S. Soylemez, S. O. Hacioglu, M. Kesik, H. Unay, Ali Cirpan, L. Toppare, Appl. Mater. Interfaces 6 (2014) 18290−18300.
[48] G. Nie, Z. Bai, W. Yu, J. Chen, Biomacromolecules 14 (2013) 834−840.
[49] E.Suresh, K. Sundaram, B. Kavitha, S. N. Kumar, Int. J. Chem. Pharm. Sci. 7 (2016) 42-47.
[50] D. W. Hatchett, M. Josowicz, Chem. Rev. 108 (2008) 746-769.
[51] G. V. Martins, A. C. Marques, E. Fortunato, M. G. F. Sales, Biosens. Bioelectron. 86 (2016) 225–234.
[52] S. S. Kurek, B. J. Laskowska, A. Stokłosa, Electrochim. Acta 51 (2006) 2306–2314.
[53] X. Gan, H. Zhao, Sens. Mater. 27 (2015) 191-215.
[54] Z. Wang, E. Liu, X. Zhao, Thin Solid Films 519 (2011) 5285–5289.
[55] V. H. Nguyen, C. Lamiel, D. Kharismadewi, V. C. Tran, J. J. Shim, J. Electroanal. Chem. 758 (2015) 148–155.
[56] Y.Yang1, R. Sun, M. Li1, B. Geng, J. Deng, M.Tang, Int. J. Electrochem. Sci. 11 (2016) 7370 – 7379.
[57] N. T. M. Hai , B. Gasparovic, K. Wandelt, P. Broekmann, Surf. Sci. 601 (2007) 2597–2602.
[58] J. H. Yu, F. Y. Li, X. S. Wang, Y. Huang, B. W. Zhang, C. H. Huang, Y. Cao, Optical Mater. 21 (2002) 467–473.
[59] G. Zuo, Q. Wang, Z. Li, J. Yang, P. Wang, Int. J. Electrochem. Sci. 10 (2015) 6703 – 6713.
[60] C. Wang, R. Yuan, Y. Chai, S. Chen, Y. Zhang, F. Hu, M. Zhang, Electrochim. Acta 62 (2012) 109– 115.
[61] K. I. Ozoemena, Sensors 6 (2006) 874-891.
[62] C.Y. Yeh1, S. H. Cheng, Tamkang J. Sci. Eng. 6 (2003) 81-86.
[63] L. M. Shi, J. X. Pan, B. Zhou, X. Jiang, J. Mater. Chem. B 3 (2015) 9340-9348.
[64] C. M. A. Brett, A. M. C.F. Oliveira Brett, J. Electroanal. Chem. 255 (1988) 199-213.
[65] R. L. Benoit, M. Fréchette, Can. J. Chem. 63 (1985) 3053–3056.
[66] S. F. Mason, J. Chem. Soc. (1954) 2071–2081.
[67] F. Zaccaria, G. Paragi, C. Fonseca Guerra, Phys. Chem. Chem. Phys. 18 (2016) 20895–20904.
[68] A. Hirano, H. Tokunaga, M. Tokunaga, T. Arakawa, K. Shiraki, Arch. Biochem. Biophys. 497 (2010) 90–96.
[69] V. Verdolino, R. Cammi, B. H. Munk, H. B. Schlegel, J. Phys. Chem. B 112 (2008) 16860–16873.

[70] K. Guille,. W. Clegg, Acta Crystallogr. C 62 (2006) O515–O517.
[71] U. Thewalt, C. E. Bugg, R. E. Marsh, Acta Crystallogr. B 27 (1971) 2358–2363.
[72] A. Hirsch, D. Gur, I. Polishchuk, D. Levy, B. Pokroy, A. J. Cruz-Cabeza, L. Addadi, L. Kronik, L. Leiserowitz, Chem. Mater. 27 (2015) 8289–8297.
[73] D. Ibañez, A. Santidrian, A. Heras, M. Kalbáč, A. Colina, J. Phys. Chem. C 119 (2015) 8191−8198.
[74] X. Li, C. Lin, C. Batchelor-McAuley, E. Laborda, L. Shao, R. G. Compton, J. Phys. Chem. Lett. 7 (2016) 1554–1558.
[75] R. R. Nazmutdinov, T. T. Zinkicheva, S. A. Shermukhamedov, J. Zhang, J. Ulstrup, Curr. Op. Electrochem. 7 (2018) 179–187.
[76] T. Darvishzad, T. Lubera, S. S. Kurek, J. Phys. Chem. B 122 (2018) Just Accepted Manuscript. DOI: 10.1021/acs.jpcb.8b04327
[77] Z. Feng, N. S. Georgescu, D. A. Scherson, Anal. Chem. 88 (2016) 1088–1091.
[78] G. P. McCallum, M. Siu, S. L. Ondovcik, J. N. Sweeting, P. G. Wells, Mol. Carcinogenesis 50 (2011) 163–172.
[79] A. M. Osman, K. K. Y. Wong, A. Fernyhough, Biochem. Biophys. Res. Commun. 346 (2006) 321–329.
[80] X. Li, J. Agric. Food Chem. 60 (2012) 6418–6424.
[81] T. Darvishzad, S. S. Kurek, Electrochim. Acta 240 (2017) 466-473.
[82] C. Li, X. Qiu, Y. Ling, J. Electroanal. Chem. 704 (2013) 44–49.